Cun, Wukuang; Pesaran, M. Hashem

Working Paper

A Spatiotemporal Equilibrium Model of Migration and Housing Interlinkages

CESifo Working Paper, No. 9343

Provided in Cooperation with:
Ifo Institute – Leibniz Institute for Economic Research at the University of Munich

Suggested Citation: Cun, Wukuang; Pesaran, M. Hashem (2021) : A Spatiotemporal Equilibrium Model of Migration and Housing Interlinkages, CESifo Working Paper, No. 9343, Center for Economic Studies and ifo Institute (CESifo), Munich

This Version is available at:
https://hdl.handle.net/10419/248888

CESifo WORKING PAPERS

9343
2021

October 2021

A Spatiotemporal Equilibrium Model of Migration and Housing Interlinkages

Wukuang Cun, M. Hashem Pesaran

CESifo

Impressum:

CESifo Working Papers
ISSN 2364-1428 (electronic version)
Publisher and distributor: Munich Society for the Promotion of Economic Research - CESifo GmbH
The international platform of Ludwigs-Maximilians University's Center for Economic Studies and the ifo Institute
Poschingerstr. 5, 81679 Munich, Germany
Telephone +49 (0)89 2180-2740, Telefax +49 (0)89 2180-17845, email office@cesifo.de
Editor: Clemens Fuest
https://www.cesifo.org/en/wp
An electronic version of the paper may be downloaded
· from the SSRN website: www.SSRN.com
· from the RePEc website: www.RePEc.org
· from the CESifo website: https://www.cesifo.org/en/wp

CESifo *Working Paper No. 9343*

A Spatiotemporal Equilibrium Model of Migration and Housing Interlinkages

Abstract

This paper develops and solves a spatiotemporal equilibrium model in which regional wages and house prices are determined jointly with location-to-location migration flows. The agent's optimal location choice and the resultant migration process are shown to be Markovian, with the transition probabilities across all location pairs given as non-linear functions of wage and housing cost differentials, endogenously responding to migration flows. The model can be used for the analysis of spatial distribution of population, income, and house prices, as well as for the analysis of the entire dynamic process of shock spill-over effects in regional economies through location-to-location migration. The model is estimated on a panel of 48 mainland U.S. states and the District of Columbia over the training sample (1976-1999) and is shown to fit the data well over the evaluation sample (2000-2014). The estimated model is then used to analyse the size and speed of spatial spill-over effects by computing spatiotemporal impulse responses of positive productivity and land-supply shocks to California, Texas, and Florida. The sensitivity of the results to migration elasticity, housing depreciation rate and local land supply conditions is also investigated.

JEL-Codes: E000, R230, R310.

Keywords: location choice, joint determination of migration and house prices, spatiotemporal impulse responses, land-use deregulation, counterfactual exercise, population allocation, productivity and land supply shocks, California, Texas and Florida.

Wukuang Cun
Shanghai University of Finance and Economics
Shanghai / China
cunwukuang@mail.shufe.edu.cn

M. Hashem Pesaran
University of Southern California
Los Angeles / CA / USA
pesaran@usc.edu

September 30, 2021
We are grateful to Alexander Chudik and Ron Smith, an anonymous referee and the Editor for helpful comments. This paper was previously circulated under the title of "Land Use Regulations, Migration and Rising House Price Dispersion in the U.S." Wukuang Cun was a postdoc at USC Dornsife INET when research for this paper was carried out.
This paper is a revised version of CESifo WP no. 7007 (April 2018).

1 Introduction

This paper contributes to the literature on housing and migration by developing a Markovian model of the migration process jointly with a regional model of house prices driven by population and exogenously given labor productivity and land supply. It extends the classical spatial equilibrium model of Rosen (1979) and Roback (1982) by explicitly modelling the dynamics of location-to-location migration flows that interact with the dynamics of housing depreciation and accumulation. The size and speed of spatial spill-over effects are quantified by means of spatiotemporal impulse response analyses of regional shocks. The proposed model is tractable and can be applied to study spill-over effects in regional housing markets, which have been the subject of a number of empirical studies by Holly et al. (2010), Bailey et al. (2016), Sinai (2012), Cotter et al. (2015) and DeFusco et al. (2018), amongst others. The model can also be used to study the spatiotemporal impacts of changes in local land supplies on regional house prices and spatial population allocation, which are recently considered by Hsieh and Moretti (2019) and Herkenhoff et al. (2018).[1] Importantly, the model can be used to quantify the effects of factors such as migration elasticity, housing depreciation rate and local land supply conditions on the spatiotemporal adjustments in regional economies through migration, which cannot be done using Rosen-Roback style models that abstract from migration by assuming perfect mobility, or by using reduced form empirical models.

Specifically, we propose a spatiotemporal equilibrium model of the housing market by solving explicitly the agent's optimal location choice problem and the dynamics of location-to-location migration flows. We model local labor and housing markets jointly with migration decisions, allowing the latter to be the function of wage and housing cost differentials. This is in contrast to conventional demographic studies on migration that use Markov chain models, such as Fuguitt (1965) and Tarver and Gurley (1965), but assume transition probabilities across locations are exogenously given, whilst in our study we allow migration flows to interact with local housing markets through endogenous and nonlinear variations in transition probabilities across location pairs and over time. As a result, in our set-up local wage rates and house prices are jointly determined with migration flows. Our theoretical framework can be viewed as an example of a dynamic network where regional labor and housing markets interact with each other via migration flows that function as a source of spatial spill-over effects. The proposed model has the advantage that it can be used for the analysis of spatial distribution of population, income and house prices, as well as for the analysis of the entire dynamic process of shock spill-over effects in regional economies through location-to-location migration.

We place location choice of individual agents at the core of our modelling strategy. At the start of each period, agents decide whether to remain where they are or migrate to a different location. The gain from migration depends on the differences in wage rates and housing costs between the origin and the destination, as well as migration costs consisting of a route-specific

[1] Furthermore, our theoretical framework can be adapted to analyze other types of spatial spill-over effects in regional economies that operate through migration, such as spill-over effects in regional labor markets, previously considered by Blanchard et al. (1992).

element plus a stochastic idiosyncratic component. The agent's optimal location choice and the resultant migration process is shown to be Markovian with the transition probabilities across all location pairs given as non-linear functions of wage and housing cost differentials. In each location, construction firms build new houses by combining land and residential structures, with housing supplies endogenously responding to migration flows. In addition, it is shown that the deterministic version of the model has a unique balanced growth path, with no location ending up with zero population.

The model is estimated on a panel of 48 mainland U.S. states plus the District of Columbia on a training sub-sample, 1976-1999, and then evaluated over 2000-2014, which we refer to as the evaluation sample.[2] The migration elasticity and route-specific migration costs, which are the key parameters affecting the spatiotemporal spill-over effects of regional shocks, are estimated *jointly* using the combined state-to-state migration flows and state level incomes and housing costs data. It is shown that a large part of variations in migration costs can be explained in terms of amenity differentials and geographical distances. Parameters that govern local housing supplies are calibrated using state level housing market data. We estimate the state level supplies of new residential land from the model using housing market and urban land acreage data. These estimates are shown to be significantly negatively correlated with the Wharton Residential Land Use Regulatory Index (WRI henceforth). In the baseline simulations, we examine the performance of the model in predicting the observed trends in house prices and migration flows over the evaluation sample. The model predicts the trends in state level house price-to-income ratios, output and population reasonably well. In addition, the model adequately captures the observed patterns of interstate migration flows.

To examine the size and speed of spatial spill-over effects, we compute spatiotemporal impulse responses of positive productivity and land-supply shocks to California, Texas and Florida in turn. A positive productivity shock in California raises local wages and induces net migration flows from other states to California. As a result, the population and house prices of all U.S. states except for California decrease. However, the responses of population and house prices tend to be stronger and quicker for states close to California than for the distant states. Similarly, the responses of U.S. states to a positive land-supply shock in California also have qualitatively similar spatiotemporal patterns. These results suggest, perhaps not surprisingly, that migration between states that are geographically close are more responsive to changes in wages and housing costs differentials. This is largely due to the fact that migration costs tend to increase with migration distance.

We obtain qualitatively similar results for Texas and Florida. However, the responses of Texas and Florida to local shocks are quantitatively different from those of California, due to the differences in land supply conditions across these states. For example, a positive productivity shock in Texas (where housing supplies are more elastic) induces more inward

[2]Ideally, we would have liked to estimate our model at MSA or even at county levels. But due to the highly non-linear nature of the model in which the dynamic interaction of location-to-location migration flows and regional housing markets are explicitly modelled, increasing the number of locations, N, will increase the computational burden significantly, by a factor N^2. There are also important data limitations to be overcome at the MSA level. Such an extension of our empirical analysis will be beyond the scope of the present paper.

migration flows and larger increases in housing stocks, while a positive productivity shock in California (where housing supplies are less elastic) translates into larger rises in house prices and less inward migration flows. In addition, a positive land-supply shock in California induces larger increases in housing supplies in California and more inward migration flows, while a positive land-supply shock in Texas has less impact on housing supplies in Texas and induces less inward migration flows. This is because new residential land is more scarce in California than in Texas, and thus a positive land-supply shock increases housing supplies more in California than in Texas.[3]

Finally, we investigate also how migration elasticity and housing depreciation rate can affect the spatiotemporal adjustment processes. Not surprisingly, when migration elasticity is larger, a regional shock tends to induce more population reallocation, and the spill-over effects are stronger, especially for the nearby states. We find also that when housing depreciation rate is low, housing stocks adjust slowly to changes in local housing demand and supply conditions, which slows down the migration flows (Glaeser and Gyourko (2005)).

1.1 Related literature

Our modelling approach is to be distinguished from Rosen-Roback style spatial equilibrium models, such as, Van Nieuwerburgh and Weill (2010), and from the dynamic population allocation models adopted in the studies on spatial labor allocations by Davis et al. (2021) and Herkenhoff et al. (2018), among others. These studies rely on static models of population allocation as an outcome of spatial sorting process under perfect population mobility, or consider a representative household that centrally allocates household members (population) across locations. In contrast, we extend the classical spatial equilibrium model of Rosen (1979) and Roback (1982) in a different direction by modeling explicitly the dynamics of location-to-location migration flows that function as a source of spatial spill-over effects. In addition, the tractability of the model allows us to analytically solve the model. Because of these features, the present model can be used to study the dynamic process of shock spill-over in regional economics through migration, which has not been dealt with in most existing Rosen-Roback style models. Furthermore, we explicitly model the dynamic process of housing depreciation and accumulation, which is a feature that most existing Rosen-Roback style models do not have. This feature allows us to capture the role of durable housing stock in slowing down population reallocation (Glaeser and Gyourko (2005)).

Our paper also sheds light on the effects of land-use regulation on regional house prices and spatial population allocation. Glaeser and Gyourko (2003), Glaeser et al. (2005), Quigley and Raphael (2005), Ihlanfeldt (2007) and Albouy and Ehrlich (2018) find that areas with faster than average growth in house prices tend to have more restrictions on residential land-use.[4] Recently, Hsieh and Moretti (2019) and Herkenhoff et al. (2018), go beyond the analysis of house prices and examine the impact of land-use regulations on spatial labor

[3] Our analyses of the differences between regional productivity and land-supply shocks are complementary to Notowidigdo (2020), who focuses on the asymmetric effects of positive and negative shocks on local population (especially for low-skill worker population), and to Monras (2018), who focuses on the different responses of in-migration and out-migration to shocks and the speed of convergence across locations.

[4] A number of studies also consider non-regulatory factors behind land supply availability. For example,

allocation and the national output.[5] Our empirical analysis is complementary to Herkenhoff et al. (2018), and following them we also adopt a macroeconomic approach and consider the impact of state-specific land-use regulation on spatial population allocation across U.S. states. However, while their study emphasizes the positive impacts of land-use deregulation in California on the national output through population reallocation, we investigate the spatiotemporal patterns of the population reallocation that results from land-use deregulation. As shown in our impulse response analyses, a positive land-supply shock to California lowers local housing costs and induces net migration inflows from other states to California, and reduces population and house prices in other U.S. states. However, the adjustment of population to the deregulation is slow and the population reallocation towards California is mostly from the nearby states. These results in turn suggest that the population reallocation from the deregulation in California can be mostly regional.

The rest of the paper is organized as follows: Section 2 sets out the migration module, and Section 3 specifies the rest of the model. Section 4 summarizes the set of equilibrium conditions and the model's solution. Section 5 proves the existence and the uniqueness of the equilibrium and the balanced growth path in the deterministic case. Section 6 estimates the model. Section 7 examines the performance of the model in predicting the observed trends in house price and migration over the evaluation sample. Section 8 presents the spatiotemporal analyses of productivity and land-supply shocks to California, Texas and Florida. Section 9 provides some sensitivity analyses to the choices of migration elasticity and the housing depreciation rate. Section 10 concludes. Mathematical derivations and data sources are provided in Appendix A. To save space, some of the simulation results and details of the computation of spatiotemporal impulse responses are provided in an online supplement.

2 A dynamic location-to-location migration model

Our theoretical framework consists of two modules: a migration module and a module for regional labor and housing markets. The migration module is a dynamic version of the residential choice model originally developed by McFadden (1978), in which the location-to-location migration choices of agents at the start of each period are explicitly modelled.[6] We begin with the migration module that forms the core of our analysis.

Saiz (2010) considers the impacts of geographical constraints on land supplies, and Kahn (2011) finds that liberal cities in California grant fewer new housing permits.

[5] In addition, Hilber and Robert-Nicoud (2013) and Parkhomenko (2016) study how regional housing supply regulations are endogenously determined in political processes, and Van Nieuwerburgh and Weill (2010) and Gyourko et al. (2013) attribute the increase in house price dispersion to spatial labor sorting.

[6] The McFadden location choice model has been used in a number of other areas in economics. Prominent recent examples include the studies by Artuc et al. (2010) and Caliendo et al. (2019) on trade and labor allocation choices.

2.1 Geography and migration flows

Time, denoted by t, is discrete and the horizon is infinite, so that $t = 0, 1, 2, ...$ There are n locations, and the collection of locations is represented by $\mathcal{I}_n = \{1, 2, ..., n\}$, where n is fixed but possibly large ($n \geq 2$). The economy is populated by workers who consume goods and housing services, and live for only one period. At the start of each period, workers decide whether to reside at locations where they are born, or migrate to a new location. Denote by $l_{ij}(t)$ the number of workers who are born at location i in period t, and choose to reside at location j, where i and $j \in \mathcal{I}_n$. Denote the population of workers born at location i at the start of period t by $l_{i\cdot}(t)$. Then

$$l_{i\cdot}(t) = \sum_{j=1}^{n} l_{ij}(t), \tag{1}$$

and the number of workers who choose to reside at location j in period t, denoted by $l_{\cdot j}(t)$, is given by

$$l_{\cdot j}(t) = \sum_{i=1}^{n} l_{ij}(t). \tag{2}$$

The number of workers who are born at location i at the start of period t equals to the number of workers who reside at that location in period $t-1$, plus an intrinsic exogenously given population change.[7] Denote the intrinsic rate of population change (growth rate if positive) of location i in period t by $g_{l,it}$. Thus, the number of workers born in location i at the start of period t is given by

$$l_{i\cdot}(t) = e^{g_{l,it}} l_{\cdot i}(t-1), \tag{3}$$

where it is assumed that $g_{l,it}$ follows an exogenously given deterministic process, for $i \in \mathcal{I}_n$, to be specified below.

We model migration probabilities as a Markov process. The probability that an individual worker born at location i chooses to reside at location j in period t is denoted by $\rho_{ij}(t)$, where $\rho_{ij}(t) \geqslant 0$ and $\sum_{j=1}^{n} \rho_{ij}(t) = 1$. Workers' location choices are assumed to be conditionally independent given the location-specific wage rates and housing service prices. Thus, according to the law of large numbers, the fraction of workers born in location i who choose to reside at location j converges to $\rho_{ij}(t)$ as population increases. We ignore any randomness due to finite population and assume the migration flow from location i to location j, $l_{ij}(t)$, is determined by

$$l_{ij}(t) = l_{i\cdot}(t)\rho_{ij}(t). \tag{4}$$

Thus, by combining (2), (3) and (4), we obtain

$$l_{\cdot j}(t) = \sum_{i=1}^{n} e^{g_{l,it}} l_{\cdot i}(t-1)\rho_{ij}(t), \quad \text{for } j = 1, 2, ..., n.$$

[7] The intrinsic population changes are made up of, for example, the net natural population increases (i.e. birth minus death) and the net migration flows from other countries.

The above system of equations can be re-written more compactly as

$$\boldsymbol{l}(t) = \boldsymbol{l}(t-1)\mathbf{G}(t)\mathbf{R}(t), \tag{5}$$

where $\boldsymbol{l}(t) \equiv [l_{\cdot 1}(t), l_{\cdot 2}(t), ..., l_{\cdot n}(t)]$ is the $1 \times n$ (row) vector of location-specific population, and $\mathbf{G}(t)$ is the $n \times n$ diagonal matrix of population growth rates and $\mathbf{R}(t)$ is the $n \times n$ Markovian migration probability matrix, defined by

$$\mathbf{G}(t) \equiv \begin{pmatrix} e^{g_{l,1t}} & 0 & \cdots & 0 \\ 0 & e^{g_{l,2t}} & \cdots & 0 \\ \vdots & \vdots & \ddots & \vdots \\ 0 & 0 & \cdots & e^{g_{l,nt}} \end{pmatrix}, \text{ and } \mathbf{R}(t) \equiv \begin{pmatrix} \rho_{11}(t) & \rho_{12}(t) & \cdots & \rho_{1n}(t) \\ \rho_{21}(t) & \rho_{22}(t) & \cdots & \rho_{2n}(t) \\ \vdots & \vdots & \ddots & \vdots \\ \rho_{n1}(t) & \rho_{n2}(t) & \cdots & \rho_{nn}(t) \end{pmatrix}.$$

In the standard Markov chain model of migration, transition matrix, $\mathbf{R}(t)$, is exogenously given. However, in our model, we allow $\mathbf{R}(t)$ to be time varying and endogenously determined. We consider the endogenous determination of $\mathbf{R}(t)$ in the following sections.

2.2 Location choice

At the start of each period, workers decide where to reside by maximizing their utilities in terms of consumption and housing services across all locations, and then choosing the location that gives them the highest level of utility. Consider an individual worker τ who is born at location i in period t, and considers moving to location $j \in \mathcal{I}_n$, where j could be i (namely not moving). We adopt a log-linear utility function and assume that if the worker decides to reside in location j, then her utility will be given by

$$u_{\tau,t,ij} = (1-\eta)\ln c_{\tau,t,ij} + \eta \ln s_{\tau,t,ij} - \ln \alpha_{ij} + \sigma_\varepsilon \varepsilon_{\tau,t,ij},$$

where $c_{\tau,t,ij}$ and $s_{\tau,t,ij}$ are her consumption of goods and housing services, respectively, η represents the relative preference for housing service to consumption goods with $\eta \in (0,1)$, $\ln \alpha_{ij}$ is the route-specific migration cost, $\varepsilon_{\tau,t,ij}$ represents the idiosyncratic component of worker's relative location preference over (i,j) location pair, and σ_ε is a strictly positive scaler constant. In our theoretical derivations we assume that the log migration cost from location i to j, $\ln \alpha_{ij}$, is given by

$$\ln \alpha_{ij} = (amenity_i - amenity_j) + rlc_{ij}, \tag{6}$$

where $amenity_i$ and $amenity_j$ denote the amenity levels at locations i and j, respectively, and rlc_{ij} is a route-specific relocation cost, with $rlc_{ij} = 0$ when $i = j$, and $rlc_{ij} > 0$ otherwise. rlc_{ij} is intended to capture factors such as distance, geographical, social and economic differences between locations i and j.[8] We also assume that $\varepsilon_{\tau,t,ij}$ is distributed independently of $c_{\tau,t,ij}$ and $s_{\tau,t,ij}$, and over time t. Also, following the literature on utility-based multiple choice decision problem, we shall assume that at each point in t, $\varepsilon_{\tau,t,ij}$ are independently

[8] In our empirical application we allow for trends in $\ln \alpha_{ij}$. See Section 6.1.2.

and identically distributed (IID) as extreme value distribution. (see, for example, McFadden (1978)).

Each worker inelastically supplies one unit of labor and allocate her wage income between consumption of goods and housing services. Denoting the wage rate and the price of housing services at location j in period t by w_{jt} and q_{jt} respectively, the budget constraint of the worker is given as

$$c_{\tau,t,ij} + q_{jt}s_{\tau,t,ij} = w_{jt}.$$

The utility maximization is done in two steps. First, the worker maximizes her utility in terms of consumption of goods and housing services across locations. Denote by $\tilde{u}_{\tau,t,ij}$ the maximized utility of worker τ if she chooses to reside at location j. It is given as

$$\tilde{u}_{\tau,t,ij} = u_{jt} - \ln \alpha_{ij} + \sigma_\varepsilon \varepsilon_{\tau,t,ij}, \tag{7}$$

where u_{jt} is the maximal utility a worker expects to get in location j, and is determined by

$$\begin{aligned} u_{jt} \equiv \max_{\{c_{\tau,t,ij},\, s_{\tau,t,ij}\}} & (1-\eta)\ln c_{\tau,t,ij} + \eta \ln s_{\tau,t,ij}, \\ s.t. \qquad & c_{\tau,t,ij} + q_{jt}s_{\tau,t,ij} = w_{jt}. \end{aligned} \tag{8}$$

By solving this optimization problem, we obtain:

$$c_{jt} = (1-\eta)w_{jt}, \tag{9}$$

$$s_{jt} = \frac{\eta w_{jt}}{q_{jt}}, \tag{10}$$

where the subscripts τ and i of $c_{\tau,t,ij}$ and $s_{\tau,t,ij}$ are dropped for convenience, since the optimal levels of consumption of goods and housing services of each worker only depend on j and t. Thus, the indirect utility function associated with location j can be obtained by substituting (9) and (10) into (8) to yield:

$$u_{jt} = u_0 + \ln w_{jt} - \eta \ln q_{jt}, \tag{11}$$

where $u_0 \equiv (1-\eta)\ln(1-\eta) + \eta \ln \eta$ is an scaler.

Second, the worker chooses the location with the highest utility. Using (7) and (11), the net utility gain of worker τ migrating to location j, denoted by $v_{\tau,t,ij}$, is given by

$$\begin{aligned} v_{\tau,t,ij} &= \tilde{u}_{\tau,t,ij} - \tilde{u}_{\tau,t,ii}, \\ &= (\ln w_{jt} - \ln w_{it}) - \eta\,(\ln q_{jt} - \ln q_{it}) + \sigma_\varepsilon\,(\varepsilon_{\tau,t,ij} - \varepsilon_{\tau,t,ii}) - \ln \alpha_{ij}. \end{aligned}$$

Given the realizations of $\{\varepsilon_{\tau,t,ij}\}_{j=1}^n$, the worker chooses the destination with the highest $v_{\tau,t,ij}$. Let $j^*_{\tau,t,i}$ denote the location chosen by the worker. Then,

$$j^*_{\tau,t,i} = arg\max_{j \in \mathcal{I}_n} \; v_{\tau,t,ij}.$$

Since by assumption $\varepsilon_{\tau,t,ij}$ is distributed as IID extreme value, it can be shown that the probability for the worker in location i to migrate to location j is given by (see Appendix A1.1 for a derivation)

$$\rho_{ij}(t) = \frac{\left[\left(w_{jt}/w_{it}\right)\left(q_{jt}/q_{it}\right)^{-\eta}/\alpha_{ij}\right]^{1/\sigma_\varepsilon}}{\sum_{s=1}^{n}\left[\left(w_{st}/w_{it}\right)\left(q_{st}/q_{it}\right)^{-\eta}/\alpha_{is}\right]^{1/\sigma_\varepsilon}}, \text{ for } i \text{ and } j \in \mathcal{I}_n. \tag{12}$$

Thus, $\rho_{ij}(t)$ is a function of wage rate differentials, w_{jt}/w_{it}, and housing cost differentials, q_{jt}/q_{it}.

3 Production and housing supplies

In this section, we focus on the module for regional labor and housing markets, and discuss how regional wage rates, housing service prices, house prices, and housing supplies endogenously respond to migration flows.

3.1 Production

We assume that location-specific wage rates are competitively determined in local labor markets, and allow for agglomeration effects in production. We further assume that the production of final goods is given by

$$y_{it} = \phi_{it}\left(a_{it}l_{\cdot i}(t)\right)^{v_l}, \tag{13}$$

where y_{it} is the output of final goods in location i in period t, $l_{\cdot i}(t)$ is the labor used in the production, a_{it} is the location-specific labor productivity, $v_l \in (0,1)$ is the share of labor costs in output, and ϕ_{it} stands for total factor productivity given by

$$\phi_{it} = \bar{\phi}_i y_{it}^{v_\phi}, \tag{14}$$

where $\bar{\phi}_i > 0$, and $v_\phi \in [0,1)$. It is assumed that total factor productivity, ϕ_{it}, increases with production scale, which captures agglomeration effects of production. Parameter v_ϕ governs the magnitude of agglomeration effects, with $v_\phi = 0$ corresponding to no agglomeration effect. The profit of the representative final goods producer at location i is given by

$$\pi_{it}^{y} = y_{it} - w_{it}l_{\cdot i}(t), \tag{15}$$

where w_{it} is the wage rate in location i. The representative final goods producer chooses $l_{\cdot i}(t)$ to maximize its profits (15) subject to (13), while taking ϕ_{it} as given. The first order condition for $l_{\cdot i}(t)$ is given by,

$$w_{it} = v_l\left(\frac{y_{it}}{l_{\cdot i}(t)}\right). \tag{16}$$

By substituting (13) and (14) into (16), we obtain the labor demand function:

$$w_{it} = \tau_{w,i}a_{it}^{\lambda_a}l_{\cdot i}(t)^{-\lambda_l}, \tag{17}$$

where $\tau_{w,i} \equiv \upsilon_l \bar{\phi}_i^{-1/(1-\upsilon_\phi)}$ is a location-specific scalar, and λ_a and λ_l are the elasticities of wage rate with respect to labor productivity and labor input respectively, which are defined by

$$\lambda_a \equiv \frac{\upsilon_l}{1-\upsilon_\phi}, \quad \text{and} \quad \lambda_l \equiv \frac{1-\upsilon_l-\upsilon_\phi}{1-\upsilon_\phi}. \tag{18}$$

To ensure that wage rates, w_{it}, decrease with labor inputs, $l_{\cdot i}(t)$, we assume $1-\upsilon_l-\upsilon_\phi > 0$, which in turn implies $1 > \lambda_l > 0$.[9] We further assume that final goods producers consume all the profits they earn in each period. Thus, $c_{it}^y = \pi_{it}^y$, where c_{it}^y denotes the consumption of final goods by producers at location i in period t.

We adopt a relatively general specification of a_{it} and assume that $\ln a_{it}$ comprises of a linear trend component, $\ln a_i + g_a t$, a national common (unobserved) component, f_t, and a local component $z_{a,it}$:

$$\ln a_{it} = \ln a_i + g_a t + \lambda_i f_t + z_{a,it}, \tag{19}$$

where g_a is the national growth rate of labor productivity, and λ_i is the location-specific coefficient on the national component, with $E(\lambda_i) > 0$. In addition, $z_{a,it}$ and f_t are assumed to follow first-order autoregressive (AR(1)) processes:

$$f_t = \rho_f f_{t-1} + \sigma_f \varepsilon_{f,t}, \tag{20}$$

$$z_{a,it} = \rho_{a,i} z_{a,i,t-1} + \sigma_{a,i} \varepsilon_{a,it}, \tag{21}$$

where $\varepsilon_{f,t}$ and $\varepsilon_{a,it}$ are IID across locations and over time.

3.2 Housing supplies

3.2.1 Housing rental markets

We assume that location-specific housing service prices are competitively determined in local rental markets. Suppose that each unit of existing houses provides a unit of housing services in each period, while new houses begin to provide housing services a period after they are built. Thus, the market clearing condition is given by

$$h_{i,t-1} = \left(\frac{\eta w_{it}}{q_{it}}\right) l_{\cdot i}(t), \tag{22}$$

where $h_{i,t-1}$ is the quantity of houses that are available for rent at location i in period t, $\eta w_{it}/q_{it}$ is the per capita consumption of housing services given by (10).

3.2.2 Construction of new houses

For determination of housing stocks, h_{it}, and house prices, p_{it}, we suppose that in each period t, a representative contractor is endowed with $\kappa_{it} > 0$ units of unused or reclaimed land in location i that can be used for new house construction. New houses are constructed

[9] It is easily seen that $\tau_{w,i} > 0$ and $\lambda_a > 0$, since $\bar{\phi}_i$ and $\upsilon_l > 0$, and $\upsilon_\phi \in [0, 1)$.

by combing residential land and final goods using a Cobb-Douglas technology. Denote the amount of new houses built at location i in period t by x_{it}, and note that

$$x_{it} = \tau_{x,i} \kappa_{it}^{\vartheta_{\kappa,i}} m_{it}^{1-\vartheta_{\kappa,i}}, \tag{23}$$

where $\tau_{x,i} > 0$ is a scalar constant, $\vartheta_{\kappa,i} \in (0,1)$ is the share of land in house value, and m_{it} is the amount of final goods used for investments in residential structures at location i. Contractors are assumed to be homogeneous and operate competitively across locations. The profit of the representative contractor in period t, denoted by π_t^c, is given as

$$\pi_t^c = \sum_{i=1}^{n} p_{it} x_{it} - m_{it}.$$

The contractor chooses $\{x_{it}, m_{it}\}_{i=1}^n$ to maximize her profits subject to house construction technology, (23), while taking the new land supplies, κ_{it}, as given. By solving the contractor's optimization problem, we obtain the supply function for new houses

$$x_{it} = \tau_{\kappa,i} \kappa_{it} p_{it}^{\lambda_{p,i}}, \tag{24}$$

where $\tau_{\kappa,i} \equiv \tau_{x,i}^{1+\lambda_{p,i}} (1-\vartheta_{\kappa,i})^{\lambda_{p,i}}$ is the location-specific scalar, and $\lambda_{p,i}$ is the elasticity of the new housing supply with respect to the house price, defined by

$$\lambda_{p,i} \equiv \frac{1-\vartheta_{\kappa,i}}{\vartheta_{\kappa,i}} \quad . \tag{25}$$

We assume that contractors consume all the profits they earn in each period. Thus, $c_t^c = \pi_t^c$, where c_t^c denotes the consumption of contractors in period t. Finally, we assume

$$\ln \kappa_{it} = \ln \kappa_i + g_{\kappa,i} t + z_{\kappa,it} \tag{26}$$

where $g_{\kappa,i}$ is the trend growth rate of new land supplies, and $z_{\kappa,it}$ is the state-specific land-supply shock assumed to follow the AR(1) process:

$$z_{\kappa,it} = \rho_{\kappa,i} z_{\kappa,i,t-1} + \sigma_{\kappa,i} \varepsilon_{\kappa,it}, \tag{27}$$

where $\varepsilon_{\kappa,it}$ are IID across locations and over time.

3.2.3 Housing accumulation process

It is assumed that housing stock depreciates at rate $\delta \in (0,1)$ in all locations. Let $h_{i,t-1}$ be the quantity of housing stock in location i at the end of period $t-1$, which is carried over to period t. In period t, after depreciation the housing stock is given by $(1-\delta)h_{i,t-1}$, which is then augmented with x_{it} units of new houses constructed during period t. Thus, the total stock of housing in location i at the end of period t is given by

$$h_{it} = (1-\delta) h_{i,t-1} + x_{it}. \tag{28}$$

In addition, homogeneous landlords own local housing stocks and rent them to workers, and derive utility from consuming their profits. The population of landlords in location i, denoted by l_{it}^o, grows over time at the common rate of g_l, where $g_l > 0$. Thus, $l_{it}^o = e^{g_l t} l_{i0}^o$, where $l_{i0}^o > 0$ is the initial population of landlords in location i. The life time utility of landlords (as a group) in location i is given by

$$E_t \sum_{s=0}^{\infty} (\beta e^{g_l})^s \ln(c_{i,t+s}^o), \tag{29}$$

where c_{it}^o is the consumption of the 'representative' landlord in location i, and $\beta e^{g_l} \in (0,1)$ is the adjusted discount factor that allows for the growing number of landlords. The realized net return on housing investment in location i in period t, denoted by r_{it}^o, is given by

$$r_{it}^o = (1-\theta_i)\left[\frac{q_{it} + (1-\delta)p_{it}}{p_{i,t-1}}\right], \tag{30}$$

where $\theta_i \in (0,1)$ is the location-specific cost of housing investment. The landlords' budget constraint is then given by

$$c_{it}^o l_{it}^o + p_{it} h_{it} = r_{it}^o \left(p_{i,t-1} h_{i,t-1}\right). \tag{31}$$

Landlords maximize (29) subject to (31). The Euler condition for this optimization is given by

$$E_t\left(\Lambda_{i,t+1} r_{i,t+1}^o\right) = 1, \tag{32}$$

where $\Lambda_{i,t+1}$ is the stochastic discount factor, defined by $\Lambda_{i,t+1} = \beta\left(c_{it}^o / c_{i,t+1}^o\right)$. Pre-multiplying both sides of (32) by p_{it}, and using (30), we can write the house price, p_{it}, as the sum of the expected present value of rents net of depreciation:

$$p_{it} = \sum_{s=1}^{\infty} E_t\left[(1-\delta)^{s-1}(1-\theta_i)^s \left(\prod_{\upsilon=1}^{s} \Lambda_{i,t+\upsilon}\right) q_{i,t+s}\right].$$

Since the utility function of landlords is assumed to be logarithmic, a closed form solution for landlords' optimization problem exists. The optimal rules for housing investment and consumption are given by

$$p_{it} h_{it} = \beta e^{g_l}(1-\theta_i)\left[q_{it} + (1-\delta)p_{it}\right] h_{i,t-1}, \tag{33}$$

and

$$c_{it}^o l_{it}^o = \left(1 - \beta e^{g_l}\right)(1-\theta_i)\left[q_{it} + (1-\delta)p_{it}\right] h_{i,t-1}.$$

4 Model solution

We first summarize the set of equilibrium conditions by which the key variables are determined. We use bold lowercase letters with only time subscripts to denote the vectors of

prices and quantities for all locations. For example, $\boldsymbol{p}_t \equiv [p_{1t}, p_{2t}, ..., p_{nt}]$, which is a $1 \times n$ vector. We focus only on the key variables that are related to migration and local housing markets, including $\boldsymbol{p}_t, \boldsymbol{q}_t, \boldsymbol{w}_t, \boldsymbol{x}_t, \boldsymbol{h}_t, \boldsymbol{l}(t)$ and $\mathbf{R}(t)$, and the subset of equilibrium conditions by which they are determined, which can be categorized into two groups:

- **Migration.** The first block of equilibrium conditions correspond to the migration module set up in Section 2**,** and describe how migration probabilities, $\mathbf{R}(t)$, and local population values, $\boldsymbol{l}(t)$, are determined, given wage rates, $\boldsymbol{w}_t$, and housing service prices, $\boldsymbol{q}_t$, which include (5) and (12).

- **Regional labor and housing markets**. The second block of equilibrium conditions correspond to the module for regional labor and housing markets set up in Section 3**,** and describe how wage rates, $\boldsymbol{w}_t$, housing service prices, $\boldsymbol{q}_t$, house prices, $\boldsymbol{p}_t$, and housing supplies, $\boldsymbol{h}_t$, are determined given local population, $\boldsymbol{l}(t)$, which include (17), (22), (24), (28) and (33), for $i \in \mathcal{I}_n$.

As shown in equations (5) and (12), the agent's optimal location choice and the resultant migration process is Markovian, where the transition probabilities across all location pairs, $\rho_{ij}(t)$, are functions of wage and housing cost differentials, i.e., w_{jt}/w_{it} and q_{jt}/q_{it}. In turn, wage rates, $\boldsymbol{w}_t$, housing service prices, $\boldsymbol{q}_t$, house prices, $\boldsymbol{p}_t$, and housing supplies, $\boldsymbol{h}_t$, endogenously respond to migration flows according to (17), (22), (24), (28) and (33).

It is now clear that for given values of the exogenous variables, $\boldsymbol{a}_t, \boldsymbol{\kappa}_t$, and $\boldsymbol{g}_{l,t}$, and the initial values for local population and housing stocks, $\boldsymbol{l}_{t-1}$ and $\boldsymbol{h}_{t-1}$, prices, $\boldsymbol{p}_t, \boldsymbol{q}_t$, and $\boldsymbol{w}_t$, and allocations, $\mathbf{R}(t), \boldsymbol{l}(t), \boldsymbol{x}_t$,and $\boldsymbol{h}_t$, can be solved for by using equations (5), (12), (17), (22), (24), (28) and (33). In addition, as shown in Appendix A1.2, these equations can be written compactly as:

$$\boldsymbol{\zeta}_t = \boldsymbol{f}\left(\boldsymbol{\zeta}_{t-1}, \boldsymbol{a}_t, \boldsymbol{a}_{t-1}, \boldsymbol{\kappa}_{t-1}, \boldsymbol{g}_{l,t}; \Theta\right), \tag{34}$$

$$\boldsymbol{\chi}_t = \boldsymbol{g}\left(\boldsymbol{\zeta}_t, \boldsymbol{a}_t, \boldsymbol{\kappa}_t; \Theta\right), \tag{35}$$

where Θ is a row vector that contains all the parameters, $\boldsymbol{\zeta}_t = [\boldsymbol{l}(t), \boldsymbol{q}_t]$ is a $1 \times 2n$ vector, and $\boldsymbol{\chi}_t = [\boldsymbol{p}_t, \boldsymbol{h}_t]$ is a $1 \times 2n$ vector. The stochastic processes of $\boldsymbol{a}_t$ are given by

$$\ln \boldsymbol{a}_t = \ln \boldsymbol{a} + \boldsymbol{g}_a t + \boldsymbol{\lambda} f_t + \boldsymbol{z}_{a,t}, \tag{36}$$

$$f_t = \rho_f f_{t-1} + \sigma_f \varepsilon_{f,t}, \tag{37}$$

$$\boldsymbol{z}_{a,t} = \boldsymbol{z}_{a,t-1}\mathbf{diag}(\rho_{a,1}, \rho_{a,2}, ...\rho_{a,n}) + \boldsymbol{\varepsilon}_{a,t}\mathbf{diag}(\sigma_{a,1}, \sigma_{a,2}, ...\sigma_{a,n}), \tag{38}$$

and the stochastic processes of $\boldsymbol{\kappa}_t$ are given by

$$\ln \boldsymbol{\kappa}_t = \ln \boldsymbol{\kappa} + \boldsymbol{g}_\kappa t + \boldsymbol{z}_{\kappa,t}, \tag{39}$$

$$\boldsymbol{z}_{\kappa,t} = \boldsymbol{z}_{\kappa,t-1}\mathbf{diag}(\rho_{\kappa,1}, \rho_{\kappa,2}, ...\rho_{\kappa,n}) + \boldsymbol{\varepsilon}_{\kappa,t}\mathbf{diag}(\sigma_{\kappa,1}, \sigma_{\kappa,2}, ...\sigma_{\kappa,n}). \tag{40}$$

and the values of $\boldsymbol{g}_{l,t}$, for $t = 1, 2, ...$, are exogenously given.

5 The balanced growth path

We now consider the *non-stochastic* version of the model economy set out in Sections 2 and 3, characterize its short-run and long-run equilibria and prove the existence and uniqueness of the short-run equilibrium and the balanced growth path. The non-stochastic specification is obtained by setting to zero the innovations to the national and location-specific components of labor productivities ($\varepsilon_{f,t}$ and $\varepsilon_{a,it}$ in (20) and (21)), and the innovations to the location-specific land-supply shocks ($\varepsilon_{\kappa,it}$ in (27)), namely $\varepsilon_{f,t} = 0$, $\varepsilon_{a,it} = 0$, and $\varepsilon_{\kappa,it} = 0$, for $i = 1, 2, ...n$, and $t = 1, 2, ...$ In this set up, local productivities are given by

$$a_{it} = e^{g_a t} a_i, \text{ for } i = 1, 2, ...n, \text{ and } t = 1, 2, ... \tag{41}$$

In addition, to obtain a balanced growth path we assume the same intrinsic population growth rate, g_l, across locations:

$$g_{l,it} = g_l, \text{ for } i = 1, 2, ...n, \text{ and } t = 1, 2, ... \tag{42}$$

Finally, we assume that the location-specific land supplies are given by

$$\kappa_{it} = e^{g^*_{\kappa,i} t} \kappa_i, \text{ for } i = 1, 2, ...n, \text{ and } t = 1, 2, ..., \tag{43}$$

where $g^*_{\kappa,i}$ is the state-specific land supply growth rate. On the balanced growth path, prices $\boldsymbol{p}_t, \boldsymbol{q}_t, \boldsymbol{w}_t$ (quantities $\boldsymbol{l}(t), \boldsymbol{x}_t, \boldsymbol{h}_t$) should grow at a common rate as $t \to \infty$. To find conditions under which the economy has a balanced growth path, using (24) we note that

$$\ln\left(\frac{x_{it}}{x_{i,t-1}}\right) = \ln\left(\frac{\kappa_{it}}{\kappa_{i,t-1}}\right) + \lambda_{p,i} \ln\left(\frac{p_{it}}{p_{i,t-1}}\right).$$

Note also that on the balanced growth path by definition we have $\ln(x_{it}/x_{i,t-1}) = g_l$, $\ln(\kappa_{it}/\kappa_{i,t-1}) = g^*_{\kappa,i}$, and $\ln(p_{it}/p_{i,t-1}) = g_w$, where g_w is the wage growth rate, and (17) implies $g_w = \lambda_a g_a - \lambda_l g_l$. Hence, for a balanced growth path to exist we must have

$$g^*_{\kappa,i} = (1 + \lambda_{p,i}\lambda_l) g_l - \lambda_{p,i}\lambda_a g_a, \text{ for } i = 1, 2, ..., n. \tag{44}$$

The above condition states that the growth rate of new land supplies, $g^*_{\kappa,i}$, and the growth of productivity for production of residential structures, g_a, should ensure that enough new houses can be produced to accommodate the housing requirements of the growing population in all locations. The land supply regime under which land growth rates are given by (44) will be referred to as the *balanced growth path land supply regime*. The analysis of the equilibrium properties of the stochastic version of the model is complicated, and will be conducted by simulations. The deterministic solution provides information on the local equilibrating properties of the stochastic version for sufficiently small-size shocks.

We use letters with stars and time subscripts to denote the corresponding detrended variables. Specifically, $w^*_{it} \equiv e^{-g_w t} w_{it}$, $\boldsymbol{w}^*_t \equiv [w^*_{1t}, w^*_{2t}, ..., w^*_{nt}]$, $p^*_{it} \equiv e^{-g_w t} p_{it}$, $\boldsymbol{p}^*_t \equiv [p^*_{1t}, p^*_{2t}, ..., p^*_{nt}]$, $h^*_{it} \equiv e^{-g_l t} h_{it}$, and $\boldsymbol{h}^*_t \equiv [h^*_{1t}, h^*_{2t}, ..., h^*_{nt}]$. We denote the detrended aggregate population by

$L_t^* \equiv \sum_{i=1}^n l_{.i}^*(t)$. Note that the detrended exogenous variables are time invariant by construction (see (41)-(43)). For example, $a_{it}^* = a_i$ and $\kappa_{it}^* = \kappa_i$. Hence equilibrium conditions (5), (12), (17), (22), (24), (28) and (33) can be re-written in terms of the detrended variables as (A.9)-(A.15) in Appendix A1.3. Then the short-run and the balanced growth path equilibria of the economy can be defined in terms of detrended variables as follows:

Definition 1 ***(Short-run equilibrium)*** *Consider the dynamic spatial equilibrium model set up in Sections 2 and 3 by equations (5), (12), (17), (22), (24), (28) and (33), which can be written equivalently in terms of detrended variables by equations (A.9) to (A.15) in Appendix A1.3. Suppose that the vectors of exogenous processes for labor productivities, $\boldsymbol{a}_t$, land supplies, $\boldsymbol{\kappa}_t$, and the intrinsic population growth rates, $\boldsymbol{g}_{lt}$, for $t = 1, 2, ...$, are given by (41)-(43), condition (44) holds, and the initial values for local population and housing stocks ($\boldsymbol{l}_0$ and $\boldsymbol{h}_0$) are strictly positive. Then, a short-run equilibrium is defined as series of non-negative prices $[\boldsymbol{p}_t^*, \boldsymbol{q}_t^*, \boldsymbol{w}_t^*]$ and allocations $[\boldsymbol{l}^*(t), \boldsymbol{x}_t^*, \boldsymbol{h}_t^*]$ that solve the system of equations (A.9)-(A.15) in Appendix A1.3, for given values $l_{.i}^*(t-1)$ and $h_{i,t-1}^*$, for $i \in \mathcal{I}_n$.*

Definition 2 ***(Balanced growth path equilibrium)*** *Consider the dynamic spatial equilibrium model set up in Sections 2 and 3 by equations (5), (12), (17), (22), (24), (28) and (33), which can be written equivalently in terms of detrended variables by equations (A.9) to (A.15) in Appendix A1.3. Suppose that the vectors of exogenous processes for labor productivities, $\boldsymbol{a}_t$, land supplies, $\boldsymbol{\kappa}_t$, and the intrinsic population growth rates, $\boldsymbol{g}_{lt}$, for $t = 1, 2, ...$, are given by (41)-(43), condition (44) holds, and the initial values for local population and housing stocks ($\boldsymbol{l}_0$ and $\boldsymbol{h}_0$) are strictly positive. Then, a balanced growth path equilibrium is defined as a path on which the economy is in short-run equilibrium in the sense set out in Definition 1 in each period, and the de-trended prices $[\boldsymbol{p}_t^*, \boldsymbol{q}_t^*, \boldsymbol{w}_t^*]$ and quantities $[\boldsymbol{l}^*(t), \boldsymbol{x}_t^*, \boldsymbol{h}_t^*]$ converge to non-negative limits as $t \to \infty$.*

The existence and uniqueness of the short-run equilibrium is established in Appendix A1.5. In what follows we focus on the existence and uniqueness of the long-run balanced growth path which plays a more fundamental role in our simulation exercises.

Proposition 1 ***(Existence and uniqueness of the long-run balanced growth path)*** *Consider the dynamic spatial equilibrium model set up in Sections 2 and 3 by equations (5), (12), (17), (22), (24), (28) and (33), which can be written equivalently in terms of detrended variables by equations (A.9) to (A.15) in Appendix A1.3. Suppose that the vectors of exogenous processes for labor productivities, $\boldsymbol{a}_t$, land supplies, $\boldsymbol{\kappa}_t$, and intrinsic population growth rates, $\boldsymbol{g}_{lt}$, for $t = 1, 2, ...$, are given by (41)-(43), and condition (44) holds, and the initial values for local population and housing stocks ($\boldsymbol{l}_0$ and $\boldsymbol{h}_0$) are strictly positive. Then the model has a unique balanced growth path as set out in Definition 2.*

Proof: By post-multiplying both sides of (A.9) by $\boldsymbol{\tau}$, an $n \times 1$ vector of ones, we have

$$L_t^* = \boldsymbol{l}^*(t)\boldsymbol{\tau} = \boldsymbol{l}^*(t-1)\mathbf{R}^*(t)\boldsymbol{\tau} = \boldsymbol{l}^*(t-1)\boldsymbol{\tau} = L_{t-1}^*,$$

which implies

$$L_t^* = L_{t-1}^*, ..., = L_1^* = L_0, \tag{45}$$

where L_0 is the detrended total population for $t = 0, 1, ...$ Using (A.9), $\boldsymbol{l}^*(t)$ can be written as

$$\boldsymbol{l}^*(t) = \boldsymbol{l}(0) \left[\Pi_{s=1}^{t} \mathbf{R}^*(s)\right], \tag{46}$$

where $\boldsymbol{l}(0) > 0$ is the vector of the initial local populations, and $\mathbf{R}^*(1), \mathbf{R}^*(2), ..., \mathbf{R}^*(t)$, are a series of stochastic matrices. Lemma A1 in Appendix A1.6 establishes the existence of the balanced growth path by showing that $\boldsymbol{l}^*(t)$ converges to some time invariant non-negative population vector $\boldsymbol{l}^*$, as $t \to \infty$.

We use letters with only stars to denote the steady states of the corresponding detrended variables. To establish that $\boldsymbol{l}^*$ is unique, we first note that (45) implies

$$\sum_{i=1}^{n} l_{.i}^* = L_0. \tag{47}$$

By imposing the balance growth path conditions, the equilibrium conditions (A.9) to (A.15) can be written as follows

$$\boldsymbol{l}^* = \boldsymbol{l}^* \mathbf{R}^*, \tag{48}$$

where $\mathbf{R}^* \equiv \left(\rho_{ij}^*\right)$ is the $n \times n$ matrix of migration probabilities, and

$$\rho_{ij}^* = \frac{(w_j^*/w_i^*)^{1/\sigma_\varepsilon} (q_j^*/q_i^*)^{-\eta/\sigma_\varepsilon} (\alpha_{ij})^{-1/\sigma_\varepsilon}}{\sum_{s=1}^{n} (w_s^*/w_i^*)^{1/\sigma_\varepsilon} (q_s^*/q_i^*)^{-\eta/\sigma_\varepsilon} (\alpha_{is})^{-1/\sigma_\varepsilon}}, \text{ for } i \text{ and } j \in \mathcal{I}_n, \tag{49}$$

and

$$w_i^* = \tau_{w,i} a_i^{\lambda_a} \left(l_{.i}^*\right)^{-\lambda_l}, \text{ for } i \in \mathcal{I}_n, \tag{50}$$

$$h_i^* = \left(\eta w_i^*/q_i^*\right) l_{.i}^*, \text{ for } i \in \mathcal{I}_n, \tag{51}$$

$$x_i^* = \tau_{\kappa,i} \kappa_i (p_i^*)^{\lambda_{p,i}}, \text{ for } i \in \mathcal{I}_n \tag{52}$$

$$h_i^* = \left[1 - (1-\delta) e^{-g_l}\right]^{-1} x_i^*, \text{ for } i \in \mathcal{I}_n, \tag{53}$$

$$p_i^* = \beta (1 - \theta_i) \left[q_i^* + (1-\delta) p_i^*\right], \text{ for } i \in \mathcal{I}_n, \tag{54}$$

Thus, to prove the uniqueness of the balanced growth path, in what follows we show that the system of equations given by (47)-(54), has a *unique positive* solution. In the rest of the proof, we show that given L_0, $\boldsymbol{a}$ and $\boldsymbol{\kappa}$, then $\boldsymbol{w}^*, \boldsymbol{p}^*, \boldsymbol{q}^*, \boldsymbol{x}^*, \boldsymbol{h}^*, \boldsymbol{l}^*$ and $\mathbf{R}^*$ are uniquely determined.

We first show that for given values of $\boldsymbol{l}^*$, $\boldsymbol{a}$ and $\boldsymbol{\kappa}$, the solution for $\boldsymbol{w}^*, \boldsymbol{p}^*, \boldsymbol{q}^*, \boldsymbol{x}^*$ and $\boldsymbol{h}^*$ is unique and can be obtained using (50)-(54), and then ρ_{ij}^* can be written as a function of $\boldsymbol{l}^*$ as

$$\rho_{ij}^* = \frac{\psi_{ij} \left(l_{.j}^*\right)^{-\varphi_j}}{\sum_{s=1}^{n} \psi_{is} \left(l_{.s}^*\right)^{-\varphi_s}}, \tag{55}$$

where φ_j and ψ_{ij} are positive constants. See the detailed derivation of the above equation in Appendix A1.4. Recall that $\mathbf{R}^*$ is the migration probability matrix on the balanced growth path, with a typical element ρ_{ij}^* given by (49). Thus, $\mathbf{R}^*$ can be written as a function of $\boldsymbol{l}^*$, namely $\mathbf{R}^* \equiv \mathbf{R}(\boldsymbol{l}^*)$. Then, (48) can be written as

$$\boldsymbol{l}^* = \boldsymbol{l}^* \mathbf{R}(\boldsymbol{l}^*), \tag{56}$$

which is a system of non-linear equations in $\boldsymbol{l}^*$. Lemma A1 in Appendix A1.6 establishes that there exists a $\boldsymbol{l}^*$ that solves (56), and Lemma A2 establishes that (56) cannot have more than one solution. Therefore, $\boldsymbol{l}^*$ exists and is unique. Then, using the solution of $\boldsymbol{l}^*$, the other variables of the model, namely, $\boldsymbol{w}^*, \boldsymbol{p}^*, \boldsymbol{q}^*, \boldsymbol{x}^*, \boldsymbol{h}^*$and $\mathbf{R}^*$, can be solved for using equations (50) and (A.20)-(A.24) in Appendix A1.4.■

6 Estimation and calibration of the model

Parameters of the model are estimated, as far as possible, using panel data on 48 mainland U.S. states plus the District of Columbia, a total of $n = 49$ locations or states.[10] To avoid over-fitting, the parameters are estimated using the subset of available data on interstate migration flows and housing markets over the period 1976-1999 (training sample). The year indexed by 0 (i.e., the initial period) corresponds to 1976, and the subsequent periods indexed by $1, 2, ..., T_1$ correspond to the years 1977 to 1999 (inclusive). Out-of-sample simulations are carried out over the period 2000-2014 (evaluation sample) in Section 7, with the periods indexed by $T_1 + 1, T_1 + 2, ..., T$ corresponding to the years 2000 to 2014.

The model parameters can be divided into three groups; namely the parameters that characterize migration flows, housing supplies and the exogenous processes. In what follows, we consider these three sets of parameters in turn. Table A3 of Appendix A3.4 gives a summary of the key parameters.

6.1 Estimation of the migration module

We start by presenting some important facts about state-to-state migration in the U.S. in Section 6.1.1, and in Section 6.1.2, we estimate the migration costs that are the key parameters in our model.

6.1.1 Facts about state-to-state migration in the U.S.

Before estimating route-specific migration cost parameters, α_{ij}, we first consider how the scale of migration varies with the distance between origin and destination states. Population and migration flows are measured using annual data from the Internal Revenue Service (IRS).[11] The distance between two states is measured as the distance between their centers of population that are defined by Census.[12] Note that the gross migration flow between states i and j in period t is $l_{ij}(t) + l_{ji}(t)$, and recall that $l_{.i}(t)$ and $l_{.j}(t)$ are the population of states i and j in period t, respectively. Thus, $(1/10)\sum_{t_{1990}}^{t_{1999}} [l_{ij}(t) + l_{ji}(t)]$ is the average annual gross migration flow between states i and j, and $(1/10)\sum_{t_{1990}}^{t_{1999}} [l_{.i}(t) + l_{.j}(t)]$ is their

[10] Data sources for estimation and calibration are described in Appendix A2.

[11] For further details, see Appendix A2.1.

[12] For further details about the definitions of population centers, see `https://www.census.gov`.

average population. The average rate of migration between states i and j over the 1990-1999 period, denoted by $\hat{\pi}_{ij}$, is given by[13]

$$\hat{\pi}_{ij} = \frac{\sum_{t_{1990}}^{t_{1999}} [l_{ij}(t) + l_{ji}(t)]}{\sum_{t_{1990}}^{t_{1999}} [l_{.i}(t) + l_{.j}(t)]}. \tag{57}$$

Figure 1 plots $\ln \hat{\pi}_{ij}$ against the migration distance, d_{ij}, measured as the geographical distance between states i and j. Each dot represents a pair of migration distance and migration scale, $(d_{ij}, \ln \hat{\pi}_{ij})$, for location pair (i, j). As the figure shows, $\ln \hat{\pi}_{ij}$ decreases with migration distance, d_{ij}, indicating that migration cost tends to increase with the distance between origin and destination states.

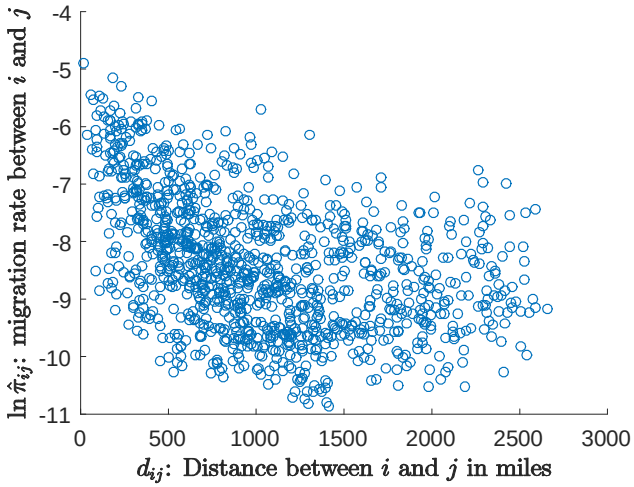

Figure 1: Patterns of migration and geographical distance

Notes: This figure plots $\ln \hat{\pi}_{ij}$ against d_{ij}, where $\hat{\pi}_{ij}$ is defined by (57) and refers to the average annual gross migration flow between States i and j relative to their population, and d_{ij} refers to the geographical distance between States i and j.

6.1.2 Estimation of migration costs

Recall that in the model set out in Sections 2 and 3, migration costs, $\ln \alpha_{ij}$, are the sum of relocation costs, rlc_{ij}, which are intended to capture route-specific factors such as migration distance, and amenity differentials, $amenity_i - amenity_j$ (see (6)). To capture the persistent decline in internal migration in the U.S. since 1980s, we allow for a national time trend, reflecting the general rise in migration costs due to common factors such as population aging (Karahan and Rhee (2014)) and increasing labor market frictions (Davis et al. (2010) and

[13]It makes little difference if we compute the average rate of migration by averaging the annual migration rates over the period 1990-1999.

Fujita (2018)). Accordingly, in our empirical analysis we use the more general specification

$$\ln \alpha_{ij,t} = c_\alpha + g_\alpha t + (amenity_i - amenity_j) + rlc_{ij}, \tag{58}$$

$$for\ i \neq j, \text{and } i \text{ and } j \in \mathcal{I}_n,$$

where c_α is a constant, $g_\alpha t$ is the national time trend in migration costs, $amenity_i$ is an average index of amenity for state i, rlc_{ij} is the relocation cost between states i and j. As before, we normalize $\alpha_{ii,t}$ to one, for $i \in \mathcal{I}_n$ and $t = 0, 1, ...$ Let $\lambda_{\alpha,ij}$ denote the route-specific component in migration cost (i.e., the sum of amenity differential and route-specific relocation cost), and note that

$$\lambda_{\alpha,ij} = (amenity_i - amenity_j) + rlc_{ij}. \tag{59}$$

To identify $\lambda_{\alpha,ij}$, using (59) in (58) we first note that

$$\ln \alpha_{ij,t} = c_\alpha + g_\alpha t + \lambda_{\alpha,ij}, \quad \text{for } i \neq j. \tag{60}$$

Also using (4) we have

$$\frac{\rho_{ij}(t)}{\rho_{ii}(t)} = \frac{l_{ij}(t)}{l_{i.}(t)} \frac{l_{i.}(t)}{l_{ii}(t)} = \frac{l_{ij}(t)}{l_{ii}(t)}. \tag{61}$$

Since by construction $\alpha_{ii,t} = 1$, then (12) implies

$$\begin{aligned} \frac{\rho_{ij}(t)}{\rho_{ii}(t)} &= \left(\frac{w_{jt} q_{jt}^{-\eta} / \alpha_{ij,t}}{w_{it} q_{it}^{-\eta} / \alpha_{ii,t}} \right)^{1/\sigma_\varepsilon}, \Rightarrow \\ \ln \left(\frac{\rho_{ij}(t)}{\rho_{ii}(t)} \right) &= \frac{1}{\sigma_\varepsilon} \ln \left(\frac{w_{jt} q_{jt}^{-\eta}}{w_{it} q_{it}^{-\eta}} \right) - \frac{1}{\sigma_\varepsilon} \ln \left(\alpha_{ij,t} \right). \end{aligned} \tag{62}$$

Using (61) and (60) in the above now yields

$$\ln \left(\frac{l_{ij}(t)}{l_{ii}(t)} \right) = \frac{1}{\sigma_\varepsilon} \ln \left(\frac{w_{jt} q_{jt}^{-\eta}}{w_{it} q_{it}^{-\eta}} \right) - \frac{1}{\sigma_\varepsilon} c_\alpha - \frac{1}{\sigma_\varepsilon} g_\alpha t - \frac{1}{\sigma_\varepsilon} \lambda_{\alpha,ij}, \tag{63}$$

$$for\ i \neq j, \text{and } i \text{ and } j \in \mathcal{I}_n.$$

Note that the relative weight of housing in workers' utility function (8), η, is set to 0.24, as estimated by Davis and Ortalo-Magné (2011).[14] Also data on w_{it} are inferred using (16), and q_{it} and $l_{ij}(t)$ are directly observed data.[15] Thus, to estimate $1/\sigma_\varepsilon$, c_α, g_α and $\lambda_{\alpha,ij}$, we run a least square regression of $\ln(l_{ij}(t)/l_{ii}(t))$ on $\ln(w_{jt} q_{jt}^{-\eta} / w_{it} q_{it}^{-\eta})$, with a linear time trend and

[14] These authors also provide evidence that the shares of expenditure on housing are constant over time and across U.S. MSAs.

[15] For further details, see Sections A2.1, A2.2 and A2.3 of Appendix A.

fixed effects to allow for route (i, j) specific fixed costs and a constant.[16] Then, to decompose $\hat{\lambda}_{\alpha,ij}$ into amenity differentials and relocation costs (see (59)), we estimate

$$\hat{\lambda}_{\alpha,ij} = c_\lambda + \boldsymbol{\beta}'_{\mathbf{d}}\mathbf{dis}_{ij} + \boldsymbol{\beta}'_{\mathbf{a}}\left(\mathbf{am}_i - \mathbf{am}_j\right) + \xi_{\lambda,ij}, \tag{64}$$

where c_λ is a constant, $\mathbf{dis}_{ij}$ is a vector of distance measures (geography and climate) between states i and j, $\mathbf{am}_i$ is a vector of amenities for state i, and $\xi_{\lambda,ij}$ is the error term that captures the unobserved attributes of location pair (i, j).[17] Then, the amenity index, $amenity_i$, for state i is defined as a linear combination of different measures of amenities:

$$amenity_i = \boldsymbol{\beta}'_{\mathbf{a}}\mathbf{am}_i, \text{ for } i \in \mathcal{I}_n, \tag{65}$$

and the relocation cost is given in terms of distance measures as

$$rlc_{ij} = c_\lambda + \boldsymbol{\beta}'_{\mathbf{d}}\mathbf{dis}_{ij} + \xi_{\lambda,ij}, \text{ for } i \neq j, \text{and } i \text{ and } j \in \mathcal{I}_n. \tag{66}$$

Migration costs over the training sample (1990-1999). Since the Internal Revenue Service (IRS) migration flow data that we use are only available from 1990 onward, we use data over the period 1990-1999 for estimation.[18] Note that $1/\sigma_\varepsilon$ is the elasticity of $\rho_{ij}(t)/\rho_{ii}(t)$, with respect to the income ratio w_{jt}/w_{it} (see (62)). Our estimate of $1/\sigma_\varepsilon$ is 0.812 (with a standard error of 0.051), which is broadly in agreement with the estimates reported in Moretti and Wilson (2017).[19] Figure 2 displays the scatter plot of the estimated route-specific costs, $\hat{\lambda}_{\alpha,ij}$, with $i \neq j$, against migration distance, d_{ij}. As can be seen, $\hat{\lambda}_{\alpha,ij}$ is an increasing concave function of migration distance, d_{ij}. This may be due to the fact that areas that are geographically close to each other tend to share more similarities in terms of natural and cultural conditions. In addition, $\hat{\lambda}_{\alpha,ij}$ start to decline slightly when migration distance is more than 2000 miles. This could be because migration between the East and West Coasts, which covers a distance more than 2000 miles, is relatively easier due to the similarities between the eastern and western coastal states. The positive relationship between $\hat{\lambda}_{\alpha,ij}$ and migration distance explains why the rate of migration tends to decrease with migration distance (Figure 1).

To decompose $\hat{\lambda}_{\alpha,ij}$ into amenity differentials and relocation costs, we estimate (64) using data over the period 1990-1999. The sources for the amenity data used in the regression are summarized in Table A1 in Appendix A2.5, which include natural amenities, such as climate and geography, and non-natural amenities, such as local public goods, air quality and population densities, as suggested in the studies by Blomquist et al. (1988), Gyourko and Tracy (1991), Bieri et al. (2014) and Ahlfeldt and Pietrostefani (2019). The R^2 from

[16] The purpose of running this regression is for calibration only. In addition, to separate the constant, c_α, from the route-specific costs $\lambda_{\alpha,ij}$, we set $\lambda_{\alpha,12}$ to zero.

[17] For a list of potential elements of $\mathbf{dis}_{ij}$ and $\mathbf{am}_i$ see Table A1 in the Appendix.

[18] For further details, see Appendix A2.1.

[19] Moretti and Wilson (2017) estimate the migration elasticity (with respect to after tax income) of "star scientists", and their estimates range from 0.6 to 2 (with the benchmark estimate being 1.8). Our estimated migration elasticity is in the lower-range of these estimates. This is because we consider all state-to-state migrants, the average mobility of whom is lower than those of star scientists.

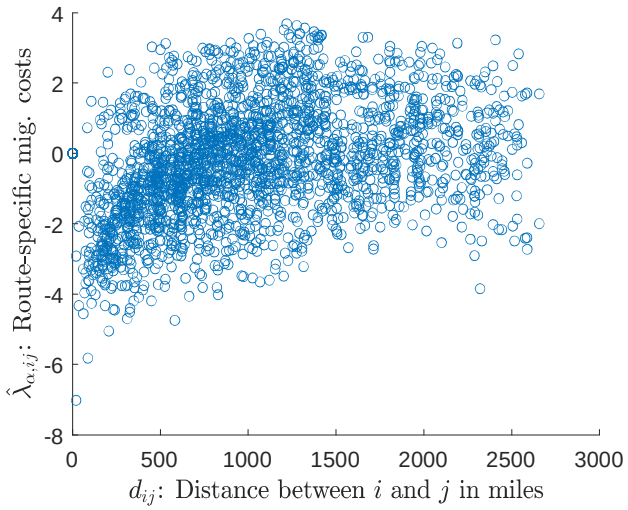

Figure 2: Route-specific migration costs estimated based on data during 1990-1999, $\hat{\lambda}_{\alpha,ij}$

Notes: This figure shows the route-specific migration costs estimated based on data during 1990-1999, $\hat{\lambda}_{\alpha,ij}$, against migration distance, d_{ij}, where d_{ij} refers to the geographical distance between States i and j. Each dot represents a pair $(d_{ij}, \hat{\lambda}_{\alpha,ij})$ for migration route (i, j).

this regression is 0.76, indicating that $\hat{\lambda}_{\alpha,ij}$ can be largely explained by amenity differentials and distances between origin and destination states. It is noteworthy that the coefficients associated with distances are positive and significant as shown in Table A2 in Appendix A3.1, confirming that distance have an important role in determining migration costs.

Then, we measure state level amenity and relocation costs by evaluating (65) and (66) using the estimates for c_λ, $\boldsymbol{\beta}'_{\mathbf{d}}, \boldsymbol{\beta}'_{\mathbf{a}}$ and $\xi_{\lambda,ij}$ and amenity and distance data. The five states with highest amenity indices are California, Texas, Florida, New York, and Pennsylvania (ordered from high to low), and the five states with lowest amenity indices are South Dakota, North Dakota, Delaware, Vermont and Wyoming (ordered from high to low).

Finally, the estimated de-trended migration costs are given by (note that (60) implies $\ln \alpha_{ij,t} - g_\alpha t = c_\alpha + \lambda_{\alpha,ij}$)

$$\ln \hat{\alpha}_{ij} = \hat{c}_\alpha + \hat{\lambda}_{\alpha,ij}. \tag{67}$$

Migration costs over the evaluation sample (2000-2014). The state level amenity is extrapolated for 2000-2014 as

$$\widehat{amenity}_{i,2000-2014} = \hat{\boldsymbol{\beta}}'_{\mathbf{a}} \mathbf{am}_{i,2000-2014}, \text{ for } i \in \mathcal{I}_n,$$

where $\mathbf{am}_{i,2000-2014}$ is the vector of amenities in state i for period 2000-2014, in which the time-varying amenities (e.g., public goods and air quality) are measured using data during 2000-2014.[20] Then, migration costs are extrapolated for 2000-2014 as (see (58))

[20] Note that some of the amenities considered are time-invariant (e.g., climate and geography), whereas others may vary over time (e.g., public goods and air quality).

$$\ln \hat{\alpha}_{ij,t} = \hat{c}_\alpha + \hat{g}_\alpha t + (\widehat{amenity}_{i,2000-2014} - \widehat{amenity}_{j,2000-2014}) + \widehat{rlc}_{ij},$$

for $i \neq j$, and i and $j \in \mathcal{I}_n$, and for $t = t_{2000}, t_{2001}, ..., t_{2014}$.

6.2 Labor demand and housing supplies

To calibrate the state-specific labor demand functions, given by (17), we set the share of labor costs in output, v_l, to 0.67 as estimated by Valentinyi and Herrendorf (2008). Following Davis et al. (2014), the elasticity of TFP with respect to local production scale (namely the agglomeration effect), v_ϕ, is set to 0.06.[21] To distinguish between scale effects of ϕ_{it} and a_{it} in (13), we set $\bar{\phi}_i$ defined by (14) to 1.

To calibrate the state-specific supply functions for new houses, given by (24), we estimate, $\vartheta_{\kappa,i}$, location-specific share of land in house values, by the state level average land values relative to total value of housing stocks over the 1977-1999 period.[22] We estimate the housing depreciation rate, δ, as the average ratio of aggregate depreciation to aggregate housing stock over the period 1977-1999 using the data from the Fixed Assets Tables compiled by the Bureau of Economic Analysis (BEA), and obtain $\hat{\delta} = 2\%$. The discount factor of landlord, β, is set to 0.98 to match the risk-free annual real interest rate of the U.S. over the period 1960-1999, which is estimated to be around 2 per cent. The location-specific housing investment cost parameter, θ_i, is estimated as follows. Using the housing investment function on the balanced growth path given by (54), we have

$$\theta_i = 1 - \frac{1}{\hat{\beta}} \left[\frac{q_i^*}{p_i^*} + (1 - \delta) \right]^{-1},$$

which suggests the following estimate

$$\hat{\theta}_i = 1 - \frac{1}{\beta} \left[\frac{1}{\frac{1}{T_1} \sum_{t=1}^{T_1} q_{it}/p_{it} + (1 - \hat{\delta})} \right], \tag{68}$$

where periods 1 and T_1 correspond to 1977 and 1999, respectively, δ and β are previously calibrated and estimated, and q_{it} and p_{it} are observed data.[23]

6.3 Exogenous processes

We now estimate the parameters that characterize the exogenous processes of regional productivities, land supplies and intrinsic population growth.

[21] Note that in Davis et al. (2014), parameter λ is estimated to be 1.069 (Table 1), which indicates that the estimated elasticity of TFP with respect to local production scale, $(\hat{\lambda} - 1)/\hat{\lambda}$, is 0.06 (equation (19)).

[22] The data on state level land share in house values are obtained from Davis and Heathcote (2007).

[23] For the details on the sources for q_{it} and p_{it}, see Appendix A2.3.

6.3.1 Productivity processes

To infer the state-specific labor productivities, a_{it}, we first note that (16), (17) and (18) imply

$$\ln a_{it} = -\frac{1}{1-\upsilon_\phi}\ln\bar{\phi}_i + \frac{1-\upsilon_\phi}{\upsilon_l}\ln y_{it} - \ln l_{.i}(t), \tag{69}$$

where υ_ϕ,υ_l and $\bar{\phi}_i$ are previously calibrated and estimated in Section 6.2, and $l_{.i}(t)$ and y_{it} are observed data.[24] Thus, the estimates of a_{it} are obtained by evaluating (69) using the parameter estimates and realized values of $l_{.i}(t)$ and y_{it}, for $t = 0, 1, ..., T_1$. Then, we estimate the stochastic processes of state-specific productivities, defined by (19), (20) and (21), using the estimates of a_{it}.[25]

6.3.2 Land supplies

To estimate κ_{it}, we first note that equilibrium conditions (16), (22), (24), (33) and (28) imply

$$\kappa_{it} = \frac{\gamma_{it}}{\tau_{\kappa,i}}, \tag{70}$$

where[26]

$$\gamma_{it} = \frac{\left\{\beta e^{g_l}(1-\theta_i)\left[\frac{q_{it}}{p_{it}} + (1-\delta)\right] - (1-\delta)\right\}\eta\upsilon_l\left(\frac{y_{it}}{q_{it}}\right)}{p_{it}^{(1-\vartheta_{\kappa,i})/\vartheta_{\kappa,i}}}. \tag{71}$$

Note that $\beta, g_l, \theta_i, \eta, \vartheta_{\kappa,i}, \upsilon_l$ and δ are previously calibrated and estimated, and that y_{it}, q_{it} and p_{it} are observed data.[27] Thus, an estimator of γ_{it} can be obtained by evaluating (71) using the parameter estimates and realized values of y_{it}, q_{it} and p_{it}, for $t = 0, 1, ..., T_1$, which corresponds to the period of 1976-1999. Then, the scalars, $\tau_{\kappa,i}$, in equation (70), are calibrated such that the implied accumulated new land flows, κ_{it}, over the sample period match the realized increases in state level urban area sizes over the same period. Details of the calibration of $\tau_{\kappa,i}$ are provided in Appendix A3.3.1. Finally, we compute $\hat{\kappa}_{it}$ using (70) as

$$\ln\hat{\kappa}_{it} = \ln\hat{\gamma}_{it} - \ln\hat{\tau}_{\kappa,i}, \text{ for } i = 1, 2, ..., n \text{ and } t = 0, 1, ..., T_1. \tag{72}$$

We estimate κ_i and $g_{\kappa,i}$ in (26) by running OLS regressions of $\ln\hat{\kappa}_{it}$ on a linear time trend (including a constant), for $i = 1, 2, ..., n$, and obtain the residuals, $\hat{z}_{\kappa,it}$, for $t = 0, 1, ..., T_1$.[28] Finally, for each i we estimate $\rho_{\kappa,i}$ and $\sigma_{\kappa,i}$ by running OLS regressions of $\hat{z}_{\kappa,it}$ on $\hat{z}_{\kappa,i,t-1}$, over the period $t = 1, 2, ..., T_1$.

Our estimates of land supply growth rates, $\hat{g}_{\kappa,i}$, are significantly negatively correlated with the state level Wharton Residential Land Use Regulatory Index compiled by Gyourko et al. (2008), and suggest that land use regulation can be an important factor that affects local house prices through the supplies of new land.[29]

[24] For the details on the sources for $l_{.i}(t)$ and y_{it}, see Appendices A2.1 and A2.2.

[25] For further details see Appendix A3.2.

[26] For details of the derivations, see Appendix A1.7.

[27] For the details on the sources for y_{it}, q_{it} and p_{it}, see Appendices A2.2 and A2.3.

[28] It is worth noting that our estimates of $g_{\kappa,i}$ reflect the average tightness of state level land-use regulations over the period 1977-1999, and need not to be good proxies for particular years or sub-periods.

[29] For further details, see Appendix A3.3.2.

6.3.3 Intrinsic population growth

The balanced growth path intrinsic population growth rate, g_l, defined by (42), is set to 1%, which is the average growth rate of the U.S. population over the period 1977-1999. The actual state level intrinsic population growth rates, $g_{l,it}$, over the period 1977-1999 are measured using the IRS data. For further details, see Appendix A2.1.

7 Model evaluation

We here simulate the model given by (34) and (35) over the evaluation sample (2000-2014) using the realized state level productivities, land supplies and intrinsic population growth rates. To do so, we set $\boldsymbol{a}_t$, $\boldsymbol{\kappa}_t$ and $\boldsymbol{g}_{l,t}$ to their realized values, for $t = T_1 + 1, T_1 + 2, ..., T$.[30] The initial values, $\boldsymbol{\zeta}_{T_1}$, correspond to the realized values in 1999. Recall that $\boldsymbol{\zeta}_t \equiv [\boldsymbol{l}(t), \boldsymbol{q}_t]$, and $\boldsymbol{l}(T_1)$ and $\boldsymbol{q}_{T_1}$ are observed data.

Figure 3 shows the simulated changes in log house price-to-income ratio and log output by states over the evaluation sample (2000-2014) against the realized values. As can be seen from the figure, the simulated and realized values are quite close.

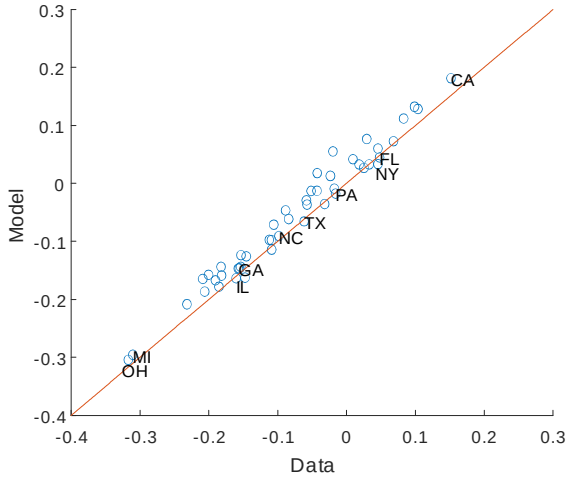

Panel 1: Changes in log house price-to-income ratio

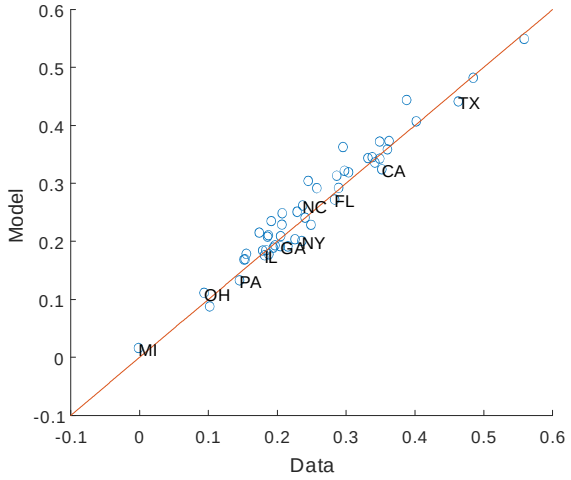

Panel 2: Changes in log output

Figure 3: Changes in log house price-to-income ratio and log output by states over the evaluation sample (2000-2014)

Notes: This figure displays the model predicted changes in log house price-to-income ratios and log output of U.S. states over the evaluation sample (2000-2014) against the realized values. Only the abbreviations of the ten most populated states are displayed.

Figure 4 compares the actual accumulated net inward migration flows and the actual

[30] For further details, see Appendix A4.

changes in log population of U.S. states over the evaluation sample with the model generated counterparts. As can be seen, the model captures the significant migration outflows from states with rising house price-to-income ratios, such as California and New York, and the substantial inflows towards states with decreasing house price-to-income ratios, such as Florida and Texas.

The model also replicates reasonably well the trends in the bilateral migration flows between the U.S. states. Figure 5 shows the realized and simulated migration flows between California, Texas, Florida and other U.S. states cumulated over the evaluation sample (2000-2014). Panels 1.a, 2.a and 3.a of the figure give the migration flows from California, Texas, Florida to other states, and Panels 1.b, 2.b and 3.b show the migration flows from other states to California, Texas, Florida. Only ten states with the largest migration flows are displayed. Similarly, Figure S1 in Section S1.1 of the online supplement shows the realized and simulated cumulated migration flows over the evaluation sample between New York, Pennsylvania, Illinois and other U.S. states. As can be seen, the simulated and realized values match reasonably well.

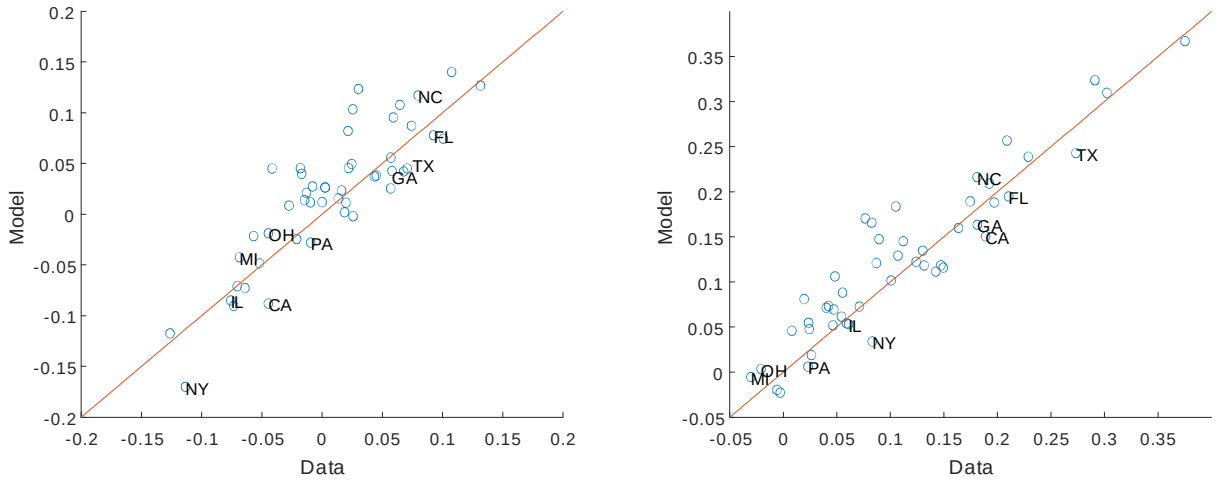

Panel 1: Net inward migration rates

Panel 2: Changes in log population

Figure 4: Net inward migration rates and changes in log population by states over the evaluation sample (2000-2014)

Notes: Panel 1 displays the model predicted accumulated net inward migration rates (i.e., the ratios of net inward migration to local population) of U.S. states during the period 2000-2014 against the counterpart realized values. Panel 2 displays the model predicted changes in log population by states over the evaluation sample (2000-2014) against the counterpart realized values. Only the abbreviations of the ten most populated states are displayed.

The results show that migration linkages tend to be stronger between two nearby states as compared to between two distant states. For example, as shown in Panels 1.a and 1.b of Figure 5, the bilateral migration flows between California and the nearby states tend to be

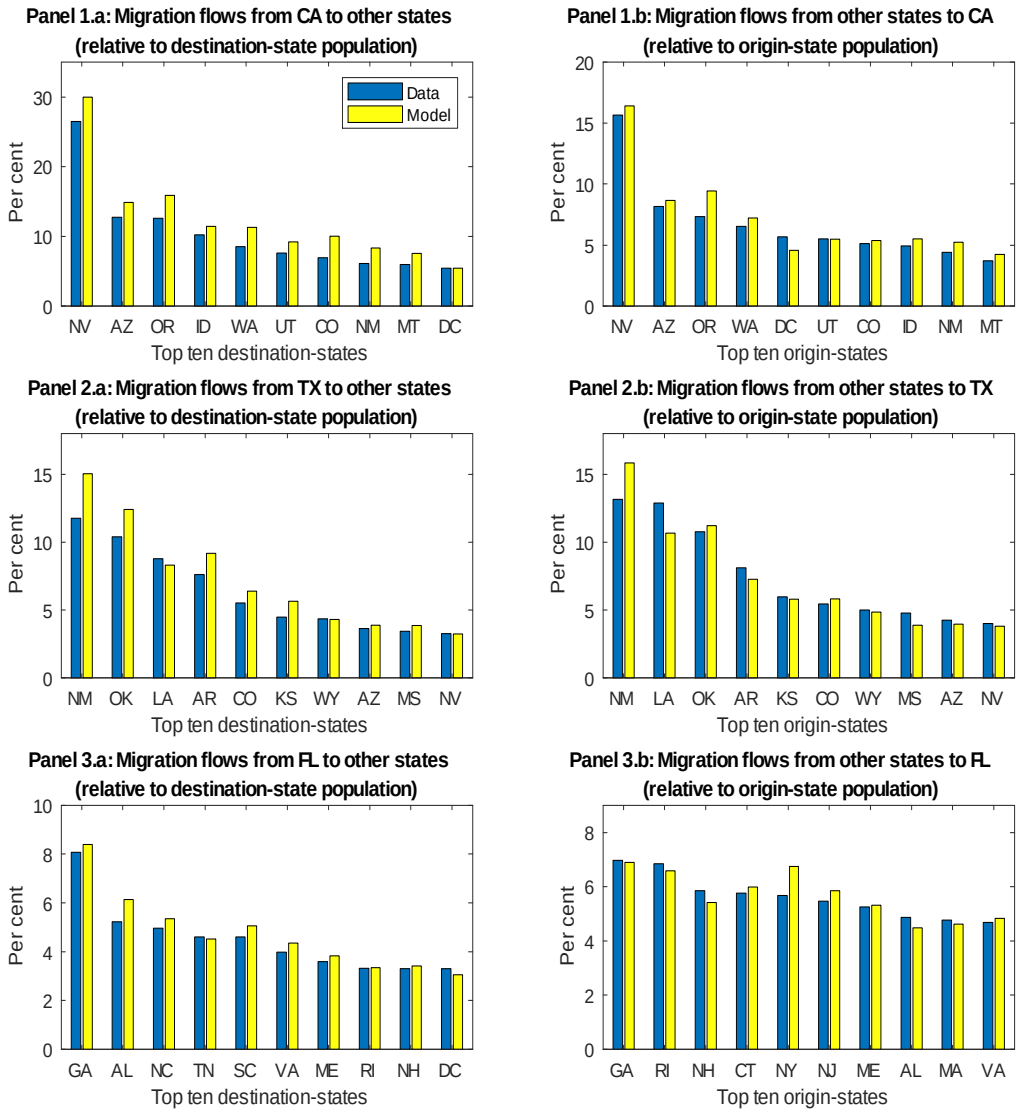

Figure 5: Bilateral migration flows between U.S. states during the evaluation sample (2000-2014)

Notes: Panel 1.a shows the realized and simulated accumulated migration flows from California to other states during the period 2000-2014 relative to destination-state population in 2014. Only the ten destination-states with the largest migration flows from California (relative to their own population) are displayed. Panel 1.b shows the realized and simulated accumulated migration flows from other states to California relative to origin-state population. Similarly, Panels 2.a and 2.b show the bilateral migration flows between Texas and other U.S. states, and Panels 3.a and 3.b show the bilateral migration flows between Florida and other U.S. states.

larger than the flows between California and other states, and the nearby states, including both the adjacent states, such as Arizona, Nevada and Oregon, and the nonadjacent states, such as Washington, Utah and Colorado, have the highest rates of migrations with California as compared to other states.

Finally, California has experienced considerable net outward migration to other states during 2000-2014. As shown in Panels 1.a and 1.b of Figure 5, the outward migration flows of California tend to be larger than the inward flows. The migration flows from California have also substantially impacted the population of its nearby states. For example, as can be seen in Panels 1.a and 1.b of Figure 5, the migration flow from California to Nevada is equivalent to around 25% of Nevada's population, while the migration flow from Nevada to California is equivalent to around 15% of Nevada's population. This indicates a net migration flow from California to Nevada that is equivalent to around 10% of Nevada population in 2014. Similarly, the net migration flow from California to Arizona is equivalent to around 5% of Arizona's population in 2014.

8 Spatiotemporal impulse responses

One of the important features of our theoretical analyses is the explicit modelling of dynamic location-to-location migration flows that function as a source of spatiotemporal spill-over effects. Here we examine the quantitative importance of such spill-over effects using spatiotemporal impulse responses. In particular, we consider not only the spatial patterns of the responses of different locations to shocks but also the time profile of state-specific shocks from one location to another. We shall focus on the effects of productivity and land-supply shocks in California, Texas and Florida. The results for California are discussed in some detail in sub-section 8.1, and then compared to those for Texas and Florida in sub-section 8.2. Finally, Section 9 provides some sensitivity analysis with respect to two key parameters of the model, namely migration elasticity and housing depreciation rate.

8.1 Productivity and land-supply shocks in California

We start by considering the effects of a positive productivity shock and a positive land-supply shock in California in turn. We assume that the economy is initially on the balanced growth path, and simulate the outcomes and the resultant impulse responses using independent Gaussian draws for the model's innovations.[31]

We first consider the effects of a one per cent positive shock to the labor productivity in California. Figure 6 displays the responses of real wages, house prices, rent and migration flows in California to the shock. In response to an exogenous increase in labor productivity local wages rise, which in turn induces net inward migration towards California, leading to an increases in local population. Due to rising wage rate and population, the housing demand in California increases, which raises local rents and house prices. As house prices rise, more

[31] Details are provided in Section S2 of the online supplement.

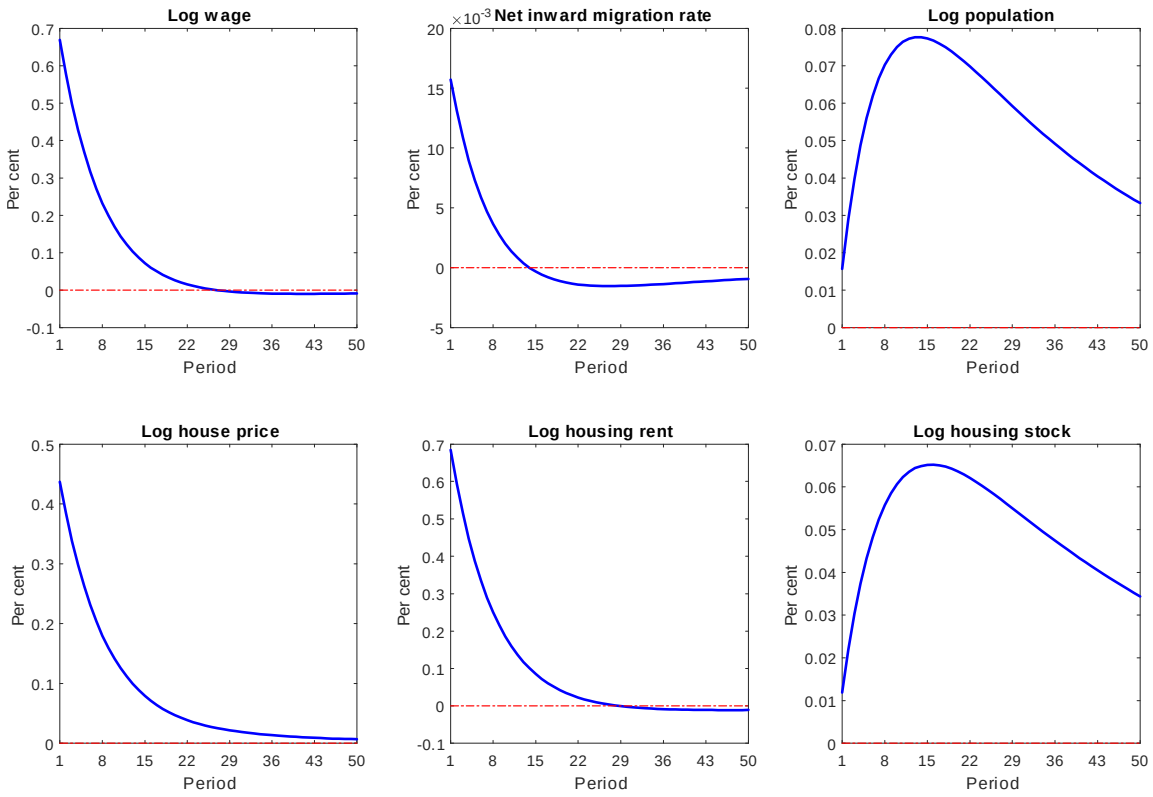

Figure 6: Reponses of California to a positive productivity shock in California

Notes: This figure shows the responses of log wage rate, net inward migration rate (i.e., the ratio of net inward migration to local population), log population, log house price, log housing rent and log housing stock in California to a one per cent positive shock to the labor productivity in California.

new homes are constructed, which increases the housing stock in California. Due to the slow depreciation of houses, the adjustment of housing stock and population is very slow, taking decades before the economy returns to its steady state.

Figures 7 and 8 show the spatiotemporal responses of population and house price-to-income ratios of U.S. states to the positive productivity shock in California.[32] The different plots show the responses of U.S. states, except for California, arranged by the number of periods after the shock, with the states ordered by their average distance to California on the horizontal axis. The rise in wages in California induces net migration flows from other states to California, leading to population declines in all other states. (see Figure 7). This in turn leads to lower house prices and higher wages, causing a drop in the house price-to-income ratios (Figure 8). However, the responses tend to be stronger in the states that are geographically close to California, including both the adjacent states, such as Nevada, Arizona and Oregon, and the nonadjacent states, such as Washington, Colorado and Utah.

[32]The responses of each of the U.S. states are shown in Figures S10 and S11 in Section S1.3.1 of the online supplement.

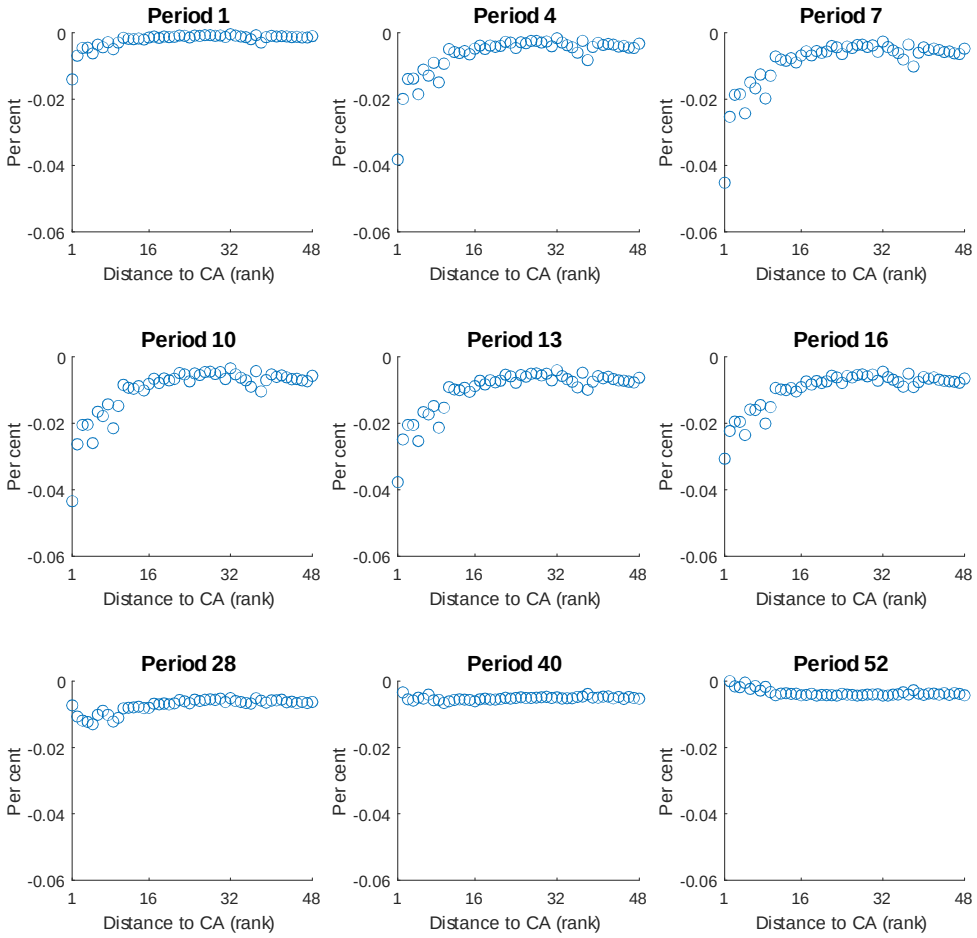

Figure 7: Spatiotemporal responses of log population of U.S. states to a positive productivity shock in California

Notes: Each panel shows the responses of log population of U.S. states (except for California) to a one per cent positive shock to the labor productivity in California, for the period noted at the top. Each dot represents a state. States are ordered ascendingly by their distances to California, and the horizontal axis corresponds to state's rank in terms of distance to California.

In addition, the responses in some of the East Coast states (e.g., Washington, D.C. and New York) are also strong. Thus, the snapshots of the responses tend to have an inverse U-shape.

Furthermore, the responses of the nearby states to a California productivity shock are not only stronger but also take place much more quickly. See Figures 7, 8, and 9.

To quantify the length of time it takes for the effects of the productivity shock in California to reach other states, let $|\check{z}_t|$ denote the absolute response of variable z to the shock

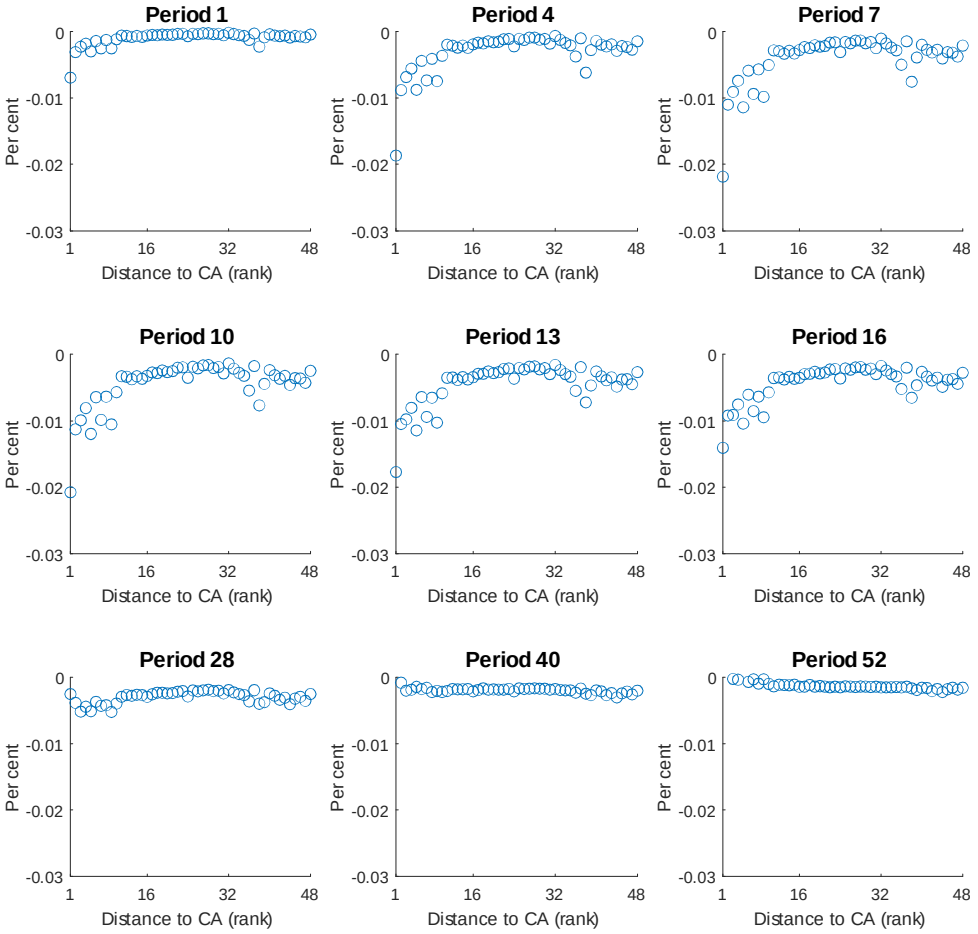

Figure 8: Spatiotemporal responses of log house price-to-income ratios of U.S. states to a positive productivity shock in California

Notes: Each panel shows the responses of log house price-to-income ratios of U.S. states (except for California) to a one per cent positive shock to the labor productivity in California, for the period noted at the top. Each dot represents a state. States are ordered ascendingly by their distances to California, and the horizontal axis corresponds to state's rank in terms of distance to California.

after t periods, with $t = 1, 2, ...$ Define the response time of variable z, denoted by RT_z, as

$$RT_z = \frac{\sum_{t=1}^{\infty} |\check{z}_t| \, t}{\sum_{t=1}^{\infty} |\check{z}_t|}. \tag{73}$$

In the above expression, $|\check{z}_t| \, / \left(\sum_{t=1}^{\infty} |\check{z}_t|\right)$ is the weight atatched to period t responses. Therefore, RT_z can be interpreted as the average length of time it takes for z to respond to the

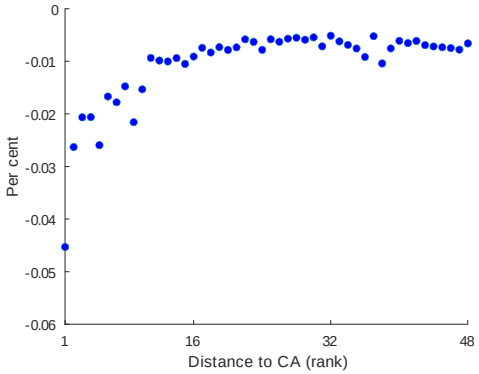

Panel 1.a: Bottom values of the responses of log population (by states)

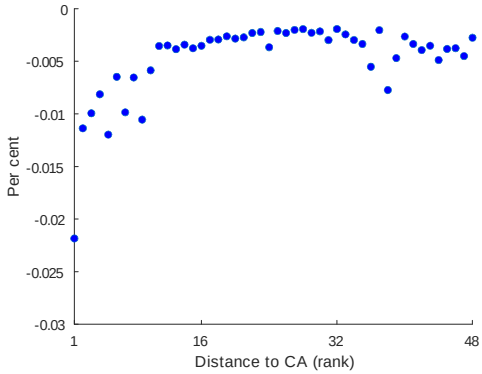

Panel 1.b: Bottom values of the responses of log house price-to-income ratios (by states)

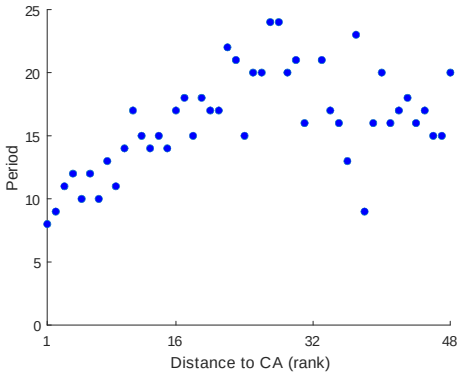

Panel 2.a: Periods in which the responses of log population reach their bottom values (by states)

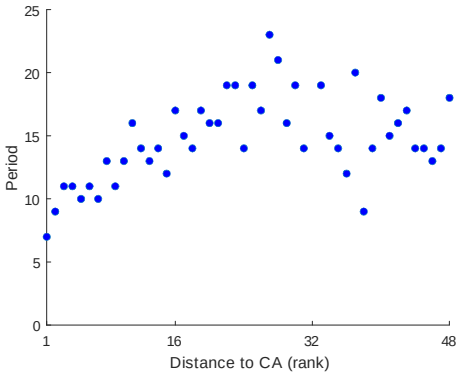

Panel 2.b: Periods in which the responses of log house price-to-income ratios reach their bottom values (by states)

Figure 9: Size and speed of responses of mainland U.S. states (except for California) to a positive productivity shock in California

Notes: In each panel, a dot represents a state. In Panels 1.a and 1.b, the vertical axis corresponds to the extreme value of state's response after a one per cent positive productivity shock in California, and in Panels 2.a and 2.b, the vertical axis corresponds to period in which state's response reaches its extreme value. States are ordered ascendingly by their distances to California, and the horizontal axis corresponds to state's rank in terms of distance to California.

shock.[33] Figure 10 display the approximated response time of the log population and log house price-to-income ratios of U.S. states (except for California) after the California productivity shock. In each panel, the states are ordered by their distances to California and the

[33]Note that if the model is stable, $|\check{z}_t|$ should converge to zero as t goes to ∞. Thus, $\sum_{t=1}^{\infty} |\check{z}_t| t$ and $\sum_{t=1}^{\infty} |\check{z}_t|$ should be finite if $|\check{z}_t|$ converge to zero fast enough as t goes to ∞.

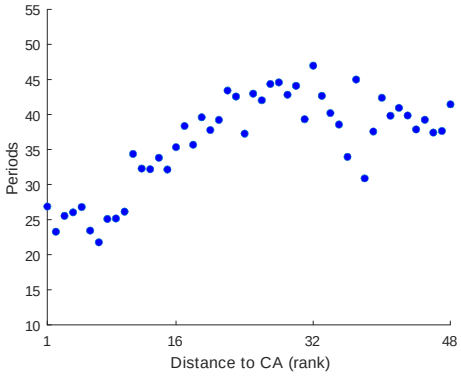

Panel 1: Response time of log population (by states)

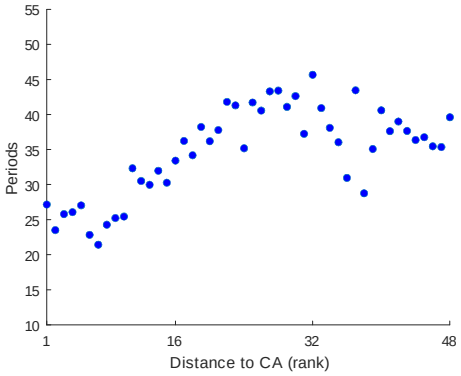

Panel 2: Response time of log house price-to-income ratios (by states)

Figure 10: Response time of U.S. mainland states after a positive productivity shock in California

Notes: In each panel, a dot represents a state. States are ordered ascendingly by their distances to California, and the horizontal axis corresponds to state's rank in terms of distance to California. The vertical axes correspond to the response time of state's population and house price-to-income ratio computed according to (73).

horizontal axis corresponds to state's rank in terms of geographical closeness to California. As shown in the figure, the response time of the nearby states of California tends to be shorter.

In sum, the California productivity shock tends to have larger impacts for the nearby states than for the distant states. In addition, it tends to take longer time for the shock's effects to reach more distant states. This can be due to the fact that migration cost tends to increase with migration distance (see Section 6.1).

We have also computed the impulse responses for the effects of a ten per cent positive land-supply shock in California.[34] The results are shown in Figures S6, S7, S8 and S9 in Section S1.3.1 of the online supplement. As can be seen, the spatiotemporal patterns of the responses of U.S. states to this shock are similar as those presented above for the productivity shock. However, the effects of the California land-supply shock are more persistent when compared to the effects of California productivity shock considered above. This is because the positive shock to the land supply in California raises the housing supply in California. Since houses depreciate slowly, the housing rent in California will be kept low for a long time, leading to persistent net inward migration to California.

[34]Note that the annual supply of new land in California (estimated from the model) has been declining over 1976-1999 (the training sample). The ten per cent land-supply shock would raise the annual supply of new land in California from its steady state level (corresponding to the average during the training sample, 1976-1999) to its level in the late 1970s.

8.2 Comparing impulse responses for California,Texas and Florida

Impulse responses of productivity and land-supply shocks for Texas and Florida are presented in Sections S1.3.2, S1.3.3 and S1.3.4 of the online supplement. We find that responses of Texas and Florida to the shocks are qualitatively similar to those of California but differ quantitatively, which is mainly due to the differences in land supply conditions across these states.[35] Residential land uses are much more regulated in California (with a WRI of 0.59) than in Florida (with a WRI of 0.37) and Texas (with a WRI of -0.45).[36] As a result, available land for residential construction is more limited in supply in California than in Florida and Texas. During 1976-1999 (the training sample), the share of land in house value is about 50% in Californian, but only 14% in Florida and less than 10% in Texas (Davis and Heathcote (2007)). Our model captures such differences in land supply reasonably well.

As shown in Panel 1 of Figure S24 in Section S1.3.4 of the online supplement, following a one per cent positive productivity shock in Texas, the net migration flows towards Texas increase considerably, while inducing only mild increases in local house prices. In contrast, a one per cent positive productivity shock in California translates into sizeable increases in house prices in California with less net inward migration flows. The responses in Florida are somewhere between those of California and Texas.

We also find that a ten per cent positive land-supply shock in California results in large increases in housing supplies which is accompanied with large drops in house prices in California and sizable net inward migration flows. See Panel 2 of Figure S24 in Section S1.3.4 of the online supplement. In contrast, a ten per cent positive land-supply shock in Texas induces less increases in housing supplies in Texas, resulting in less inward migration flows. Again, responses in Florida are somewhere between those of California and Texas.

Finally, as shown in Figures S13, S14, S16, S17, S19, S20, S22, S23 in Sections S1.3.2 and S1.3.3 of the online supplement, the spatiotemporal patterns of the responses of U.S. states to shocks in Texas and Florida are qualitatively similar to those of California, and confirm that spatial spill-over effects tend to be larger for the nearby states than for the distant states.

9 Calibration sensitivity

We now consider the sensitivity of the model results to our calibration choices for the migration elasticity, $1/\sigma_\varepsilon$, and the housing depreciation rate, δ.

Migration elasticity. As described in Section 6.1.2, we estimate the migration elasticity jointly with migration costs over the period 1990-1999. Our estimate of $1/\sigma_\varepsilon$ is 0.812 (with a standard error of 0.051), which is in line with Moretti and Wilson (2017) whose estimates range between 0.6 and 2 (with the benchmark estimate being 1.8). To investigate the sensitivity of the model results to migration elasticity, we repeat the impulse response

[35] See Figure S24 in Section S1.3.4 of the online supplement.

[36] See Table 10 of Gyourko et al. (2008)

analyses we conducted for California in Section 8.1 but with migration elasticity set to 0.6, 1.8 and 2. The results are shown in Figures S25 and S26 in Section S1.3.5 of the online supplement.

When migration elasticity is higher, spatial population reallocation after positive productivity and land-supply shocks in California is significantly larger and net migration flows towards California rises significantly more, leading to larger increases in the population of California. We also note that the spatial spill-over effects are significantly stronger, especially for the nearby states, when migration elasticity is increased. See Figure S26 in Section S1.3.5 of the online supplement.

Housing depreciation rate. To gauge the sensitivity of our results to the choice of the depreciation rate, we conducted the impulse response analyses for California presented in Section 8.1 but with δ set to 0.01 as compared to the value of 0.02 used in the baseline simulations. In this way we also shed some light on how housing depreciation rate can affect the size and speed of population reallocation after regional shocks (Glaeser and Gyourko (2005)).[37] The results are presented in Figures S27 and S28 in Section S1.3.5 of the online supplement. When the housing depreciation rate, δ, is lower, housing supplies adjust more slowly to changes in local housing demand and supply conditions. This reduces and slows down population reallocation, and the effects are quantitatively larger for land-supply shocks than for productivity shocks.

When the housing depreciation rate, δ, is lower, the increases in housing stocks in California are smaller and the decreases in housing stocks in other states are also smaller, after a positive productivity shock in California. See Panel 1 of Figure S27 and Panel 1 of Figure S28 in Section S1.3.5 of the online supplement. Thus, when the housing depreciation rate, δ, is lower, due to the slow adjustment of housing supplies, a positive productivity shock in California induces less population reallocation from other states to California. Similarly, when the housing depreciation rate, δ, is lower, housing supplies in California increase less after a positive land-supply shock in California, inducing less population reallocation towards California. See Panel 2 of Figure S27 in Section S1.3.5 of the online supplement.

10 Concluding remarks

This paper presents and solves a spatiotemporal equilibrium model in which regional wage rates and house prices are jointly determined with migration flows. It extends existing studies on regional economies by explicitly modelling the dynamics of location-to-location migration flows. The model can be viewed as an example of a dynamic network where regional labor and housing markets interact with each other via migration flows, and provides a theoretically coherent framework to study the spatiotemporal impacts of changes in regional supply and demand conditions on regional house prices and spatial population allocation through endogenized migration flows. The theoretical model can also be adapted to study other types of spatial spill-overs in regional economies that operate through migration; for example, spill-over effects in regional labor markets.

[37] Glaeser and Gyourko (2005) argue that urban decline is highly persistent because of durable housing.

The estimated model is shown to simultaneously account for the observed trends in the state level house prices and interstate migration flows over our evaluation sample (2000-2014). By using spatiotemporal impulse responses we are also able to capture both the dynamic and equilibrium outcomes of local productivity and land-supply shocks over time and across states. We also investigate the sensitivity of our results to migration elasticity, housing depreciation rate, and local land supply conditions.

The analysis of this paper on regional housing markets can be extended in a number of directions. An econometrically estimated version of the model can be used for the analysis and predication of house price diffusion across states or MSAs. In addition, given the importance of labor mobility for population reallocation, it is also worth considering the factors that determine population mobility, their nature and variations overtime and across space.

References

Ahlfeldt, G.M. and Pietrostefani, E. (2019). The economic effects of density: A synthesis. *Journal of Urban Economics*, 111, 93–107.

Albouy, D. and Ehrlich, G. (2018). Housing productivity and the social cost of land-use restrictions. *Journal of Urban Economics*, 107, 101–120.

Artuc, E., Chaudhuri, S., and McLaren, J. (2010). Trade shocks and labor adjustment: A structural empirical approach. *American Economic Review*, 100, 1008–45.

Bailey, N., Holly, S., and Pesaran, M.H. (2016). A two-stage approach to spatio-temporal analysis with strong and weak cross-sectional dependence. *Journal of Applied Econometrics*, 31, 249–280.

Bieri, D.S., Kuminoff, N.V., and Pope, J.C. (2014). National expenditures on local amenities. *Department of Economics, Arizona State University, Manuscript.*

Blanchard, O.J., Katz, L.F., Hall, R.E., and Eichengreen, B. (1992). Regional evolutions. *Brookings papers on economic activity*, 1992, 1–75.

Blomquist, G.C., Berger, M.C., and Hoehn, J.P. (1988). New estimates of quality of life in urban areas. *The American Economic Review*, pages 89–107.

Caliendo, L., Dvorkin, M., and Parro, F. (2019). Trade and labor market dynamics: General equilibrium analysis of the china trade shock. *Econometrica*, 87, 741–835.

Cotter, J., Gabriel, S., and Roll, R. (2015). Can housing risk be diversified? a cautionary tale from the housing boom and bust. *The Review of Financial Studies*, 28, 913–936.

Davis, M.A., Fisher, J.D., and Veracierto, M. (2021). Migration and urban economic dynamics. *Journal of Economic Dynamics and Control*, page 104234.

Davis, M.A., Fisher, J.D., and Whited, T.M. (2014). Macroeconomic implications of agglomeration. *Econometrica*, 82, 731–764.

Davis, M.A. and Heathcote, J. (2007). The price and quantity of residential land in the united states. *Journal of Monetary Economics*, 54, 2595–2620.

Davis, M.A. and Ortalo-Magné, F. (2011). Household expenditures, wages, rents. *Review of Economic Dynamics*, 14, 248–261.

Davis, S.J., Faberman, R.J., Haltiwanger, J., Jarmin, R., and Miranda, J. (2010). Business volatility, job destruction, and unemployment. *American Economic Journal: Macroeconomics*, 2, 259–87.

DeFusco, A., Ding, W., Ferreira, F., and Gyourko, J. (2018). The role of price spillovers in the american housing boom. *Journal of Urban Economics*, 108, 72–84.

Fuguitt, G.V. (1965). The growth and decline of small towns as a probability process. *American Sociological Review*, 30, 403–411.

Fujita, S. (2018). Declining labor turnover and turbulence. *Journal of Monetary Economics*, 99, 1–19.

Glaeser, E.L. and Gyourko, J. (2003). The impact of building restrictions on housing affordability. *Federal Reserve Bank of New York Economic Policy Review*, 9, 21–39.

Glaeser, E.L. and Gyourko, J. (2005). Urban decline and durable housing. *Journal of Political Economy*, 113, 345–375.

Glaeser, E.L., Gyourko, J., and Saks, R.E. (2005). Why have housing prices gone up? *The American Economic Review*, 95, 329–333.

Gyourko, J., Mayer, C., and Sinai, T. (2013). Superstar cities. *American Economic Journal: Economic Policy*, 5, 167–199.

Gyourko, J., Saiz, A., and Summers, A. (2008). A new measure of the local regulatory environment for housing markets: The Wharton Residential Land Use Regulatory Index. *Urban Studies*, 45, 693–729.

Gyourko, J. and Tracy, J. (1991). The structure of local public finance and the quality of life. *Journal of Political Economy*, 99, 774–806.

Herkenhoff, K.F., Ohanian, L.E., and Prescott, E.C. (2018). Tarnishing the golden and empire states: Land-use restrictions and the US economic slowdown. *Journal of Monetary Economics*, 93, 89–109.

Hilber, C.A. and Robert-Nicoud, F. (2013). On the origins of land use regulations: Theory and evidence from us metro areas. *Journal of Urban Economics*, 75, 29–43.

Holly, S., Pesaran, M.H., and Yamagata, T. (2010). A spatio-temporal model of house prices in the usa. *Journal of Econometrics*, 158, 160–173.

Hsieh, C.T. and Moretti, E. (2019). Housing constraints and spatial misallocation. *American Economic Journal: Macroeconomics*, 11, 1–39.

Ihlanfeldt, K.R. (2007). The effect of land use regulation on housing and land prices. *Journal of Urban Economics*, 61, 420–435.

Kahn, M.E. (2011). Do liberal cities limit new housing development? evidence from california. *Journal of Urban Economics*, 69, 223–228.

Karahan, F. and Rhee, S. (2014). Population aging, migration spillovers, and the decline in interstate migration. *FRB of New York Staff Report*.

Koop, G., Pesaran, M.H., and Potter, S.M. (1996). Impulse response analysis in nonlinear multivariate models. *Journal of Econometrics*, 74, 119–147.

McFadden, D. (1978). Modelling the Choice of Residential Location. In *Spatial Interaction Theory and Planning Models*, pages 75–96. North-Holland Publishing Company.

Monras, J. (2018). Economic shocks and internal migration. *CEPR Discussion Paper No. DP12977*.

Moretti, E. and Wilson, D.J. (2017). The effect of state taxes on the geographical location of top earners: evidence from star scientists. *American Economic Review*, 107, 1858–1903.

Notowidigdo, M.J. (2020). The incidence of local labor demand shocks. *Journal of Labor Economics*, 38, 687–725.

Parkhomenko, A. (2016). The rise of housing supply regulation in the us: Local causes and aggregate implications. Technical report, mimeo.

Quigley, J.M. and Raphael, S. (2005). Regulation and the high cost of housing in california. *The American Economic Review*, 95, 323–328.

Roback, J. (1982). Wages, rents, and the quality of life. *Journal of Political Economy*, 90, 1257–1278.

Rosen, S. (1979). Wage-based indexes of urban quality of life. In *Current issues in urban economics*, pages 74–104. Johns Hopkins University Press.

Saiz, A. (2010). The geographic determinants of housing supply. *Quarterly Journal of Economics*, 125.

Sinai, T. (2012). House price moments in boom-bust cycles. In *Housing and the Financial Crisis*, pages 19–68. University of Chicago Press.

Tarver, J.D. and Gurley, W.R. (1965). A stochastic analysis of geographic mobility and population projections of the census divisions in the united states. *Demography*, 2, 134–139.

Valentinyi, A. and Herrendorf, B. (2008). Measuring factor income shares at the sectoral level. *Review of Economic Dynamics*, 11, 820–835.

Van Nieuwerburgh, S. and Weill, P.O. (2010). Why has house price dispersion gone up? *The Review of Economic Studies*, 77, 1567–1606.

Appendices

A1 Mathematical derivations and proofs

A1.1 Derivation of migration probabilities

Here we derive the migration probability equation (12). For the worker τ who is born in location i, the probability of residing in location j^* is

$$Prob\ (j^* \text{ is chosen}) = Prob\ \left(v_{\tau,t,ij^*} > v_{\tau,t,ij}\ \forall j \neq j^*\right),$$

where

$$v_{\tau,t,ij} = (\ln w_{jt} - \ln w_{it}) - \eta\,(\ln q_{jt} - \ln q_{it}) + \sigma_\varepsilon\,(\varepsilon_{\tau,t,ij} - \varepsilon_{\tau,t,ii}) - \ln \alpha_{ij}.$$

Recall that $\varepsilon_{\tau,t,ij}$ is IID for all τ, t, i and j, and has an extreme value distribution, with the cumulative distribution function $F(\varepsilon) = e^{-e^{-\varepsilon}}$, and the probability density function $f(\varepsilon) = e^{-\varepsilon}e^{-e^{-\varepsilon}}$. Consider the following decomposition of $v_{\tau,t,ij}$,

$$v_{\tau,t,ij} = v_{t,ij} + \sigma_\varepsilon\,(\varepsilon_{\tau,t,ij} - \varepsilon_{\tau,t,ii})$$

where

$$v_{t,ij} = (\ln w_{jt} - \ln w_{it}) - \eta\,(\ln q_{jt} - \ln q_{it}) - \ln \alpha_{ij}.$$

Note that $v_{t,ij}$ is known by worker τ, and will be treated as given. The probability that worker τ selects region j^* as her migration destination can be written as

$$\begin{aligned} Prob\ (j^* \text{ is chosen}) &= Prob\ \left(v_{t,ij^*} + \sigma_\varepsilon\varepsilon_{\tau,t,ij^*} - \sigma_\varepsilon\varepsilon_{\tau,t,ii} > v_{t,ij} + \sigma_\varepsilon\varepsilon_{\tau,t,ij} - \sigma_\varepsilon\varepsilon_{\tau,t,ii},\ \forall j \neq j^*\right), \\ &= Prob\ \left(\varepsilon_{\tau,t,ij^*} + \sigma_\varepsilon^{-1}v_{t,ij^*} - \sigma_\varepsilon^{-1}v_{t,ij} > \varepsilon_{\tau,t,ij},\quad \forall j \neq j^*\right). \end{aligned}$$

Conditional on $\varepsilon_{\tau,t,ij^*}$, the probability that location j^* is chosen by worker τ is given by

$$Prob\ (j^* \text{ is chosen } |\varepsilon_{\tau,t,ij^*}) = \prod_{j \neq j^*} F\left(\varepsilon_{\tau,t,ij^*} + \sigma_\varepsilon^{-1}v_{t,ij^*} - \sigma_\varepsilon^{-1}v_{t,ij}\right).$$

Since $\varepsilon_{\tau,t,ij^*}$ is also random, the probability that location j^* is chosen is the integral of $Prob$ (j^* is chosen $|\varepsilon_{\tau,t,ij^*}$) over its support and weighted by its density function, namely

$$\begin{aligned}
Prob\ (j^* \text{ is chosen}) &= \int_{-\infty}^{+\infty} \left[\prod_{j\neq j^*} e^{-e^{-\left(\varepsilon+\sigma_\varepsilon^{-1}v_{t,ij^*}-\sigma_\varepsilon^{-1}v_{t,ij}\right)}}\right] e^{-\varepsilon}e^{-e^{-\varepsilon}}d\varepsilon \\
&= \int_{-\infty}^{+\infty} \left[\prod_{j\neq j^*} e^{-e^{-\left(\varepsilon+\sigma_\varepsilon^{-1}v_{t,ij^*}-\sigma_\varepsilon^{-1}v_{t,ij}\right)}}\right] e^{-\varepsilon}e^{-e^{-\left(\varepsilon+\sigma_\varepsilon^{-1}v_{t,ij^*}-\sigma_\varepsilon^{-1}v_{t,ij^*}\right)}}d\varepsilon \\
&= \int_{-\infty}^{+\infty} \left[\prod_{j} e^{-e^{-\left(\varepsilon+\sigma_\varepsilon^{-1}v_{t,ij^*}-\sigma_\varepsilon^{-1}v_{t,ij}\right)}}\right] e^{-\varepsilon}d\varepsilon \\
&= \int_{-\infty}^{+\infty} exp\left[-e^{-\varepsilon}\sum_j e^{-\sigma_\varepsilon^{-1}\left(v_{t,ij^*}-v_{t,ij}\right)}\right] e^{-\varepsilon}d\varepsilon.
\end{aligned}$$

Define $s = e^{-\varepsilon}$. Thus, $ds = -e^{-\varepsilon}d\varepsilon$. Then,

$$\begin{aligned}
Prob\ (j^* \text{ is chosen}) &= \int_0^{+\infty} exp\left[-s\sum_j e^{-\sigma_\varepsilon^{-1}\left(v_{t,ij^*}-v_{t,ij}\right)}\right] ds \\
&= -\left.\frac{exp\left[-s\sum_j e^{-\sigma_\varepsilon^{-1}\left(v_{t,ij^*}-v_{t,ij}\right)}\right]}{\sum_j e^{-\sigma_\varepsilon^{-1}\left(v_{t,ij^*}-v_{t,ij}\right)}}\right|_0^{+\infty} \\
&= \frac{1}{\sum_j e^{-\sigma_\varepsilon^{-1}\left(v_{t,ij^*}-v_{t,ij}\right)}} = \frac{e^{\sigma_\varepsilon^{-1}v_{t,ij^*}}}{\sum_j e^{\sigma_\varepsilon^{-1}v_{t,ij}}}.
\end{aligned}$$

A1.2 Compact form of equilibrium conditions

To derive the compact form of the equilibrium conditions, i.e., (34)-(35), we first note that (33) implies

$$p_{it} = \frac{\beta e^{g_l}\left(1-\theta_i\right)q_{it}}{h_{it}/h_{i,t-1} - \beta e^{g_l}\left(1-\theta_i\right)\left(1-\delta\right)}. \tag{A.1}$$

Also, by substituting (24) into (28), we have

$$h_{it} = (1-\delta)h_{i,t-1} + \tau_{\kappa,i}\kappa_{it}p_{it}^{\lambda_{p,i}}. \tag{A.2}$$

Then, substituting (A.1) into (A.2) we obtain

$$\begin{aligned}
h_{it} \;=\; & (1-\delta)h_{i,t-1} + \\
& \tau_{\kappa,i}\kappa_{it}\left[\frac{\beta e^{g_l}\left(1-\theta_i\right)q_{it}}{h_{it}/h_{i,t-1} - \beta e^{g_l}\left(1-\theta_i\right)\left(1-\delta\right)}\right]^{\lambda_{p,i}}.
\end{aligned} \tag{A.3}$$

Then, by substituting (22) into (A.3), we can eliminate h_{it} and $h_{i,t-1}$, and after lagging the resultant equation by one period we have

$$\eta\left(\frac{w_{it}}{q_{it}}\right)l_{\cdot i}(t)=(1-\delta)\eta\left(\frac{w_{i,t-1}}{q_{i,t-1}}\right)l_{\cdot i}(t-1)+ \\ \tau_{\kappa,i}\kappa_{i,t-1}\left[\frac{\beta e^{g_l}\left(1-\theta_i\right)q_{i,t-1}}{\left(\frac{w_{it}}{w_{i,t-1}}\right)\left(\frac{l_{\cdot i}(t)}{l_{\cdot i}(t-1)}\right)\left(\frac{q_{i,t-1}}{q_{it}}\right)-\beta e^{g_l}\left(1-\theta_i\right)\left(1-\delta\right)}\right]^{\lambda_{p,i}}. \tag{A.4}$$

Thus, equations (5), (12) and (17), together with (A.4), provide $2n$ non-linear dynamic equations in $l_{\cdot i}(t)$, $i=1,2,...,n$, and q_{it}, $i=1,2,...,n$, which can be written compactly as:

$$\boldsymbol{\zeta}_t=\boldsymbol{f}\left(\boldsymbol{\zeta}_{t-1},\boldsymbol{a}_t,\boldsymbol{a}_{t-1},\boldsymbol{\kappa}_{t-1},\boldsymbol{g}_{l,t};\Theta\right), \tag{A.5}$$

where Θ is a row vector that contains all the parameters, $\boldsymbol{\zeta}_t=[\boldsymbol{l}(t),\boldsymbol{q}_t]$ is a $1\times 2n$ vector. In addition, using (17), (22) in (A.2) and (A.1) to eliminate w_{it} and $h_{i,t-1}$, we have

$$p_{it} = \frac{\beta e^{g_l}\left(1-\theta_i\right)q_{it}}{h_{it}q_{it}/\left(\eta\tau_{w,i}a_{it}^{\lambda_a}l_{\cdot i}(t)^{1-\lambda_l}\right)-\beta e^{g_l}\left(1-\theta_i\right)\left(1-\delta\right)}, \tag{A.6}$$

$$h_{it} = (1-\delta)\left(\frac{\eta\tau_{w,i}a_{it}^{\lambda_a}}{q_{it}}\right)l_{\cdot i}(t)^{1-\lambda_l}+\tau_{\kappa,i}\kappa_{it}p_{it}^{\lambda_{p,i}}. \tag{A.7}$$

Note that using (A.6) and (A.7), we can solve for p_{it} and h_{it}, for given values of $l_{\cdot i}(t), q_{it}, a_{it}$ and κ_{it}. Thus, $\boldsymbol{p}_t$ and $\boldsymbol{h}_t$ are functions of $\boldsymbol{l}(t)$, $\boldsymbol{q}_t$, $\boldsymbol{a}_t$ and $\boldsymbol{\kappa}_t$:

$$\boldsymbol{\chi}_t=\boldsymbol{g}\left(\boldsymbol{\zeta}_t,\boldsymbol{a}_t,\boldsymbol{\kappa}_t;\Theta\right), \tag{A.8}$$

where $\boldsymbol{\chi}_t=[\boldsymbol{p}_t,\boldsymbol{h}_t]$ is a $1\times 2n$ vector.

A1.3 Equilibrium conditions written in terms of the detrended variables

Recall that we use letters with stars and time subscripts to denote the corresponding detrended variables, and that we use bold lowercase letters with only time subscripts to denote the vectors of prices and quantities for all locations. For example, $w_{it}^*\equiv e^{-g_w t}w_{it}$, $\boldsymbol{w}_t^*\equiv[w_{1t}^*,w_{2t}^*,...,w_{nt}^*]$, $p_{it}^*\equiv e^{-g_w t}p_{it}$, $\boldsymbol{p}_t^*\equiv[p_{1t}^*,p_{2t}^*,...,p_{nt}^*]$, $h_{it}^*\equiv e^{-g_l t}h_{it}$, and $\boldsymbol{h}_t^*\equiv[h_{1t}^*,h_{2t}^*,...,h_{nt}^*]$. Hence equilibrium conditions (5), (12), (17), (22), (24), (28) and (33) can be re-written in terms of the detrended variables as

$$\boldsymbol{l}^*(t)=\boldsymbol{l}^*(t-1)\mathbf{R}^*(t), \tag{A.9}$$

where $\mathbf{R}^*(t)\equiv\left(\rho_{ij}^*(t)\right)$ is the $n\times n$ matrix of migration probabilities, and

$$\rho_{ij}^*(t)=\frac{(w_{jt}^*/w_{it}^*)^{1/\sigma_\varepsilon}(q_{jt}^*/q_{it}^*)^{-\eta/\sigma_\varepsilon}(\alpha_{ij})^{-1/\sigma_\varepsilon}}{\sum_{s=1}^n(w_{st}^*/w_{it}^*)^{1/\sigma_\varepsilon}(q_{st}^*/q_{it}^*)^{-\eta/\sigma_\varepsilon}(\alpha_{is})^{-1/\sigma_\varepsilon}},\ \text{for } i \text{ and } j\in\mathcal{I}_n, \tag{A.10}$$

and

$$w_{it}^{*} = \tau_{w,i} a_i^{\lambda_a} \left(l_{\cdot i}^{*}(t)\right)^{-\lambda_l}, \text{ for } i \in \mathcal{I}_n, \tag{A.11}$$

$$h_{i,t-1}^{*} = \left(\eta w_{it}^{*}/q_{it}^{*}\right) l_{\cdot i}^{*}(t), \text{ for } i \in \mathcal{I}_n, \tag{A.12}$$

$$x_{it}^{*} = \tau_{\kappa,i}\kappa_i (p_{it}^{*})^{\lambda_{p,i}}, \text{ for } i \in \mathcal{I}_n, \tag{A.13}$$

$$h_{it}^{*} = (1-\delta)e^{-g_l} h_{i,t-1}^{*} + x_{it}^{*}, \text{ for } i \in \mathcal{I}_n, \tag{A.14}$$

$$p_{it}^{*} h_{it}^{*} = \beta\left(1-\theta_i\right)\left[q_{it}^{*} + (1-\delta)p_{it}^{*}\right] h_{i,t-1}^{*}, \text{ for } i \in \mathcal{I}_n, \tag{A.15}$$

A1.4 Derivation of balanced growth path migration probabilities

To derive the balanced growth path migration probability equation (55), we first observe that the long run rent-to-price ratio in location i can be obtained from (54) and is given by

$$\frac{q_i^{*}}{p_i^{*}} = \Gamma_i, \tag{A.16}$$

where Γ_i is given by

$$\Gamma_i = \frac{1}{\beta\left(1-\theta_i\right)} - (1-\delta). \tag{A.17}$$

Note that β and $\theta_i \in (0,1)$, which implies $\beta^{-1}\left(1-\theta_i\right)^{-1} > 1$. Since $\delta > 0$, it follows that $\Gamma_i > \delta > 0$. Using this result in (51), we obtain the long-run demand function for housing in location i:

$$h_i^{*} = \frac{\eta w_i^{*} l_{\cdot i}^{*}}{\Gamma_i p_i^{*}} \tag{A.18}$$

By substituting (53) into (52), we obtain the long-run housing supply function in location i:

$$h_i^{*} = \tilde{\delta}^{-1}\tau_{\kappa,i}\kappa_i (p_i^{*})^{\lambda_{p,i}}, \tag{A.19}$$

where $\tilde{\delta} \equiv 1 - (1-\delta)\, e^{-g_l}$. By substituting (A.19) into (A.18) for h_i^{*}, we have

$$\tilde{\delta}^{-1}\tau_{\kappa,i}\kappa_i (p_i^{*})^{\lambda_{p,i}} = \frac{\eta w_i^{*} l_{\cdot i}^{*}}{\Gamma_i p_i^{*}}.$$

Using the above equation, we can solve for p_i^{*}

$$p_i^{*} = \left(\frac{\tilde{\delta}\eta}{\tau_{\kappa,i}\kappa_i}\right)^{\frac{1}{1+\lambda_{p,i}}} \Gamma_i^{-\frac{1}{1+\lambda_{p,i}}} \left(w_i^{*} l_{\cdot i}^{*}\right)^{\frac{1}{1+\lambda_{p,i}}}, \tag{A.20}$$

and by substituting (A.20) into (A.16) for p_i^{*}, we have

$$q_i^{*} = \left(\frac{\tilde{\delta}\eta}{\tau_{\kappa,i}\kappa_i}\right)^{\frac{1}{1+\lambda_{p,i}}} \Gamma_i^{\frac{\lambda_{p,i}}{1+\lambda_{p,i}}} \left(w_i^{*} l_{\cdot i}^{*}\right)^{\frac{1}{1+\lambda_{p,i}}}. \tag{A.21}$$

By substituting (A.20) into (A.19) for p_i^*, we obtain

$$h_i^* = \left(\frac{\tilde{\delta}}{\tau_{\kappa,i}\kappa_i}\right)^{-\frac{1}{1+\lambda_{p,i}}} \left(\frac{\eta}{\Gamma_i}\right)^{\frac{\lambda_{p,i}}{1+\lambda_{p,i}}} \left(w_i^* l_{\cdot i}^*\right)^{\frac{\lambda_{p,i}}{1+\lambda_{p,i}}}. \tag{A.22}$$

Finally, by substituting (A.22) into (53) for h_i^*, we obtain

$$x_i^* = \left(\frac{1}{\tau_{\kappa,i}\kappa_i}\right)^{-\frac{1}{1+\lambda_{p,i}}} \left(\frac{\tilde{\delta}\eta}{\Gamma_i}\right)^{\frac{\lambda_{p,i}}{1+\lambda_{p,i}}} \left(w_i^* l_{\cdot i}^*\right)^{\frac{\lambda_{p,i}}{1+\lambda_{p,i}}}, \tag{A.23}$$

Therefore, p_i^*, q_i^*, x_i^* and h_i^* can be obtained uniquely in terms of $l_{\cdot i}^*, w_i^*$,and κ_i using (51) - (54).

By substituting (50) and (A.21) into (49) for $q_i^*$and w_i^*, then ρ_{ij}^* can be written as a function of $\boldsymbol{l}^*$:

$$\rho_{ij}^* = \frac{\psi_{ij}\left(l_{\cdot j}^*\right)^{-\varphi_j}}{\sum_{s=1}^n \psi_{is}\left(l_{\cdot s}^*\right)^{-\varphi_s}}, \tag{A.24}$$

where

$$\begin{aligned}
\varphi_j &= \frac{1}{\sigma_\varepsilon}\left[\frac{\eta}{1+\lambda_{p,j}} + \lambda_l\left(1 - \frac{\eta}{1+\lambda_{p,j}}\right)\right], \\
\psi_{ij} &= \alpha_{ij}^{-1/\sigma_\varepsilon}\left(\frac{\tilde{\delta}\eta}{\tau_{\kappa,j}\kappa_j}\right)^{-\frac{\eta}{\sigma_\varepsilon\left(1+\lambda_{p,j}\right)}} \Gamma_j^{-\frac{\eta\lambda_{p,j}}{\sigma_\varepsilon\left(1+\lambda_{p,j}\right)}} \left(\tau_{w,j}a_j^{\lambda_a}\right)^{\frac{1}{\sigma_\varepsilon}\left(1-\frac{\eta}{1+\lambda_{p,j}}\right)}.
\end{aligned}$$

Since σ_ε, λ_l and $\lambda_{p,j} > 0$, and $\eta \in (0,1)$, it follows that $\varphi_j > 0$, for any $i \in \mathcal{I}_n$. In addition, note that $\psi_{ij} > 0$, for any i and $j \in \mathcal{I}_n$, since $\alpha_{ij}, \tilde{\delta}, \eta, \tau_{\kappa,i}, \tau_{w,i}, \kappa_j, \sigma_\varepsilon$ and $a_j > 0$, and Γ_j, given by (A.17), is strictly positive as previously shown.

A1.5 Existence and uniqueness of short-run equilibrium

Proposition A1 *Consider the dynamic spatial equilibrium model set up in Sections 2 and 3 by equations (5), (12), (17), (22), (24), (28) and (33), which can be written equivalently in terms of detrended variables by equations (A.9) to (A.15) in Appendix A1.3. Suppose that the vectors of exogenous processes for labor productivities, $\boldsymbol{a}_t$, land supplies, $\boldsymbol{\kappa}_t$, and the intrinsic population growth rates, $\boldsymbol{g}_{lt}$, for $t = 1, 2, ...$, are given by (41)-(43), condition (44) holds, and the initial values for local population and housing stocks ($\boldsymbol{l}_0$ and $\boldsymbol{h}_0$) are strictly positive. Then the model has a unique short-run equilibrium in the sense set out in Definition 1.*

Proof: To prove the existence and uniqueness of the short-run equilibrium, we show that given $\boldsymbol{l}_{t-1}^*$ and $\boldsymbol{h}_{t-1}^*$, where $\boldsymbol{l}_{t-1}^*$ and $\boldsymbol{h}_{t-1}^*$ are strictly positive, then $\boldsymbol{w}_t^*, \boldsymbol{q}_t^*, \boldsymbol{p}_t^*, \boldsymbol{l}_t^*, \boldsymbol{x}_t^*, \boldsymbol{h}_t^*$ and $\mathbf{R}_t^*$ are uniquely determined by equations (A.9) to (A.15). We first establish that $l_{\cdot i}^*(t) > 0$, for all i, and hence $1 > \rho_{ij}^*(t) > 0$, for all i and $j \in \mathcal{I}_n$. Since by assumption aggregate

population across all locations cannot be negative, then $\sum_{i=1}^{n} l_{\cdot i}^{*}(t) > 0$, where $l_{\cdot i}^{*}(t)$ denotes the i^{th} element of $\boldsymbol{l}_t^{*}$. Hence, there must be at least one location with non-zero population, such that $l_{\cdot i}^{*}(t) > 0$ for at least one $i \in \mathcal{I}_n$. Here without loss of generality we assume that $l_{\cdot 1}^{*}(t) > 0$. Also since $l_{\cdot 1}^{*}(t)$ is the first element in $\boldsymbol{l}_t^{*}$, then from (A.9) we have

$$l_{\cdot 1}^{*}(t) = \sum_{i=1}^{n} \rho_{i1}^{*}(t) l_{\cdot i}^{*}(t-1), \tag{A.25}$$

and upon using (A.10), (A.11) and (A.12), we obtain

$$\rho_{ij}^{*}(t) = \frac{\alpha_{ij}^{-\frac{1}{\sigma_\varepsilon}} \left(\tau_{w,j} a_j^{\lambda_a}\right)^{\frac{1-\eta}{\sigma_\varepsilon}} \left(h_{j,t-1}^{*}\right)^{\frac{\eta}{\sigma_\varepsilon}} \left(l_{\cdot j}^{*}(t)\right)^{-\frac{\eta+\lambda_l(1-\eta)}{\sigma_\varepsilon}}}{\sum_{s=1}^{n} \alpha_{is}^{-\frac{1}{\sigma_\varepsilon}} \left(\tau_{w,s} a_s^{\lambda_a}\right)^{\frac{1-\eta}{\sigma_\varepsilon}} \left(h_{s,t-1}^{*}\right)^{\frac{\eta}{\sigma_\varepsilon}} \left(l_{\cdot s}^{*}(t)\right)^{-\frac{\eta+\lambda_l(1-\eta)}{\sigma_\varepsilon}}}, \tag{A.26}$$

which implies $\rho_{i1}^{*}(t)$ in equation (A.25) is given by

$$\begin{aligned}
\rho_{i1}^{*}(t) &= \frac{\alpha_{i1}^{-\frac{1}{\sigma_\varepsilon}} \left(\tau_{w,1} a_1^{\lambda_a}\right)^{\frac{1-\eta}{\sigma_\varepsilon}} \left(h_{1,t-1}^{*}\right)^{\frac{\eta}{\sigma_\varepsilon}} \left(l_{\cdot 1}^{*}(t)\right)^{-\frac{\eta+\lambda_l(1-\eta)}{\sigma_\varepsilon}}}{\sum_{s=1}^{n} \alpha_{is}^{-\frac{1}{\sigma_\varepsilon}} \left(\tau_{w,s} a_s^{\lambda_a}\right)^{\frac{1-\eta}{\sigma_\varepsilon}} \left(h_{s,t-1}^{*}\right)^{\frac{\eta}{\sigma_\varepsilon}} \left(l_{\cdot s}^{*}(t)\right)^{-\frac{\eta+\lambda_l(1-\eta)}{\sigma_\varepsilon}}}, \\
&= \frac{1}{1 + \sum_{s \neq i} \left(\frac{\alpha_{is}^{-\frac{1}{\sigma_\varepsilon}} \left(\tau_{w,s} a_s^{\lambda_a}\right)^{\frac{1-\eta}{\sigma_\varepsilon}} \left(h_{s,t-1}^{*}\right)^{\frac{\eta}{\sigma_\varepsilon}}}{\alpha_{i1}^{-\frac{1}{\sigma_\varepsilon}} \left(\tau_{w,1} a_1^{\lambda_a}\right)^{\frac{1-\eta}{\sigma_\varepsilon}} \left(h_{1,t-1}^{*}\right)^{\frac{\eta}{\sigma_\varepsilon}}} \right) \left(\frac{l_{\cdot 1}^{*}(t)}{l_{\cdot s}^{*}(t)} \right)^{\frac{\eta+\lambda_l(1-\eta)}{\sigma_\varepsilon}}}.
\end{aligned} \tag{A.27}$$

Note that $\eta \in (0,1)$ and $\lambda_l, \tau_{w,s}, \sigma_\varepsilon$, α_{is} and $a_s > 0$ by assumption, and also that $h_{s,t-1}^{*} > 0$, for $t = 1, 2, ...$, since $h_{s0} > 0$ and the depreciation rate of housing stock δ is less than one. Thus, $\alpha_{is}^{-1/\sigma_\varepsilon} \left(\tau_{w,s} a_s^{\lambda_a}\right)^{(1-\eta)/\sigma_\varepsilon} \left(h_{s,t-1}^{*}\right)^{\eta/\sigma_\varepsilon} > 0$. In addition, it is supposed that $l_{\cdot 1}^{*}(t) > 0$. Hence, if $l_{\cdot s}^{*}(t) = 0$, for any $s \in \{2, 3, ..., n\}$, then $\rho_{i1}^{*}(t) = 0$, for all $i \in \mathcal{I}_n$, and using (A.27) it follows that $l_{\cdot 1}^{*}(t) = 0$, which contradicts our supposition. The same line of reasoning can be applied to any other elements of $\boldsymbol{l}_t^{*}$, and we must have $l_{\cdot 1}^{*}(t) > 0$, for any $i \in \mathcal{I}_n$.

Second, let $\mathcal{L}_t(\epsilon)$ with $\epsilon > 0$, be a set of population vector:

$$\mathcal{L}_t(\epsilon) \equiv \left\{ (l_{\cdot 1}^{*}(t), ..., l_{\cdot n}^{*}(t)) \,\middle|\, L_0 \geq l_{\cdot i}^{*}(t) \geq \epsilon \text{ for any } i, \text{ where } \epsilon > 0, \sum_{i=1}^{n} l_{\cdot i}^{*}(t) = L_0 \right\}$$

Consider a mapping F, define

$$F(\boldsymbol{l}_t^{*}) = \boldsymbol{l}_{t-1}^{*} \mathbf{R}(\boldsymbol{l}_t^{*}; \boldsymbol{h}_{t-1}^{*}),$$

where $\boldsymbol{l}_{t-1}^{*}$ and $\boldsymbol{h}_{t-1}^{*}$ are given, and $\mathbf{R}(\boldsymbol{l}_t^{*}, \boldsymbol{h}_{t-1}^{*})$ is the migration probability matrix with typical element $\rho_{ij}^{*}(t)$, which is given by (A.26). Thus, for (A.9) to hold, the above mapping

should have a fixed point. Consider a $\boldsymbol{l}_t^* \in \mathcal{L}_t(\epsilon)$. Note that $l_{\cdot i}^*(t)$ is the ith element of $\boldsymbol{l}_t^*$ and satisfies $L_0 \geq l_{\cdot i}^*(t) \geq \epsilon$, for $i = 1, 2, ..., n$. Then, by using (A.26), we have

$$\begin{aligned}
\rho_{ij}^*(t) &= \frac{\alpha_{ij}^{-\frac{1}{\sigma_\varepsilon}} \left(\tau_{w,j} a_j^{\lambda_a}\right)^{\frac{1-\eta}{\sigma_\varepsilon}} \left(h_{j,t-1}^*\right)^{\frac{\eta}{\sigma_\varepsilon}} \left(l_{\cdot j}^*(t)\right)^{-\frac{\eta+\lambda_l(1-\eta)}{\sigma_\varepsilon}}}{\sum_{s=1}^n \alpha_{is}^{-\frac{1}{\sigma_\varepsilon}} \left(\tau_{w,s} a_s^{\lambda_a}\right)^{\frac{1-\eta}{\sigma_\varepsilon}} \left(h_{s,t-1}^*\right)^{\frac{\eta}{\sigma_\varepsilon}} \left(l_{\cdot s}^*(t)\right)^{-\frac{\eta+\lambda_l(1-\eta)}{\sigma_\varepsilon}}} \\
&> \frac{\alpha_{ij}^{-\frac{1}{\sigma_\varepsilon}} \left(\tau_{w,j} a_j^{\lambda_a}\right)^{\frac{1-\eta}{\sigma_\varepsilon}} \left(h_{j,t-1}^*\right)^{\frac{\eta}{\sigma_\varepsilon}} (L_0)^{-\frac{\eta+\lambda_l(1-\eta)}{\sigma_\varepsilon}}}{\sum_{s=1}^n \alpha_{is}^{-\frac{1}{\sigma_\varepsilon}} \left(\tau_{w,s} a_s^{\lambda_a}\right)^{\frac{1-\eta}{\sigma_\varepsilon}} \left(h_{s,t-1}^*\right)^{\frac{\eta}{\sigma_\varepsilon}} (\epsilon)^{-\frac{\eta+\lambda_l(1-\eta)}{\sigma_\varepsilon}}} \\
&= \frac{\alpha_{ij}^{-\frac{1}{\sigma_\varepsilon}} \left(\tau_{w,j} a_j^{\lambda_a}\right)^{\frac{1-\eta}{\sigma_\varepsilon}} \left(h_{j,t-1}^*\right)^{\frac{\eta}{\sigma_\varepsilon}} (L_0)^{1-\frac{\eta+\lambda_l(1-\eta)}{\sigma_\varepsilon}}}{\sum_{s=1}^n \alpha_{is}^{-\frac{1}{\sigma_\varepsilon}} \left(\tau_{w,s} a_s^{\lambda_a}\right)^{1-\eta} \left(h_{s,t-1}^*\right)^{\frac{\eta}{\sigma_\varepsilon}} (\epsilon)^{1-\frac{\eta+\lambda_l(1-\eta)}{\sigma_\varepsilon}}} \frac{\epsilon}{L_0}.
\end{aligned}$$

Since η and $\lambda_l \in (0,1)$, and $\sigma_\varepsilon \geq 1$, then $1 - [\eta + \lambda_l (1-\eta)] / \sigma_\varepsilon > 0$. Suppose ϵ is small enough such that

$$\rho_{ij}^*(t) > \frac{\epsilon}{L_0}, \text{ for } i \text{ and } j \in \mathcal{I}_n.$$

Define $\boldsymbol{l}_t^{*'} = F(\boldsymbol{l}_t^*) = \boldsymbol{l}_{t-1}^* \mathbf{R}(\boldsymbol{l}_t^*; \boldsymbol{h}_{t-1}^*)$. Thus we have

$$l_{\cdot j}^{*'}(t) = \sum_{i=1}^n \rho_{ij}^*(t) l_{\cdot i}^*(t-1) > \sum_{i=1}^n \left(\frac{\epsilon}{L_0}\right) l_{\cdot i}^*(t-1) = \left(\frac{\epsilon}{L_0}\right) L_0 = \epsilon \qquad \text{for any } j \in \mathcal{I}_n.$$

In addition,

$$\sum_{j=1}^n l_{\cdot j}^{*'}(t) = \sum_{j=1}^n \sum_{i=1}^n \rho_{ij}^*(t) l_{\cdot i}^*(t-1) = \sum_{i=1}^n l_{\cdot i}^*(t-1) \sum_{j=1}^n \rho_{ij}^*(t) = \sum_{i=1}^n l_{\cdot i}^*(t-1) = L_0.$$

Therefore, when ϵ is small enough such that $\rho_{ij}^*(t) > \epsilon / L_0$ for any $i, j \in \mathcal{I}_n$, then $\boldsymbol{l}_t^* \in \mathcal{L}_t(\epsilon) \Rightarrow \boldsymbol{l}_t^{*'} = F(\boldsymbol{l}_t^*) \in \mathcal{L}_t(\epsilon)$. Thus, F is a continuous mapping from $\mathcal{L}_t(\epsilon)$ to itself, where $\mathcal{L}_t(\epsilon)$ is a compact convex set. Thus, Brouwer Fix Point Theorem is applicable to ensure the existence of fixed point. Then, using the solution of $\boldsymbol{l}_t^*$, the other variables of the model, namely, $\boldsymbol{w}_t^*, \boldsymbol{p}_t^*, \boldsymbol{q}_t^*, \boldsymbol{x}_t^*, \boldsymbol{h}_t^*$and $\mathbf{R}_t^*$, can be solved for using equations (A.10) to (A.15).

Third, to show the uniqueness, suppose there are $\boldsymbol{l}_t^{*(1)}, \boldsymbol{l}_t^{*(2)} \in \mathcal{L}_t(\epsilon)$, with $\boldsymbol{l}_t^{*(1)} \neq \boldsymbol{l}_t^{*(2)}$, and $\boldsymbol{l}_t^{*(1)} = F(\boldsymbol{l}_t^{*(1)})$, $\boldsymbol{l}_t^{*(2)} = F(\boldsymbol{l}_t^{*(2)})$. Define $\mathcal{I}_n^+ \equiv \{j |\ l_{\cdot j}^{*(2)}(t) > l_{\cdot j}^{*(1)}(t),\ j \in \mathcal{I}_n\}$ and $\mathcal{I}_n^- \equiv \{j |\ l_{\cdot j}^{*(2)}(t) \leq l_{\cdot j}^{*(1)}(t),\ j \in \mathcal{I}_n\}$. Thus, neither $\mathcal{I}_n^+$ nor $\mathcal{I}_n^-$ is empty, and we have

$$\sum_{j \in \mathcal{I}_n^+} l_{\cdot j}^{*(2)}(t) > \sum_{j \in \mathcal{I}_n^+} l_{\cdot j}^{*(1)}(t). \tag{A.28}$$

Note that by using (A.26), we have

$$\begin{aligned}\frac{\sum_{j\in\mathcal{I}_n^+}\rho_{ij}^{*(2)}(t)}{\sum_{j\in\mathcal{I}_n^-}\rho_{ij}^{*(2)}(t)} &= \frac{\sum_{j\in\mathcal{I}_n^+}\alpha_{ij}^{-\frac{1}{\sigma_\varepsilon}}\left(\tau_{w,j}a_j^{\lambda_a}\right)^{\frac{1-\eta}{\sigma_\varepsilon}}\left(h_{j,t-1}^*\right)^{\frac{\eta}{\sigma_\varepsilon}}\left(l_{\cdot j}^{*(2)}(t)\right)^{-\frac{\eta+\lambda_l(1-\eta)}{\sigma_\varepsilon}}}{\sum_{j\in\mathcal{I}_n^-}\alpha_{ij}^{-\frac{1}{\sigma_\varepsilon}}\left(\tau_{w,j}a_j^{\lambda_a}\right)^{\frac{1-\eta}{\sigma_\varepsilon}}\left(h_{j,t-1}^*\right)^{\frac{\eta}{\sigma_\varepsilon}}\left(l_{\cdot j}^{*(2)}(t)\right)^{-\frac{\eta+\lambda_l(1-\eta)}{\sigma_\varepsilon}}},\\ &< \frac{\sum_{j\in\mathcal{I}_n^+}\alpha_{ij}^{-\frac{1}{\sigma_\varepsilon}}\left(\tau_{w,j}a_j^{\lambda_a}\right)^{\frac{1-\eta}{\sigma_\varepsilon}}\left(h_{j,t-1}^*\right)^{\frac{\eta}{\sigma_\varepsilon}}\left(l_{\cdot j}^{*(1)}(t)\right)^{-\frac{\eta+\lambda_l(1-\eta)}{\sigma_\varepsilon}}}{\sum_{j\in\mathcal{I}_n^-}\alpha_{ij}^{-\frac{1}{\sigma_\varepsilon}}\left(\tau_{w,j}a_j^{\lambda_a}\right)^{\frac{1-\eta}{\sigma_\varepsilon}}\left(h_{j,t-1}^*\right)^{\frac{\eta}{\sigma_\varepsilon}}\left(l_{\cdot j}^{*(1)}(t)\right)^{-\frac{\eta+\lambda_l(1-\eta)}{\sigma_\varepsilon}}},\\ &= \frac{\sum_{j\in\mathcal{I}_n^+}\rho_{ij}^{*(1)}(t)}{\sum_{j\in\mathcal{I}_n^-}\rho_{ij}^{*(1)}(t)}.\end{aligned}$$

Note also that

$$\sum_{j\in\mathcal{I}_n^+}\rho_{ij}^{*(2)}(t)+\sum_{j\in\mathcal{I}_n^-}\rho_{ij}^{*(2)}(t)=\sum_{j\in\mathcal{I}_n^+}\rho_{ij}^{*(1)}(t)+\sum_{j\in\mathcal{I}_n^-}\rho_{ij}^{*(1)}(t)=1.$$

Thus,

$$\sum_{j\in\mathcal{I}_n^+}\rho_{ij}^{*(2)}(t)<\sum_{j\in\mathcal{I}_n^+}\rho_{ij}^{*(1)}(t)\qquad\text{for any } i\in\mathcal{I}_n. \tag{A.29}$$

Since $\boldsymbol{l}_t^{*(1)}=F(\boldsymbol{l}_t^{*(1)})$, $\boldsymbol{l}_t^{*(2)}=F(\boldsymbol{l}_t^{*(2)})$, thus for any $j\in\mathcal{I}$

$$l_{\cdot j}^{*(2)}(t)=\sum_{i\in\mathcal{I}}\rho_{ij}^{*(2)}(t)l_{\cdot i}^*(t-1)\qquad\text{and}\qquad l_{\cdot j}^{*(1)}(t)=\sum_{i\in\mathcal{I}}\rho_{ij}^{*(1)}(t)l_{\cdot i}^*(t-1)$$

Then, we have

$$\begin{aligned}\sum_{j\in\mathcal{I}_n^+}(l_{\cdot j}^{*(2)}(t)-l_{\cdot j}^{*(1)}(t)) &= \sum_{j\in\mathcal{I}_n^+}\sum_{i\in\mathcal{I}}\rho_{ij}^{*(2)}(t)l_{\cdot i}^*(t-1)-\sum_{j\in\mathcal{I}_n^+}\sum_{i\in\mathcal{I}}\rho_{ij}^{*(1)}(t)l_{\cdot i}^*(t-1)\\ &= \sum_{i\in\mathcal{I}}\sum_{j\in\mathcal{I}_n^+}\left(\rho_{ij}^{*(2)}(t)-\rho_{ij}^{*(1)}(t)\right)l_{\cdot i}^*(t-1)\\ &= \sum_{i\in\mathcal{I}}\left(\sum_{j\in\mathcal{I}_n^+}\rho_{ij}^{*(2)}(t)-\sum_{j\in\mathcal{I}_n^+}\rho_{ij}^{*(1)}(t)\right)l_{\cdot i}^*(t-1)\\ &< 0\end{aligned}$$

Thus, the above contradicts with (A.28), which implies that $\boldsymbol{l}_t^{*(1)}\neq\boldsymbol{l}_t^{*(2)}$ cannot be true. ■

A1.6 Lemmas: statements and proofs

Lemma A1 *Consider the following Markovian process in* $\boldsymbol{l}^*(t)$

$$\boldsymbol{l}^*(t)=\boldsymbol{l}^*(t-1)\mathbf{R}^*(t) \tag{A.30}$$

where $\boldsymbol{l}^*(t) = [l^*_{\cdot 1}(t), l^*_{\cdot 2}(t), ..., l^*_{\cdot n}(t)]$ *is the* $1 \times n$ *row vector of detrended population values, and* $\mathbf{R}^*(t) = (\rho^*_{ij}(t))$ *is the* $n \times n$ *transition matrix with the typical element,* $\rho^*_{ij}(t)$ *defined by (A.10) that depends non-linearly on* $\boldsymbol{l}^*(t)$*, and* n *is a fixed integer. Suppose that the initial population vector,* $\boldsymbol{l}^*(0) = \boldsymbol{l}(0)$*, is given and satisfies the conditions* $\boldsymbol{l}(0) > 0$*, and* $\sum_{i=1}^n l_{\cdot i}(0) = L_0$*, where* $0 < L_0 < K$*. Then* $\boldsymbol{l}^*(t)$ *converges to a finite population vector,* $\boldsymbol{l}^*(\infty)$*, or simply* $\boldsymbol{l}^* = [l^*_{\cdot 1}, l^*_{\cdot 2}, ..., l^*_{\cdot n}]$*, as* $t \to \infty$*, with* $l^*_{\cdot i} \geq 0$*, and* $\sum_{i=1}^n l^*_{\cdot i} = L_0$

Proof: We first note that by construction $0 \leq \rho^*_{ij}(t) \leq 1$ for all i and j, and $\sum_{j=1}^n \rho^*_{ij}(t) = 1$, for all j. Hence, for each t, $\mathbf{R}^*(t)$ is a right stochastic matrix with $\mathbf{R}^*(t)\boldsymbol{\tau}_n = \boldsymbol{\tau}_n$, where $\boldsymbol{\tau}_n$ is an $n \times 1$ vector of ones, for all t. Recursively solving (A.30) forward from $\boldsymbol{l}^*(0)$, we have

$$\boldsymbol{l}^*(t) = \boldsymbol{l}^*(0) \left[\Pi_{s=1}^t \mathbf{R}^*(s)\right],$$

But it is easily seen that $\left[\Pi_{s=1}^t \mathbf{R}^*(s)\right] \boldsymbol{\tau}_n = \boldsymbol{\tau}_n$, and hence

$$\sum_{i=1}^n l^*_{\cdot i}(t) = \boldsymbol{l}^*(t)\boldsymbol{\tau}_n = \boldsymbol{l}^*(0)\boldsymbol{\tau}_n = L_0. \tag{A.31}$$

Also, since $\boldsymbol{l}^*(0) = \boldsymbol{l}(0) > 0$, $\rho^*_{ij}(t) \geq 0$, and n is finite, then $\boldsymbol{l}^*(t) = [l^*_{\cdot 1}(t), l^*_{\cdot 2}(t), ..., l^*_{\cdot n}(t)] \geq 0$, for all t, and in view of (A.31) we have $\sup_{it}(l^*_{\cdot i}(t)) \leq L_0 < K$. Therefore, $\boldsymbol{l}^*(t)$ must converge to some vector $\boldsymbol{l}^*$ which is bounded in t, as $t \to \infty$. ■

Lemma A2 *Consider the system of non-linear equations in* $l_{\cdot i}$*, for* $i \in \mathcal{I}_n$*:*

$$\boldsymbol{l} = \boldsymbol{l}\mathbf{R}\left(\boldsymbol{l}\right) \tag{A.32}$$

where $\boldsymbol{l} = [l_{\cdot 1}, l_{\cdot 2}, ..., l_{\cdot n}]$*,* $\boldsymbol{l} \geq 0$*,* $\sum_{i=1}^n l_{\cdot i} = L_0$*,* $0 < L_0 < K$*,* n *is fixed, and the typical element of matrix* $\mathbf{R}$ *is given by*

$$\rho_{ij} = \frac{\psi_{ij}\left(l_{\cdot j}\right)^{-\varphi_j}}{\sum_{s \in \mathcal{I}_n} \psi_{is}\left(l_{\cdot s}\right)^{-\varphi_s}}, \tag{A.33}$$

where ψ_{ij} *and* $\varphi_j > 0$*, for any* i *and* $j \in \mathcal{I}_n$*. Then, the solution to (A.32) must be strictly positive,* $l_{\cdot i} > 0$ *for* $i \in \mathcal{I}_n$*, and unique.*

Proof. We first show that $l_{\cdot i} > 0$, for all i, and hence $1 > \rho_{ij} > 0$, for all i and $j \in \mathcal{I}_n$. Consider a population vector $\boldsymbol{l} = [l_{\cdot 1}, l_{\cdot 2}, ..., l_{\cdot n}]$, that solves (A.32). Note that $\sum_{i=1}^n l_{\cdot i} > 0$, and $l_{\cdot i}$ is non-negative for any $i \in \mathcal{I}_n$. Thus, $l_{\cdot i} > 0$ has to hold for at least one i. Without loss of generality, we assume

$$l_{\cdot 1} > 0. \tag{A.34}$$

Note also that since $l_{\cdot 1}$ is the first element in $\boldsymbol{l}$, then from (A.32) we have

$$l_{\cdot 1} = \sum_{i=1}^n \rho_{i1} l_{\cdot i}, \tag{A.35}$$

where, upon using (A.33), ρ_{i1} is given by

$$\rho_{i1} = \frac{1}{1 + \sum_{s \neq i} \left(\frac{\psi_{is}}{\psi_{i1}}\right) \frac{(l_{.1})^{\varphi_1}}{(l_{.s})^{\varphi_s}}}, \text{ for } i = 1, 2, ..., n. \tag{A.36}$$

Note that by assumption ψ_{ij} and $\varphi_j > 0$, and it is supposed that $l_{.1} > 0$. Hence, if $l_{.s} = 0$, for any $s \in \{2, 3, ..., n\}$, then $\rho_{i1} = 0$, for all $i \in \mathcal{I}_n$, and using (A.35) it follows that $l_{.1} = 0$, which contradicts our supposition. The same line of reasoning can be applied to any other elements of $\boldsymbol{l}$, and we must have $l_{.i} > 0$, for any $i \in \mathcal{I}_n$.

Given that $l_{.i} > 0$, for all i, we now show that (A.32) cannot have more than one solution. Suppose there exist two solutions $\boldsymbol{l}^{(1)}$ and $\boldsymbol{l}^{(2)}$, with $\boldsymbol{l}^{(1)}$ and $\boldsymbol{l}^{(2)} > 0$, $\boldsymbol{l}^{(1)} \neq \boldsymbol{l}^{(2)}$, such that $\boldsymbol{l}^{(1)} = \boldsymbol{l}^{(1)}\boldsymbol{R}\left(\boldsymbol{l}^{(1)}\right)$ and $\boldsymbol{l}^{(2)} = \boldsymbol{l}^{(2)}\boldsymbol{R}\left(\boldsymbol{l}^{(2)}\right)$. Denote the j^{th} elements of $\boldsymbol{l}^{(1)}$ and $\boldsymbol{l}^{(2)}$ by $l_{.j}^{(1)}$ and $l_{.j}^{(2)}$, respectively. Split the locations into two groups, $\mathcal{I}_n^+$ and $\mathcal{I}_n^-$, where $\mathcal{I}_n^+ \equiv \{j \mid l_{.j}^{(2)} > l_{.j}^{(1)}, j \in \mathcal{I}_n\}$, and $\mathcal{I}_n^- \equiv \{j \mid l_{.j}^{(2)} \leq l_{.j}^{(1)}, j \in \mathcal{I}_n\}$, and note that $\mathcal{I}_n^+ \cap \mathcal{I}_n^- = \emptyset$ and $\mathcal{I}_n^+ \cup \mathcal{I}_n^- = \mathcal{I}_n$. That is,

$$l_{.j}^{(2)} \begin{cases} > l_{.j}^{(1)} & \text{if } j \in \mathcal{I}_n^+ \\ \leq l_{.j}^{(1)} & \text{if } j \in \mathcal{I}_n^- \end{cases}. \tag{A.37}$$

Further, since $\sum_{j=1}^n l_j^{(1)} = \sum_{j=1}^n l_j^{(2)} = L_0$, and $\boldsymbol{l}^{(1)} \neq \boldsymbol{l}^{(2)}$, it also follows that neither $\mathcal{I}_n^+$ nor $\mathcal{I}_n^-$ can be empty. Thus, we have

$$\sum_{j \in \mathcal{I}_n^+} l_{.j}^{(2)} > \sum_{j \in \mathcal{I}_n^+} l_{.j}^{(1)}. \tag{A.38}$$

Recall that $\rho_{ij}^{(1)}$ and $\rho_{ij}^{(2)}$ are the typical elements of $\boldsymbol{R}\left(\boldsymbol{l}^{(1)}\right)$ and $\boldsymbol{R}\left(\boldsymbol{l}^{(2)}\right)$, respectively. For any $i \in \mathcal{I}_n$, using (A.33), we have (recall that $l_{.j}^{(1)} > 0$ and $l_{.j}^{(2)} > 0$)

$$\frac{\sum_{j \in \mathcal{I}_n^+} \rho_{ij}^{(2)}}{\sum_{j \in \mathcal{I}_n^-} \rho_{ij}^{(2)}} = \frac{\sum_{j \in \mathcal{I}_n^+} \psi_{ij} \left(l_{.j}^{(2)}\right)^{-\varphi_j}}{\sum_{j \in \mathcal{I}_n^-} \psi_{ij} \left(l_{.j}^{(2)}\right)^{-\varphi_j}}, \tag{A.39}$$

$$\frac{\sum_{j \in \mathcal{I}_n^+} \rho_{ij}^{(1)}}{\sum_{j \in \mathcal{I}_n^-} \rho_{ij}^{(1)}} = \frac{\sum_{j \in \mathcal{I}_n^+} \psi_{ij} \left(l_{.j}^{(1)}\right)^{-\varphi_j}}{\sum_{j \in \mathcal{I}_n^-} \psi_{ij} \left(l_{.j}^{(1)}\right)^{-\varphi_j}}. \tag{A.40}$$

Since by (A.37), $l_{.j}^{(2)} > l_{.j}^{(1)}$, if $j \in \mathcal{I}_n^+$, and $l_{.j}^{(2)} \leq l_{.j}^{(1)}$, if $j \in \mathcal{I}_n^-$, then (recall that $\psi_{ij} > 0$ and $\varphi_j > 0$)

$$\begin{aligned} \sum_{j \in \mathcal{I}_n^+} \psi_{ij} \left(l_{.j}^{(2)}\right)^{-\varphi_j} &< \sum_{j \in \mathcal{I}_n^+} \psi_{ij} \left(l_{.j}^{(1)}\right)^{-\varphi_j}, \\ \sum_{j \in \mathcal{I}_n^-} \psi_{ij} \left(l_{.j}^{(2)}\right)^{-\varphi_j} &\geq \sum_{j \in \mathcal{I}_n^-} \psi_{ij} \left(l_{.j}^{(1)}\right)^{-\varphi_j}. \end{aligned}$$

Hence, using the above results in (A.39) and (A.40) we have

$$\frac{\sum_{j\in\mathcal{I}_n^+}\rho_{ij}^{(2)}}{\sum_{j\in\mathcal{I}_n^-}\rho_{ij}^{(2)}} < \frac{\sum_{j\in\mathcal{I}_n^+}\rho_{ij}^{(1)}}{\sum_{j\in\mathcal{I}_n^-}\rho_{ij}^{(1)}}, \qquad \forall\ i\in\mathcal{I}_n,$$

and it follows that

$$\frac{\sum_{j\in\mathcal{I}_n^+}\rho_{ij}^{(2)}+\sum_{j\in\mathcal{I}_n^-}\rho_{ij}^{(2)}}{\sum_{j\in\mathcal{I}_n^+}\rho_{ij}^{(2)}} > \frac{\sum_{j\in\mathcal{I}_n^+}\rho_{ij}^{(1)}+\sum_{j\in\mathcal{I}_n^-}\rho_{ij}^{(1)}}{\sum_{j\in\mathcal{I}_n^+}\rho_{ij}^{(1)}}, \qquad \forall\ i\in\mathcal{I}_n.$$

Since $\rho_{ij}^{(1)}$ and $\rho_{ij}^{(2)}$ are migration probabilities,

$$\sum_{j\in\mathcal{I}_n^+}\rho_{ij}^{(2)}+\sum_{j\in\mathcal{I}_n^-}\rho_{ij}^{(2)} = \sum_{j\in\mathcal{I}_n^+}\rho_{ij}^{(1)}+\sum_{j\in\mathcal{I}_n^-}\rho_{ij}^{(1)} = 1.$$

Thus, we have

$$\sum_{j\in\mathcal{I}_n^+}\rho_{ij}^{(2)} < \sum_{j\in\mathcal{I}_n^+}\rho_{ij}^{(1)}, \qquad \forall\ i\in\mathcal{I}_n. \tag{A.41}$$

Note that $l_{.j}^{(1)}$ and $l_{.j}^{(2)}$ are given by

$$l_{.j}^{(1)} = \sum_{i\in\mathcal{I}_n}\rho_{ij}^{(1)}l_{.i}^{(1)} \qquad \text{and} \qquad l_{.j}^{(2)} = \sum_{i\in\mathcal{I}_n}\rho_{ij}^{(2)}l_{.i}^{(2)}.$$

Thus, we have

$$\begin{aligned}\sum_{j\in\mathcal{I}_n^+}l_{.j}^{(2)}-\sum_{j\in\mathcal{I}_n^+}l_{.j}^{(1)} &= \sum_{j\in\mathcal{I}_n^+}\sum_{i\in\mathcal{I}_n}\rho_{ij}^{(2)}l_{.i}^{(2)}-\sum_{j\in\mathcal{I}_n^+}\sum_{i\in\mathcal{I}_n}\rho_{ij}^{(1)}l_{.i}^{(1)}\ ,\\ &= \sum_{i\in\mathcal{I}_n}l_{.i}^{(2)}\sum_{j\in\mathcal{I}_n^+}\rho_{ij}^{(2)}-\sum_{i\in\mathcal{I}_n}l_{.i}^{(1)}\sum_{j\in\mathcal{I}_n^+}\rho_{ij}^{(1)}\ .\end{aligned}$$

Since $\sum_{j\in\mathcal{I}_n^+}\rho_{ij}^{(2)} < \sum_{j\in\mathcal{I}_n^+}\rho_{ij}^{(1)}$ as previously shown in (A.41), then

$$\begin{aligned}\sum_{j\in\mathcal{I}_n^+}l_{.j}^{(2)}-\sum_{j\in\mathcal{I}_n^+}l_{.j}^{(1)} &< \sum_{i\in\mathcal{I}_n}l_{.i}^{(2)}\sum_{j\in\mathcal{I}_n^+}\rho_{ij}^{(1)}-\sum_{i\in\mathcal{I}_n}l_{.i}^{(1)}\sum_{j\in\mathcal{I}_n^+}\rho_{ij}^{(1)},\\ &= \sum_{i\in\mathcal{I}_n}\left[\left(l_{.i}^{(2)}-l_{.i}^{(1)}\right)\sum_{j\in\mathcal{I}_n^+}\rho_{ij}^{(1)}\right].\end{aligned} \tag{A.42}$$

Since by (A.37), $l_{.i}^{(2)} > l_{.i}^{(1)}$, if $i\in\mathcal{I}_n^+$, and $l_{.i}^{(2)} \le l_{.i}^{(1)}$, if $i\in\mathcal{I}_n^-$, and $\sum_{j\in\mathcal{I}_n^+}\rho_{ij}^{(1)} > 0$ by

construction, then

$$\begin{aligned}
&\sum_{i\in\mathcal{I}_n}\left[\left(l_{\cdot i}^{(2)}-l_{\cdot i}^{(1)}\right)\sum_{j\in\mathcal{I}_n^+}\rho_{ij}^{(1)}\right]\\
=&\sum_{i\in\mathcal{I}_n^+}\left[\left(l_{\cdot i}^{(2)}-l_{\cdot i}^{(1)}\right)\sum_{j\in\mathcal{I}_n^+}\rho_{ij}^{(1)}\right]+\sum_{i\in\mathcal{I}_n^-}\left[\left(l_{\cdot i}^{(2)}-l_{\cdot i}^{(1)}\right)\sum_{j\in\mathcal{I}_n^+}\rho_{ij}^{(1)}\right],\\
<&\sum_{i\in\mathcal{I}_n^+}\left[\left(l_{\cdot i}^{(2)}-l_{\cdot i}^{(1)}\right)\sum_{j\in\mathcal{I}_n^+}\rho_{ij}^{(1)}\right].
\end{aligned}$$

Note that $\rho_{ij}^{(1)}$ are migration probabilities, and $\sum_{j\in\mathcal{I}_n^+}\rho_{ij}^{(1)}<1$ by construction, and that $l_{\cdot i}^{(2)}-l_{\cdot i}^{(1)}>0$, if $i\in\mathcal{I}_n^+$. Then, we have

$$\sum_{i\in\mathcal{I}_n^+}\left[\left(l_{\cdot i}^{(2)}-l_{\cdot i}^{(1)}\right)\sum_{j\in\mathcal{I}_n^+}\rho_{ij}^{(1)}\right]<\sum_{i\in\mathcal{I}_n^+}\left(l_{\cdot i}^{(2)}-l_{\cdot i}^{(1)}\right),$$

and thus

$$\sum_{i\in\mathcal{I}_n}\left[\left(l_{\cdot i}^{(2)}-l_{\cdot i}^{(1)}\right)\sum_{j\in\mathcal{I}_n^+}\rho_{ij}^{(1)}\right]<\sum_{i\in\mathcal{I}_n^+}l_{\cdot i}^{(2)}-\sum_{i\in\mathcal{I}_n^+}l_{\cdot i}^{(1)},$$

which contradicts (A.42). Thus, $\boldsymbol{l}\neq\boldsymbol{l}^*$ cannot hold.■

A1.7 Derivation of new land supplies, κ_{it}

To derive (70), we first note that by using (16) in (22) to eliminate w_{it}, we have

$$h_{i,t-1}=\eta\upsilon_l\left(\frac{y_{it}}{q_{it}}\right). \tag{A.43}$$

By using the above equation in (33) to eliminate $h_{i,t-1}$, we have

$$h_{it}=\beta e^{g_l}\left(1-\theta_i\right)\left[\frac{q_{it}}{p_{it}}+(1-\delta)\right]\eta\upsilon_l\left(\frac{y_{it}}{q_{it}}\right). \tag{A.44}$$

Then, by using (A.43) and (A.44) in (28), we have

$$\begin{aligned}
x_{it}&=h_{it}-(1-\delta)h_{i,t-1},\\
&=\left\{\beta e^{g_l}\left(1-\theta_i\right)\left[\frac{q_{it}}{p_{it}}+(1-\delta)\right]-(1-\delta)\right\}\eta\upsilon_l\left(\frac{y_{it}}{q_{it}}\right).
\end{aligned}$$

By combing the above equation with (25) and (24), we have

$$\kappa_{it} = \frac{\gamma_{it}}{\tau_{\kappa,i}},$$

where

$$\gamma_{it} = \frac{\left\{\beta e^{g_l}\left(1-\theta_i\right)\left[\frac{q_{it}}{p_{it}}+\left(1-\delta\right)\right]-\left(1-\delta\right)\right\}\eta\upsilon_l\left(\frac{y_{it}}{q_{it}}\right)}{p_{it}^{(1-\vartheta_{\kappa,i})/\vartheta_{\kappa,i}}}.$$

A2 Data sources and measurements

A2.1 Interstate migration and population growth

Between states migration flows are measured using annual data from the Internal Revenue Service (IRS).[A1] The IRS compiles state-to-state migration data using year-to-year address changes reported on individual income tax returns filed with the IRS, which are available from 1990 to 2014.[A2] Those who file income tax returns with the IRS in two consecutive years in the same state are considered as non-migrants, and migrants otherwise. We focus on the 48 states and the District of Columbia on the U.S. mainland, and treat Alaska and Hawaii as "foreign countries" in our analysis.

For the years 1990-2014, we compute migration flows and the intrinsic population growth rates of U.S. states using the IRS state-to-state migration flow data. Migrants are considered as the residents of the destination states for the year they migrate.[A3] Thus, the population of state j in year t is measured as the number of tax filers (and their dependents) who report a home address in state j at the start of year $t+1$ as recorded by the IRS for the period from t to $t+1$. We decompose the population changes of U.S. states into an intrinsic component (due to births and deaths) and a net inward migration component. Let

$$l_{i\cdot}(t) \equiv \sum_{j=1}^{n} l_{ij}(t), \text{ and } l_{\cdot j}(t) \equiv \sum_{i=1}^{n} l_{ij}(t), \tag{A.45}$$

where for $i \neq j$, $l_{ij}(t)$ denotes the population flow from state i to state j in year t, measured using the IRS data (see also (1) and (2)). The number that remain in state i is denoted by $l_{ii}(t)$. $l_{i\cdot}(t) - l_{ii}(t)$ measures the outward migration from state i, and $l_{\cdot i}(t) - l_{ii}(t)$, measures the inward migration to state i. The change in population of state i in period t, defined by $l_{\cdot i}(t) - l_{\cdot i}(t-1)$ can now be decomposed as:

$$l_{\cdot i}(t) - l_{\cdot i}(t-1) = \left[l_{\cdot i}(t) - l_{i\cdot}(t)\right] + \left[l_{i\cdot}(t) - l_{\cdot i}(t-1)\right]. \tag{A.46}$$

where the first component $l_{\cdot i}(t) - l_{i\cdot}(t)$ is the net inward migration to state i, and the reminder term, $l_{i\cdot}(t) - l_{\cdot i}(t-1)$, which we refer to as the intrinsic population change of state i. Thus,

[A1] For further information on the IRS migration flow data, see `https://www.irs.gov`.

[A2] The total number of exemptions recorded by the IRS each year is around 80% of the U.S. population.

[A3] For example, suppose a person files income tax returns with the IRS at the starts of year t and year $t+1$, and the two addresses reported are in state i and state j respectively. If $i = j$, this person is considered as a resident in State j in year t. However, if $i \neq j$, the time she migrates to State j can be any point between the starts of year t and year $t+1$. In our analysis, we consider this person as a resident in State j for year t.

the actual state level intrinsic population growth rates, $\hat{g}_{l,it}$, for $i = 1, 2, ..., n$, are measured as

$$\hat{g}_{l,it} = \frac{l_{i\cdot}(t) - l_{\cdot i}(t-1)}{l_{\cdot i}(t-1)} \tag{A.47}$$

For the period 1976-1990, state level populations are measured using Census population data, which are scaled such that their 1990 values match those implied by the IRS migration flow data.

A2.2 State level real per capita incomes

The state level per capita annual disposable incomes are obtained from the Bureau of Economic Analysis (BEA).[A4] Real incomes are computed by dividing state level nominal incomes by state level prices of non-housing consumption goods. The relative prices of non-housing consumption goods across U.S. states for the year 2000 are estimated following the procedure in Holly et al. (2010) (see their Table A.1), where the American Chamber of Commerce Researchers Association (ACCRA) cost of living indices for non-housing items are used at the metropolitan statistical areas.[A5] Similarly, state level non-shelter Consumer Price Index (CPI) series are constructed using the U.S. Bureau of Labor Statistics (BLS) non-shelter CPIs of the cities and areas according to the Holly et al. (2010) procedure.[A6] Then, state level prices of non-housing consumption goods are complied by combining the relative prices of non-housing goods across U.S. states for 2000 and the state level non-shelter (CPI) series over 1976-2014.

We infer the state level wage rates, w_{it}, using (16), where the worker population, $l_{\cdot i}(t)$, is measured using the actual state level population (see Appendix A2.1), and the state level output, y_{it}, is measured by multiplying realized real per capita disposable income of the state by its population.

A2.3 State level real house prices and rents

The state level median house prices for 1976-2014 are complied by combining the state level median house prices in 2000 obtained from the Historical Census of Housing Tables, and the state level House Price Index obtained from U.S. Federal Housing Finance Agency (FHFA).[A7] The FHFA House Price Index are available over the period $1976Q1$ to $2015Q4$. The annual house price index is computed using the simple average of the quarter indices over the year.

[A4] For further information on the BEA state level per capita annual disposable income data (Table SA51), see `https://www.bea.gov/index.htm`.

[A5] The Cost of Living Index (COLI), formerly the ACCRA Cost of Living Index is a measure of living cost differences among urban areas in the United States compiled by the Council for Community and Economic Research. For further information, see `http://coli.org/`.

[A6] For further information on the BLS city level CPI data, see `https://www.bls.gov/data/`.

[A7] For further information on the Historical Census of Housing Tables of Home Values, see `https://www.census.gov`. For further information on the FHFA state level house price index, see `http://www.freddiemac.com`.

Real house prices are obtained by dividing nominal house prices by prices of non-housing consumption goods.

The state level annual housing rents are computed for 1976-2014 by combing the state level annual housing rents for 2000 obtained from the Historical Census of Housing Tables, and the state level shelter-CPIs.[A8] We construct the state level shelter-CPI series based on the BLS shelter-CPI data and the procedure followed by Holly et al. (2010) (Table A.1).[A9] Real annual rents are obtained by dividing the nominal annual rents by the prices of non-housing consumption goods.

A2.4 Land-use regulations and supplies

The state level Wharton Residential Land Use Regulatory Index is due to Gyourko et al. (2008), and the state level land share in house value is compiled by Davis and Heathcote (2007).[A10] The state level data on urban area sizes are from the United States Department of Agriculture (USDA).[A11]

A2.5 Amenities

The climate data are obtained from the National Centers for Environmental Information (NCEI) of the National Oceanic and Atmospheric Administration (NOAA), which include information on average annual cooling/heating degree days, precipitation, snowfall, wind speed, sunshine, number of clear days and humidity (morning and afternoon). State level climate data are derived by averaging data from all weather stations within the state.

The state level data on land, water and total areas are obtained from the U.S. Census Bureau. The state level land cover data are obtained from the United States Department of Agriculture (USDA), which include information on the acreages of cropland, grassland pasture and range, forest, urban area and other lands of U.S. states. The state level data on wilderness area are obtained from the Wilderness Connect.

The data on the expenditures of state and local governments of U.S. states are obtained from the Census of Governments, which include information on total expenditures and the amounts spent on hospitals, health, highways, airports, parks and recreation, and natural resources. The state level data on the numbers of students and instructors in public elementary and secondary schools and expenditure per pupil of local school systems are obtained from the U.S. Census Bureau.[A12] Real expenditures are computed by dividing state level nominal expenditures by state level prices of non-housing consumption goods. The state

[A8] For further information on the Historical Census of Housing Tables of Housing Rents, see `https://www.census.gov`.

[A9] For further information on the BLS city level CPI data, see `https://www.bls.gov/data/`.

[A10] For further information on the data of state level land share in house value, see `http://datatoolkits.lincolninst.edu`.

[A11] For further information on the USDA land use data, see `https://www.ers.usda.gov`.

[A12] For further information, see the Annual Survey of Public Employment and Payroll (ASPEP) and the Annual Survey of School System Finances (ASSSF) of the U.S. Census Bureau.

Table A1: Sources for amenity data

	Data sources
I. Climate and geography	
Average annual cooling degree days (1000 Df, 1901-2000)	NOAA-NCEI
Average annual heating degree days (1000 Df, 1901-2000)	NOAA-NCEI
Average annual precipitation (inches, 1901-2000)	NOAA-NCEI
Average annual snowfall (inches)	NOAA-NCEI
Average annual wind speed (m.p.h., 1984-2018)	NOAA-NCEI
Average annual sunshine (% of possible)	NOAA-NCEI
Average annual number of clear days	NOAA-NCEI
Average annual humidity: morning (1945-2018)	NOAA-NCEI
Average annual humidity: afternoon (1945-2018)	NOAA-NCEI
Coastal state (=1 if on coast)	Census
Log total used land (1000 acres, 1997)	USDA-ERS
Share of forest in total land uses (1997)	USDA-ERS
Share of crop&range in total land uses (1997)	USDA-ERS
Share of urban area in total land uses (1997)	USDA-ERS
Share of wilderness in total land area	Wilderness Connect
Share of water in total area	Census
II. Local public goods, environment and population density	
State&local government total expenditures (2000$ per capita, 1997 and 2007)	Census of Governments
State&local gov. exp. on hospitals and health (2000$ per capita, 1997 and 2007)	Census of Governments
State&local gov. exp. on highways and airports (2000$ per capita, 1997 and 2007)	Census of Governments
State&local gov. exp. on parks, rec. and nat. res. (2000$ per capita, 1997 and 2007)	Census of Governments
Average annual crime rate (per 100 persons, 1990-1999 and 2000-2014)	FBI
Teacher–to-pupil ratio (1995 and 2007)	ASPEP, ASSSF
Expenditure per pupil of local school systems (2000$, 1995 and 2007)	ASSSF
Average annual air quality index (AQI, 1990-1999 and 2000-2014)	EPA
Population density of urban area (log pop. per 1000 acres, 2000 and 2010)	Census, USDA-ERS
Population density of total area (log pop. per 1000 acres, 1990-1999 and 2000-2014)	Census

Notes: The amenity data are from the following sources: The National Centers for Environmental Information of the National Oceanic and Atmospheric Administration (NOAA-NCEI, `https://www.ncdc.noaa.gov`), the Economic Research Service of the United States Department of Agriculture (USDA-ERS, `https://www.ers.usda.gov`), the Wilderness Connect (`https://wilderness.net`), Federal Bureau of Investigation (FBI, `https://www.fbi.gov`), U.S. Environmental Protection Agency (EPA, `https://www.epa.gov`) and the Census of Government (COG), Annual Survey of Public Employment and Payroll (ASPEP), Annual Survey of School System Finances (ASSSF) conducted by the U.S. Census Bureau (`https://www.census.gov`).

level annual violent crime rates from 1990 to 2014 are obtained from the Federal Bureau of Investigation (FBI).

The county level annual Air Quality Index (AQI) from 1990 to 2014 are obtained from the U.S. Environmental Protection Agency (EPA). The state level index is derived by averaging

index values for all counties within the state.

Table A1 summarizes the amenity data used in our empirical analyses and their sources.

A3 Calibration and estimation of parameters

A3.1 Migration costs

Table A2 reports the results from regression (63) in Section (6.1.2). The distance between two states is measured as the distance between their centers of population defined by Census. The ethnic dissimilarity between two states is measured as the Euclidean distance between the ethnic distributions of populations of the two states.[A13] The dissimilarity in land cover between two states is measured as the Euclidean distance between the distributions of different types of land in the two states.[A14] The dissimilarity in annual temperature pattern is measured as the absolute difference in the ratio of cooling degree days to heating degree days. The dissimilarity in sunshine duration is measured as the absolute difference in the ratio of clear days to cloudy days. The amenity data used in the regression are summarized in Table A1 in Appendix A2.5.

A3.2 Productivity process

To estimate the stochastic process of a_{it}, defined by (19), (20) and (21), recall that a_{it} is given by

$$\ln a_{it} = \ln a_i + g_a t + \lambda_i f_t + z_{a,it}, \tag{A.48}$$

where $t = 1, 2, ..., T_1$ (1977-1999). To identify the unobserved common factor, f_t, we impose the following restrictions:

$$n^{-1} \sum_{i=1}^{n} \lambda_i = 1. \tag{A.49}$$

and

$$T_1^{-1} \sum_{t=1}^{T_1} f_t = 0, \tag{A.50}$$

Restriction (A.49) is required to distinguish between scales of λ_i and f_t, and (A.50) is required to separate the linear trend from the common factor. We take the common growth rate of state level incomes, g_a, as a known parameter, and set it to match the average annual growth

[A13] The state level data on ethnic populations are from the 2000 Decennial Census, which include information on the state level populations for different ethnic groups, including White Americans, African Americans, American Indian and Alaska Natives, Asian Americans and others.

[A14] The state level land cover data are obtained from the United States Department of Agriculture (USDA) which include information on the acreages of cropland, grassland pasture and range, forest, urban area and other lands.

Table A2: Results from the migration cost regression

Dependent variable: **Route-specific component in migration costs, $\hat{\lambda}_{ij}$**	**Coefficient**	**Std. error**
Distance (1000 miles)	2.7460†	0.1350
Distance squared	-0.7737†	0.0502
Between adjacent states (=1 if between two adjacent states)	-1.4886†	0.0716
Between coastal states (=1 if between two coastal states)	-0.3191†	0.0408
Dissimilarity in ethnic composition	0.8059†	0.1260
Dissimilarity in land cover	0.5003†	0.0787
Absolute difference in the water-to-land ratio	1.3282†	0.1129
Dissimilarity in annual temperature pattern	-0.4636†	0.0224
Dissimilarity in sunshine duration	-1.0292†	0.0433
Absolute difference in urban population share	1.2666†	0.1395
Diff in average annual cooling degree days (1000 Df, 1901-2000)	0.0811	0.0722
Diff in average annual heating degree days (1000 Df, 1901-2000)	0.0410	0.0343
Diff in average annual precipitation (inches, 1901-2000)	-0.0029	0.0061
Diff in average annual snowfall (inches)	-0.0050†	0.0018
Diff in average annual wind speed (m.p.h., 1984-2018)	0.0279	0.0180
Diff in average annual sunshine (% of possible)	0.3564	0.6407
Diff in average annual number of clear days	-0.0038*	0.0016
Diff in average annual humidity: morning (1945-2018)	0.4459	0.8695
Diff in average annual humidity: afternoon (1945-2018)	-1.1800	0.9766
Diff in coastal state dummy (=1 if on coast)	-0.0421	0.0499
Diff in log total used land (1000 acres, 1997)	0.6228†	0.0297
Diff in share of forest in total land uses (1997)	0.3021	0.5371
Diff in share of crop&range in total land uses (1997)	-0.0196	0.4115
Diff in share of urban area in total land uses (1997)	-0.2879	0.4471
Diff in share of wilderness in total land area	0.2210	0.8132
Diff in share of water in total area	0.1051	0.2735
Diff in state&local government total expenditures (2000$ per capita, 1997)	0.0450	0.0392
Diff in state&local gov. exp. on hospitals and health (2000$ per capita, 1997)	-0.0684	0.1752
Diff in state&local gov. exp. on highways and airports (2000$ per capita, 1997)	-0.2006	0.2398
Diff in state&local gov. exp. on parks, rec. and nat. res. (2000$ per capita, 1997)	-0.0885	0.4100
Diff in average annual crime rate (per 100 persons, 1990-1999)	-0.0123	0.1049
Diff in teacher–to-pupil ratio (1995)	0.6147	1.4256
Diff in expenditure per pupil of local school systems (2000$, 1995)	-0.0001*	0.0000
Diff in average annual air quality index (AQI, 1990-1999)	0.0094†	0.0038
Diff in population density of urban area (log pop. per 1000 acres, 2000)	-0.1256*	0.0753
Diff in population density of total area (log pop. per 1000 acres, 1990-1999)	0.5776†	0.0565
Constant	Yes	
Number of observations	2352	
R-squared	0.76	

Notes: This table reports the results from regression (63) in Section 6.1.2. '⋆' indicates significance at the 10% level, and '†' indicates significance at the 5% level.

rate of the U.S. real per capita income during the period 1977-1999, which is around 0.02. Then, in view of (A.50), we estimate a_i by

$$\hat{a}_i = \exp\left[T_1^{-1}\sum_{t=1}^{T_1}(\ln a_{it} - \hat{g}_a t)\right]. \tag{A.51}$$

Let $e_{a,it}$ be the deviation of $\ln a_{it}$ from its trend, which is given by

$$e_{a,it} = \lambda_i f_t + z_{a,it}, \tag{A.52}$$

and estimated as $\hat{e}_{a,it} = \ln a_{it} - \ln \hat{a}_i - \hat{g}_a t$, for $t = 0, 1, 2, ..., T$. To estimate f_t, we first note that $n^{-1}\sum_{i=1}^{n}\lambda_i = 1$ (see (A.49)). By summing up both sides of (A.52), we have $n^{-1}\sum_{i=1}^{n} e_{a,it} = f_t + n^{-1}\sum_{i=1}^{n} z_{a,it}$, where by assumption $z_{a,it}$ are cross-sectionally independent. As a result,

$$f_t = n^{-1}\sum_{i=1}^{n}\hat{e}_{a,it} + O_p\left(T_1^{-\frac{1}{2}}\right) + O_p\left(n^{-\frac{1}{2}}\right),$$

which gives a consistent estimator of f_t:

$$\hat{f}_t = n^{-1}\sum_{i=1}^{n}\hat{e}_{a,it}. \tag{A.53}$$

The parameters ρ_f and σ_f in (20) are estimated by running the OLS regression of $\hat{f}_t$ on $\hat{f}_{t-1}$, for $t = 1, 2, ..., T_1$. To estimate the associated loading coefficients, λ_i, for each i we run the OLS regressions of $\hat{e}_{a,it}$ on $\hat{f}_t$, and obtain the residuals, $\hat{z}_{a,it}$, for $t = 0, 1, 2, ..., T_1$. Then, we estimate $\rho_{a,i}$ and $\sigma_{a,i}$ in (21) by running OLS regressions of $\hat{z}_{a,it}$ on $\hat{z}_{a,i,t-1}$, over the period $t = 1, 2, ..., T_1$.

A3.3 Land supplies

A3.3.1 Estimation of $\tau_{\kappa,i}$

We assume that *used land*, denoted by UR_{it}, is turned into *unused land* when houses on these lands are depreciated. Thus, UR_{it} would shrink at rate δ in the absence of any new constructions. Therefore, UR_{it} follows as:

$$UR_{it} = \kappa_{it} + (1-\delta)\, UR_{i,t-1}. \tag{A.54}$$

To estimate $\tau_{\kappa,i}$ in (70), we make use of published data on major land uses in the U.S. compiled by the U.S. Department of Agriculture (USDA). We consider only the observations before 2000 and estimate $\tau_{\kappa,i}$ using the USDA urban area size data for 1978 and 1992 as follows. Note that (A.54) implies

$$UR_{i,t_{1992}} = \sum_{t=t_{1979}}^{t_{1992}}(1-\delta)^{t_{1992}-t}\,\kappa_{i,t} + (1-\delta)^{14}\, UR_{i,t_{1978}}, \tag{A.55}$$

where t_{1978}, t_{1979} and t_{1992} are the time indices for 1978, 1979, and 1992. Using (70) in (A.55) to eliminate κ_{it}, we obtain the following estimate of $\tau_{\kappa,i}$:

$$\hat{\tau}_{\kappa,i} = \frac{\sum_{t=t_{1979}}^{t_{1992}} (1-\delta)^{t_{1992}-t} \hat{\gamma}_{i,t}}{UR_{i,t_{1992}} - \left(1-\hat{\delta}\right)^{14} UR_{i,t_{1978}}}. \tag{A.56}$$

A3.3.2 Land-use regulation and land supply growth rates

Here we investigate the relationship between our imputed land supply growth rate by states, denoted by $\hat{g}_{\kappa,i}$, and the state level Wharton Residential Land Use Regulatory Index (WRI_i), which is based on Wharton surveys of land-use regulations conducted in 2004, intended to characterize the local residential land-use regulatory environment. WRI_i increases with the tightness of land-use regulation, and is expected to be inversely related to land supply growth rate. This index is compiled by Gyourko et al. (2008) who use factor analysis to create the aggregate index, which is then standardized so that its sample mean is zero and its standard deviation equals one. Since Alaska and Hawaii are excluded from our analysis, we re-scale the WRIs of the remaining states so that the mean and the standard deviation of the sub-sample we use are zero and one, respectively.

We then run the OLS regression of $\hat{g}_{\kappa,i}$ on WRI_i for $i = 1, 2, ..., 48$ and obtained the following estimates[A15]

$$\hat{g}_{\kappa}\left(WRI_i\right) = \underset{(0.0115)}{0.0468} - \underset{(0.0116)}{0.0607} WRI_i, \;\; R^2 = 0.37 \tag{A.57}$$

where $\hat{g}_{\kappa}\left(WRI_i\right)$ is the fitted value, R^2 is the squared correlation coefficient, and the figures in brackets are standard errors of the estimated coefficients. It is reassuring to see that our imputed land supply growth rates have a highly significant negative correlation with WRI_i, particularly noting that the way WRI is measured has little overlap with our imputed measure, $\hat{g}_{\kappa,i}$. Also by implication, our imputed measure of land supply growth indirectly allows for land use regulations that our model does not address directly.

[A15] Washington, D.C. is excluded since its WRI data is not available.

A3.4 Parameter values

Table A3: Benchmark calibration and estimation of parameters

		Value	Description
I. Preference			
η	Calibrated	0.24	Share of housing in consumption; Davis and Ortalo-Magné (2011).
β	Calibrated	0.98	Discount factor of landlords; Match the risk-free interest rate of 2%.
II. Migration and intrinsic population growth rates			
σ_ε	Estimated	1.23	Standard deviation of idiosyncratic migration cost.
g_α	Estimated	0.01	Growth rate of migration costs during 1990-2014.
α_{ij}	Estimated	See Section 6.1.2	Route-specific migration costs.
g_l	Estimated	0.01	Intrinsic population growth rate; Match the U.S. average population growth rate over the period 1977-1999.
III. Housing supplies and investment			
$\vartheta_{\kappa,i}$	Estimated	See Section 6.2	Location-specific shares of land in house values; Set to the state level average land values relative to total value of housing stocks over the period 1977-1999.
θ_i	Estimated	See Section 6.2	Location-specific housing investment costs; Match the state level average rent-to-price ratios over the period 1977-1999.
δ	Estimated	0.02	Depreciation rate of housing stocks; Set to the national housing stock depreciation rate over the period 1977-1999.
IV. Labor productivity processes			
υ_l	Calibrated	0.67	Share of labor cost in output; Valentinyi and Herrendorf (2008).
υ_ϕ	Calibrated	0.06	Effects of agglomeration on TFP; Davis et al. (2014).
$\bar{\phi}_i$	-	1.00	Location-specific intercepts in the functions for agglomeration effects; Set to one.
a_i	Estimated	See Appendix A3.2	Location-specific intercepts in the labor productivity processes.
g_a	Calibrated	0.02	Growth rate of labor productivities. Match the average annual growth rate of the U.S. real per capita income during the period 1977-1999.
ρ_f	Estimated	0.92	AR(1) autoregressive coefficient for f_t.
σ_f	Estimated	0.03	Standard deviation of the innovation to f_t.
λ_i	Estimated	See Appendix A3.2	Location-specific loading coefficients for f_t.
$\rho_{a,i}$	Estimated	See Appendix A3.2	AR(1) autoregressive coefficients for $z_{a,it}$.
$\sigma_{a,i}$	Estimated	See Appendix A3.2	Standard deviations of the innovations to $z_{a,it}$.
V. Land supply processes			
$\tau_{\kappa,i}$	Estimated	See Appendix A3.3.1	Location-specific scalars in the housing supply functions.
κ_i	Estimated	See Section 6.3.2	Location-specific intercepts in the land supply processes.
$g_{\kappa,i}$	Estimated	See Section 6.3.2	Location-specific land supply growth rates.
$\rho_{\kappa,i}$	Estimated	See Section 6.3.2	AR(1) autoregressive coefficients for $z_{\kappa,it}$.
$\sigma_{\kappa,i}$	Estimated	See Section 6.3.2	Standard deviations of the innovations to $z_{\kappa,it}$.

A4 Setting values for the exogenous variables in simulations

For the simulations conducted in Section 7, the realized state level productivities, a_{it}, for $i = 1, 2, ..., n$, and $t = T_1 + 1, T_1 + 2, ..., T$, are inferred using the estimated version of (69) and realized values of $l_{.i}(t)$ and y_{it}. The realized land supplies, κ_{it}, for $i = 1, 2, ..., n$, and $t = T_1 + 1, T_1 + 2, ..., T$, are inferred using the estimated versions of (70) and (71), and realized values of y_{it}, q_{it} and p_{it}. The realized land-supply shocks, $z_{\kappa,it}$, for $i = 1, 2, ..., n$, and $t = T_1 + 1, T_1 + 2, ..., T$, are inferred using the estimated version of (26) and estimates of κ_{it}. Finally, the actual state level intrinsic population growth rates, $\hat{g}_{l,it}$, for $i = 1, 2, ..., n$, and $t = T_1 + 1, T_1 + 2, ..., T$, are measured using the IRS state-to-state migration data (see Section A2.1).

Reference

Davis, M.A., Fisher, J.D., and Whited, T.M. (2014). Macroeconomic implications of agglomeration. *Econometrica*, 82, 731–764.

Davis, M.A. and Heathcote, J. (2007). The price and quantity of residential land in the united states. *Journal of Monetary Economics*, 54, 2595–2620

Davis, M.A. and Ortalo-Magné, F. (2011). Household expenditures, wages, rents. *Review of Economic Dynamics*, 14, 248–261.

Gyourko, J., Saiz, A., and Summers, A. (2008). A new measure of the local regulatory environment for housing markets: The wharton residential land use regulatory index. *Urban Studies*, 45, 693–729.

Holly, S., Pesaran, M.H., and Yamagata, T. (2010). A spatio-temporal model of house prices in the usa. *Journal of Econometrics*, 158, 160–173.

Valentinyi, A. and Herrendorf, B. (2008). Measuring factor income shares at the sectoral level. *Review of Economic Dynamics*, 11, 820–835.

Online Supplement to
"A Spatiotemporal Equilibrium Model of Migration and Housing Interlinkages"

by

Wukuang Cun

Shanghai University of Finance and Economics, China

M. Hashem Pesaran

University of Southern California, USA, and Trinity College, Cambridge, UK

S1 Supplementary simulation results

S1.1 Migration flows between U.S. states during 2000-2014

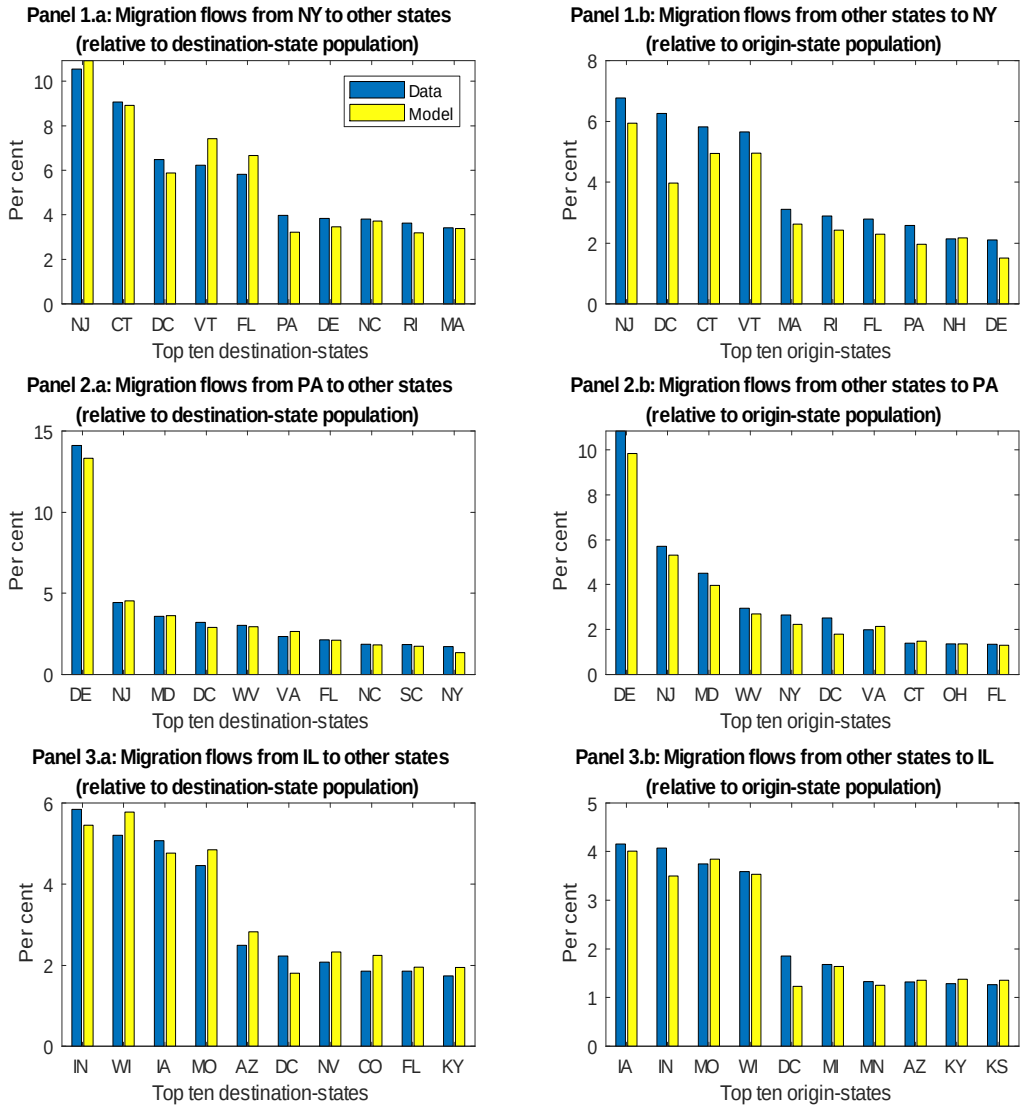

Figure S1: Bilateral migration flows between U.S. states during the evaluation sample (2000-2014)

Notes: Panel 1.a shows the realized and simulated accumulated migration flows from New York to other states during the period 2000-2014 relative to destination-state population in 2014. Only the ten destination-states with the largest migration flows from New York (relative to their own population) are displayed. Panel 1.b shows the realized and simulated accumulated migration flows from other states to New York relative to origin-state population. Similarly, Panels 2.a and 2.b show the bilateral migration flows between Pennsylvania and other U.S. states, and Panels 3.a and 3.b show the bilateral migration flows between Illinois and other U.S. states.

S1.2 Increasing land supply in California: a counterfactual exercise

Here, we consider the application of the model to study the effects of local land-use regulations on regional house prices and spatial population allocation. Our exercise is complementary to the California land-use deregulation experiment by Herkenhoff et al. (2018). These authors emphasize the positive impacts of land-use deregulation in California on the national output through population reallocation, whilst our analysis focusses on the spatiotemporal patterns of the population reallocation resulting from the land-use deregulation. It is shown that the population reallocation towards California are mainly from the nearby states, while the population reallocation from the distant states to California are both smaller in magnitude and slower in speed.

We now conduct a counterfactual experiment to examine the impacts of regional land-use regulations on spatial population allocation. In particular, we consider the effects of a land-use deregulation in California that exogenously increases the annual supply of new land in California by 10% in each year from 2000 to 2014. Increasing the annual new land supply in California by a different rate will not qualitatively change our main findings. We simulate the model using the counterfactual land supplies, within the baseline calibrated model described above.

Table S1 displays the impacts of the counterfactual increases in California land supplies on house prices, population and output in California in 2014. Due to the increases in California land supply, the house price and housing rent in California drop respectively by 3.8% and 1.5% in 2014. As a result, the net outward migration from California decreases by 0.8%, which in turn raises California's population and output in 2014 by 0.08% and 0.06%, respectively.

Table S1: Effects of increasing land supply in California

	California				
	House price in 2014	Housing rent in 2014	Net outward migration during 2000-2014	Population in 2014	Output in 2014
Baseline	273.6 (Thousands $)	11.64 (Thousands $)	2.6099 (Millions)	29.65 (Millions)	0.8772 (Trillions $)
Counterfactually increase the new land supply in CA (percentage changes from the baseline values)	-3.8229	-1.4618	-0.6559	0.0621	0.0443

Notes: This table shows the impacts of a 10% exogenous increase in the annual flows of new land released in California in each year from 2000 to 2014. The first row reports the results from the baseline simulation. The second row reports the results from the counterfactual simulation expressed as percentage changes from the counterpart values in the baseline simulation.

Figure S2 shows the counterfactual changes in U.S. population by states in 2004, 2009 and 2014, in response to the counterfactual increases in California land supplies. In each panel,

the first bar corresponds to California, and the rest of the bars correspond to other U.S. states, arranged in terms of their distances to California. First, as can be seen, the percentage change of population tends to be larger for the states that are geographically close to California, and smaller for the distant states.[S1] Second, since land-use deregulation increases stock of housing only very gradually, it takes a long time for the effects of deregulation to show up in population reallocation, although the effects are seen much more quickly in nearby states. As shown in Panel 1, in 2004, only the population changes in the nearby states are non-negligible. Third, as shown in Figure S3, the counterfactual changes of the output of U.S. states have the same spatiotemporal pattern.

Finally, the population reallocation towards California leads to an increase in California ouput, and at the same time a decrease in the output of the rest of the U.S. states. Since California has higher labor productivity than other U.S. states, the reallocation of population towards California leads to a net increase in the national output. The evidence is shown in Figure S5.

[S1] In fact, the absolute population changes of the nearby states are also the largest among all the states. See Figure S4.

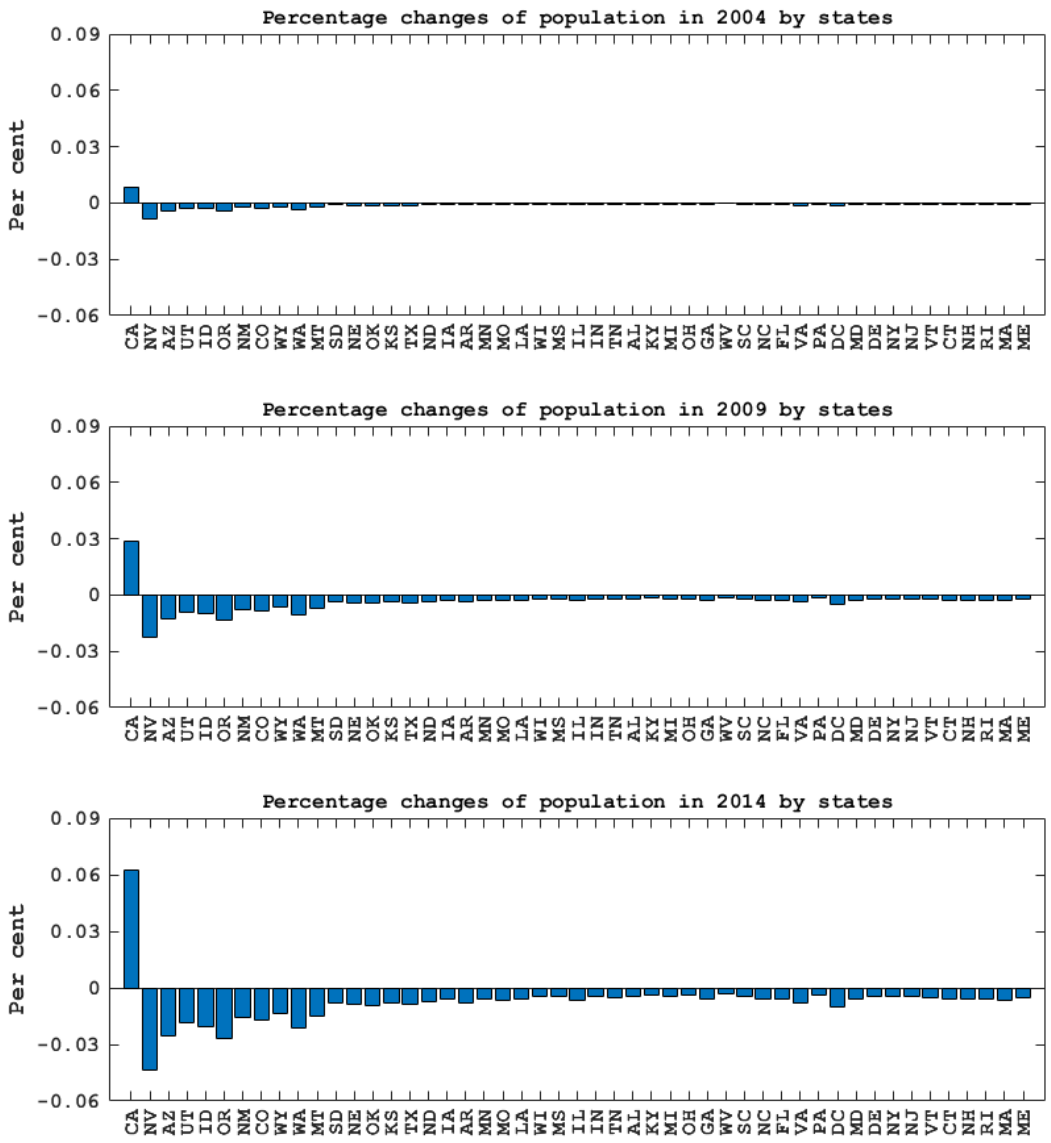

Figure S2: Effects of increasing land supply in California on population by states

Notes: Each panel shows the percentage changes of population by states for the year noted above in response to a 10% exogenous increase in the annual flows of new land released in California in each year from 2000 to 2014. States are ordered ascendingly by their distances to California.

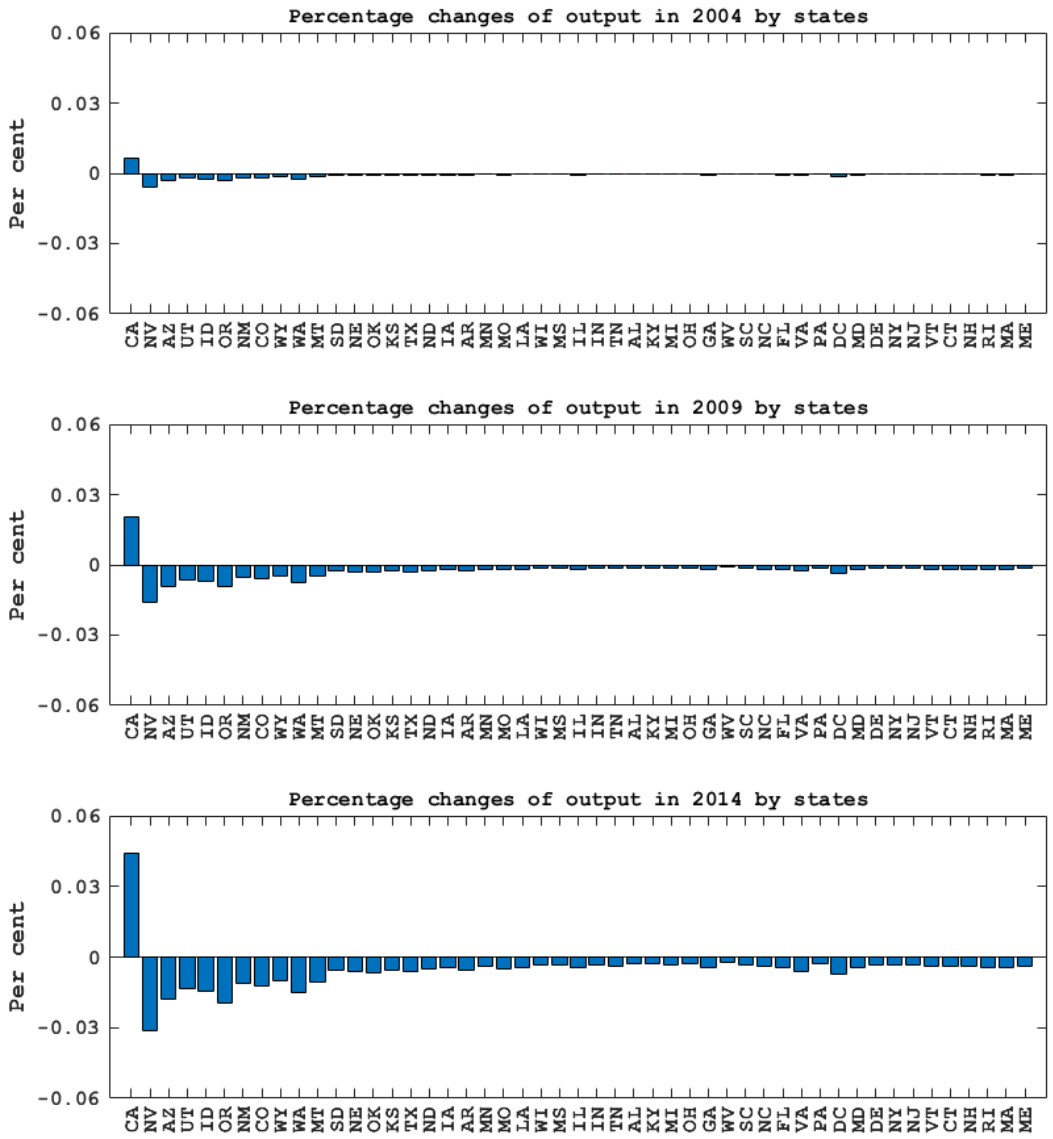

Figure S3: Effects of increasing land supply in California on output by states

Notes: Each panel shows the percentage changes of output by states for the year noted above in response to a 10% exogenous increase in the annual flows of new land released in California in each year from 2000 to 2014. States are ordered ascendingly by their distances to California.

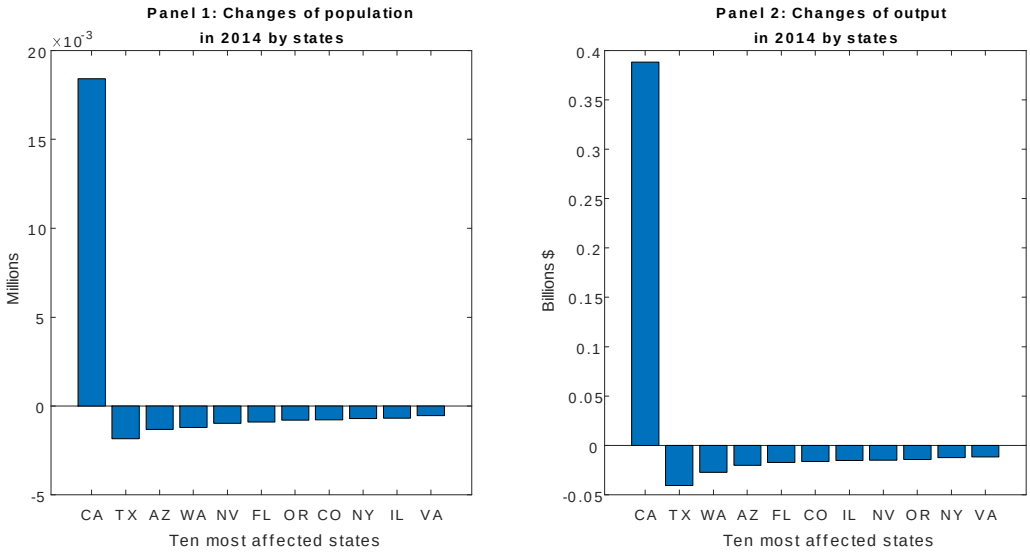

Figure S4: Effects of increasing land supply in California on population and output by states

Notes: Panels 1 and 2 show respectively the absolute changes of population and output in 2014 by states in response to a 10% exogenous increase in the annual flows of new land released in California in each year from 2000 to 2014. In each panel, only California and the ten most affected states (in terms of the magnitudes of the counterfactual changes) are displayed.

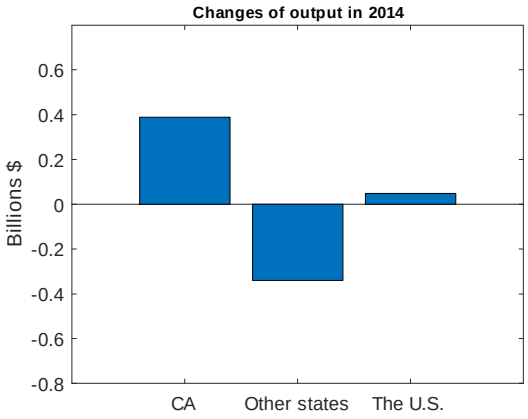

Figure S5: Effects of increasing land supply in California on the output of the U.S.

Notes: This figure shows the absolute changes of output in 2014 for California, all U.S. states except for California, and the U.S. in response to a 10% exogenous increase in the annual flows of new land released in California in each year from 2000 onward.

S1.3 Spatiotemporal impulse responses

S1.3.1 Responses to regional shocks in California

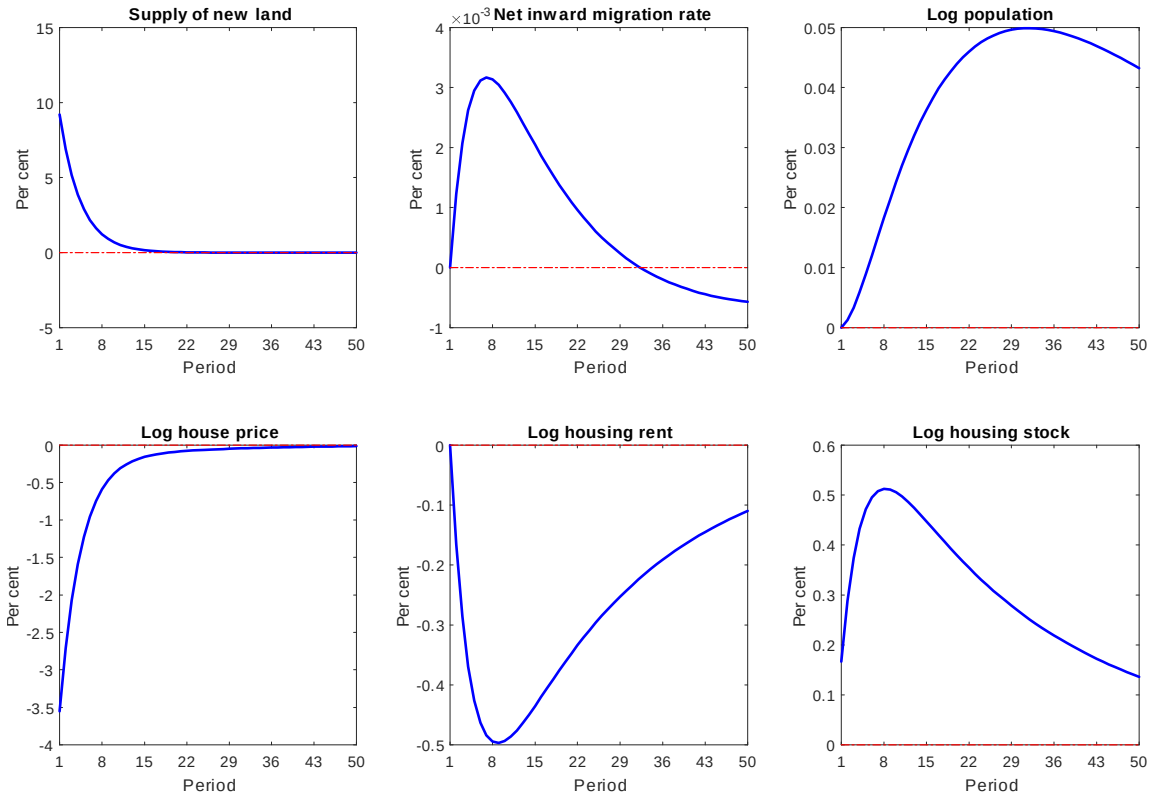

Figure S6: Reponses of California to a positive land-supply shock in California

Notes: This figure shows the responses of log wage rate, net inward migration rate (i.e., the ratio of net inward migration to local population), log population, log house price, log housing rent and log housing stock in California to a ten per cent positive shock to the annual supply of new land in California.

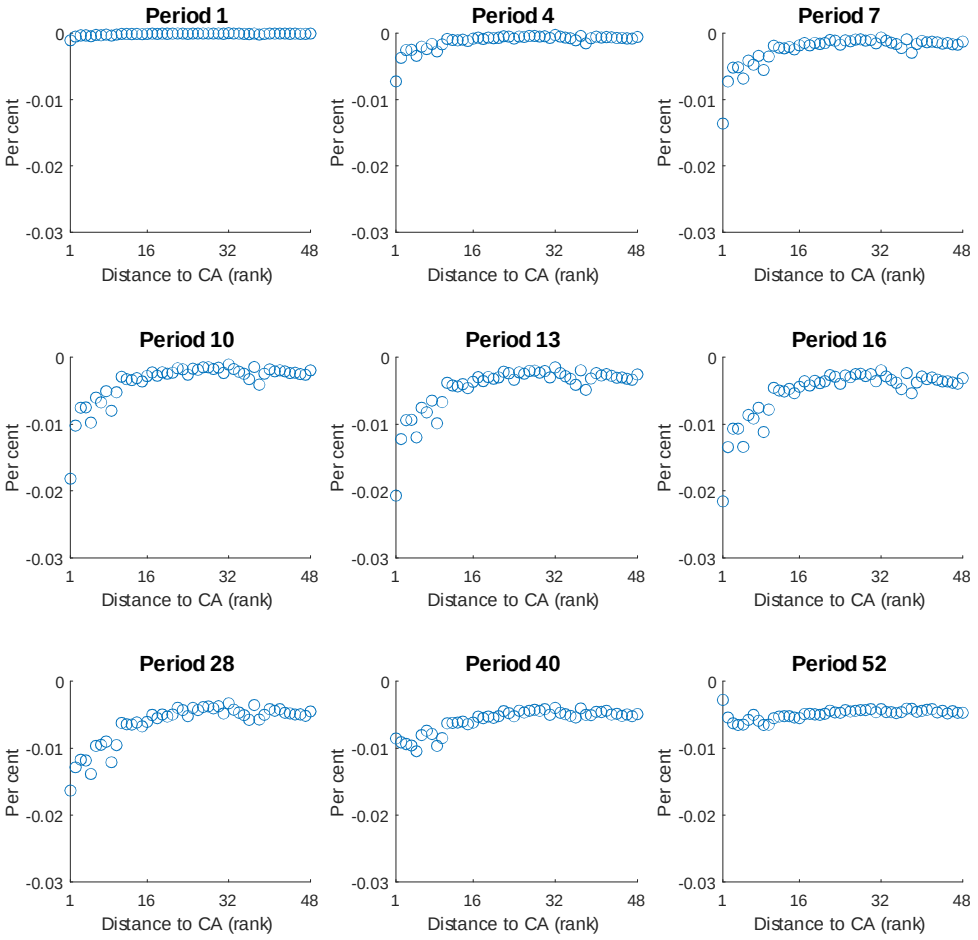

Figure S7: Spatiotemporal responses of log population of U.S. states to a positive land-supply shock in California

Notes: Each panel shows the responses of log population of U.S. states (except for California) to a ten per cent positive shock to the annul supply of new land in California, for the period noted at the top. Each dot represents a state. States are ordered ascendingly by their distances to California, and the horizontal axis corresponds to state's rank in terms of distance to California.

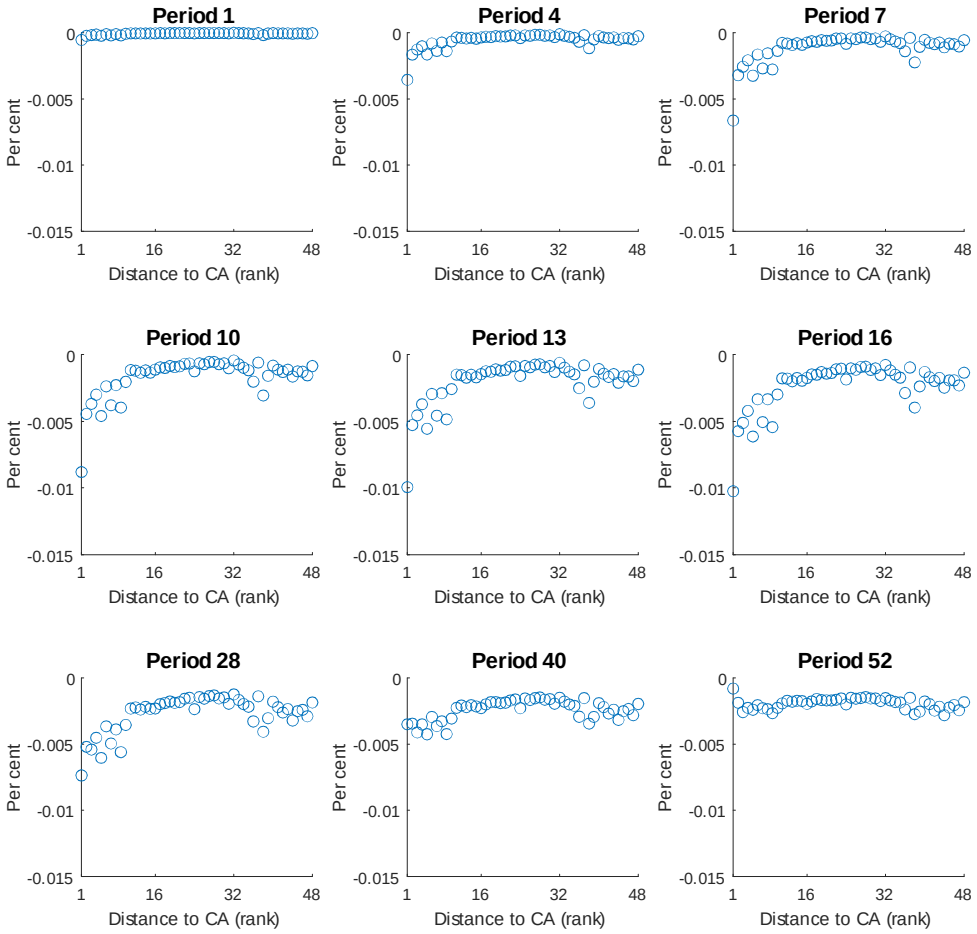

Figure S8: Spatiotemporal responses of log house price-to-income ratios of U.S. states to a positive land-supply shock in California

Notes: Each panel shows the responses of log house price-to-income ratios of U.S. states (except for California) to a ten per cent positive shock to the annul supply of new land in California, for the period noted at the top. Each dot represents a state. States are ordered ascendingly by their distances to California, and the horizontal axis corresponds to state's rank in terms of distance to California.

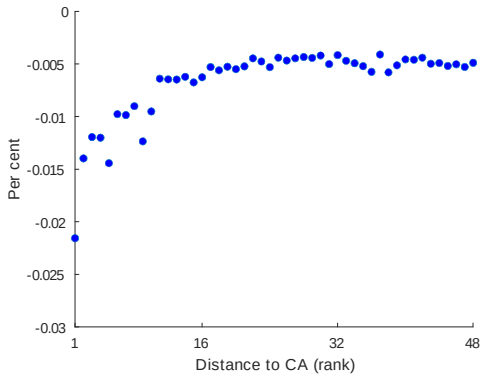

Panel 1.a: Bottom values of the responses of log population (by states)

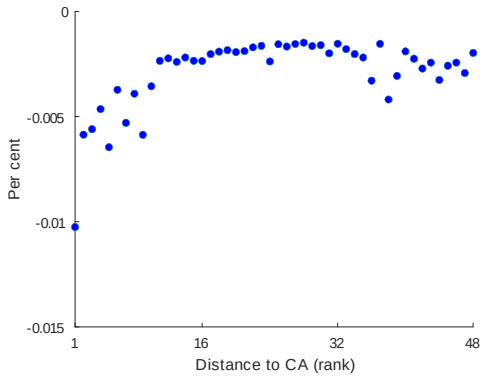

Panel 1.b: Bottom values of the responses of log house price-to-income ratios (by states)

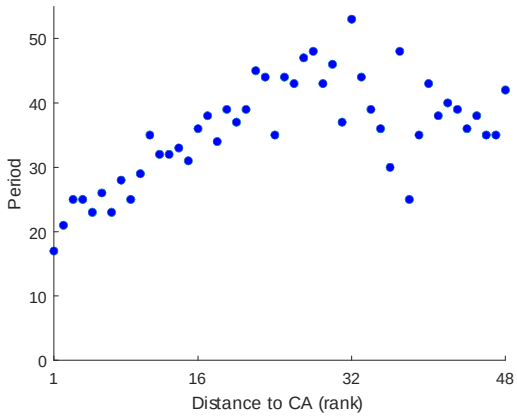

Panel 2.a: Periods in which the responses of log population reach their bottom values (by states)

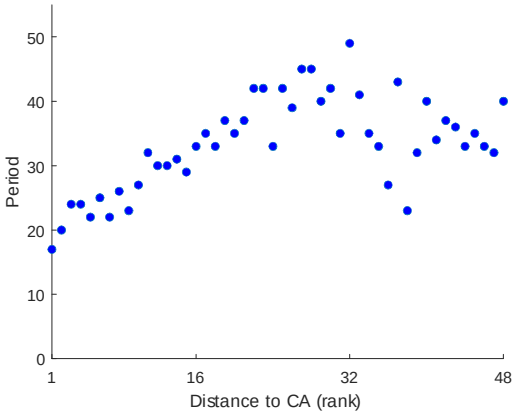

Panel 2.b: Periods in which the responses of log house price-to-income ratios reach their bottom values (by states)

Figure S9: The sizes and speed of the responses of U.S. states (except for California) to a positive land-supply shock in California

Notes: In each panel, a dot represents a state. In Panels 1.a and 1.b, the vertical axis corresponds to the extreme value of state's response after a ten per cent positive land-supply shock in California, and in Panels 2.a and 2.b, the vertical axis corresponds to period in which state's response reaches its extreme value. States are ordered ascendingly by their distances to California, and the horizontal axis corresponds to state's rank in terms of distance to California.

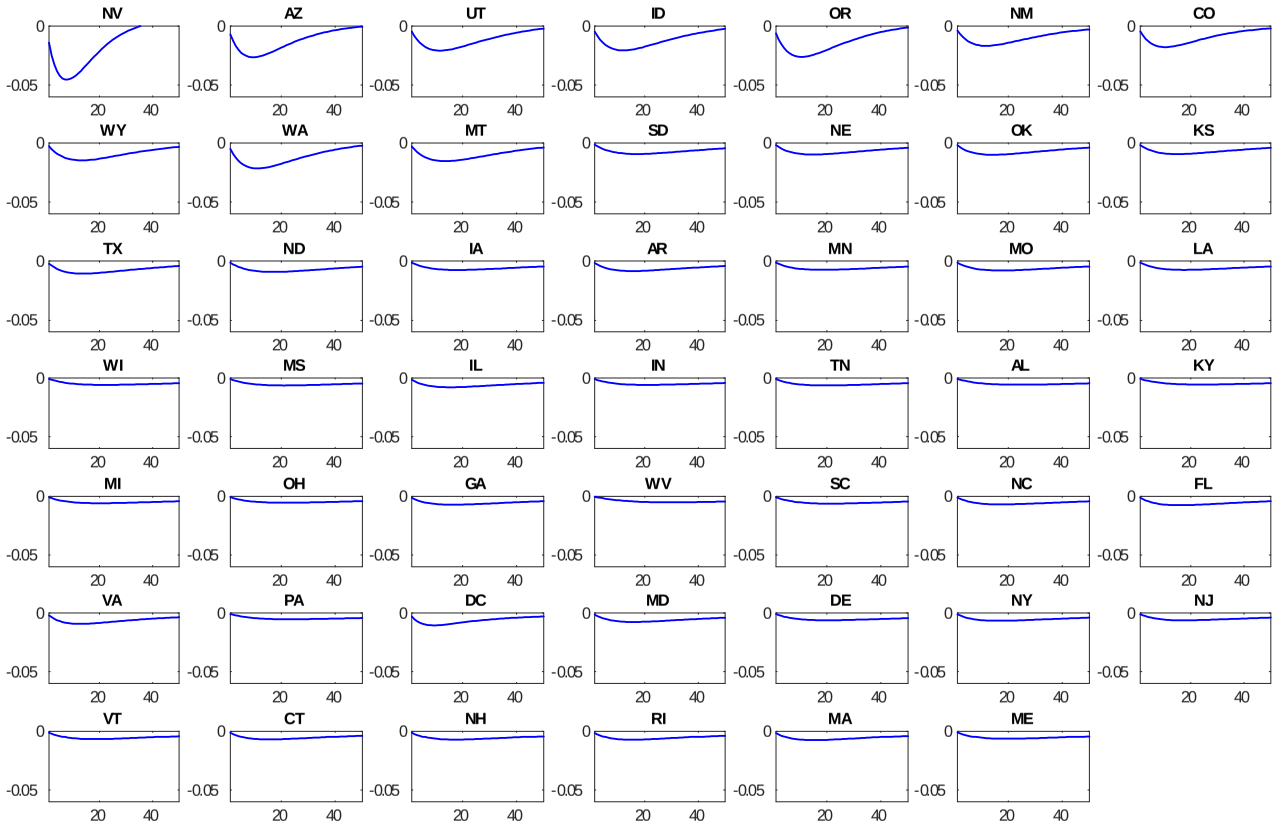

Figure S10: Spatiotemporal responses of log population of U.S. states to a positive productivity shock in California

Notes: This figure shows the responses of log population of U.S. states (except for California) to a one per cent positive shock to the labor productivity in California. States are ordered ascendingly by their distances to California. The unit on the horizontal axis is year. The unit on the vertical axis is per cent.

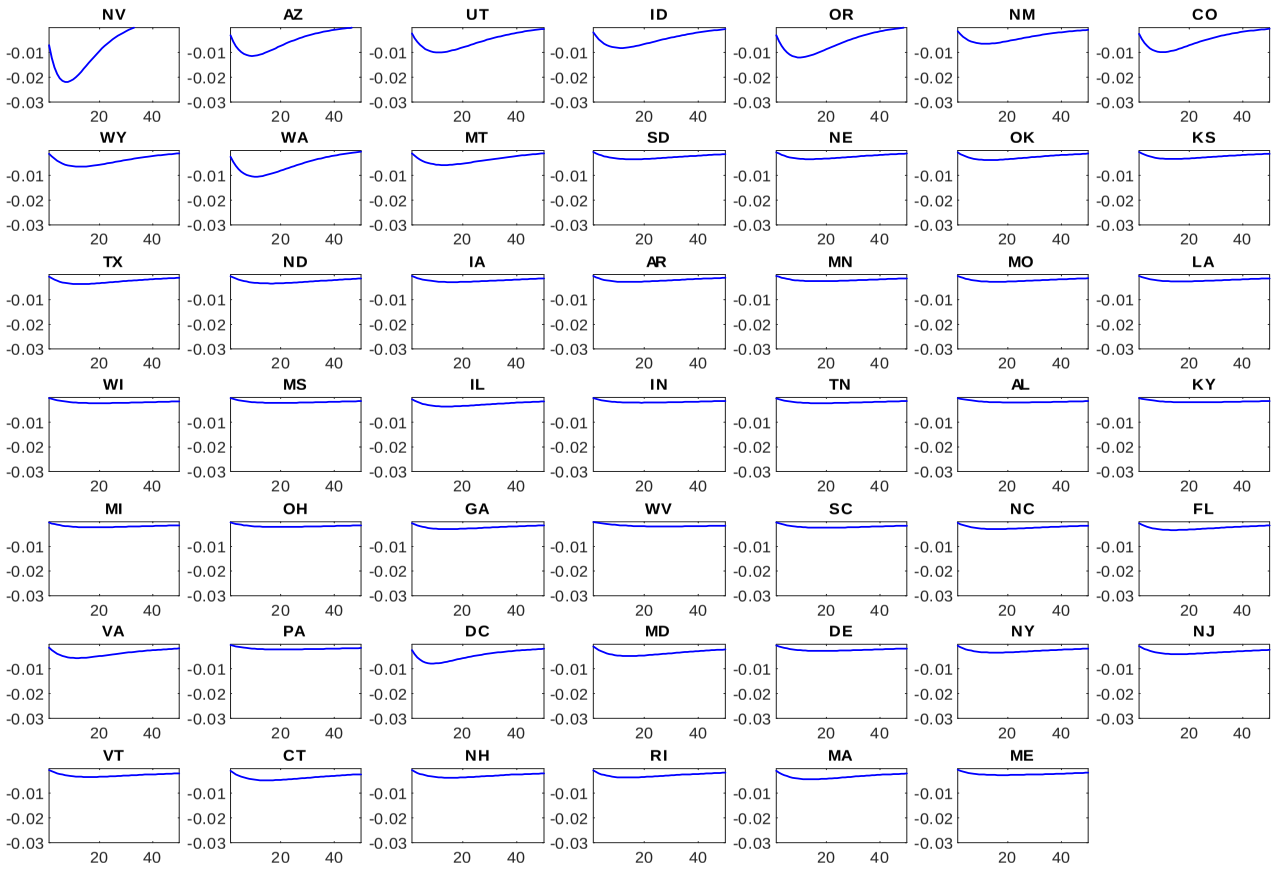

Figure S11: Spatiotemporal responses of log house price-to-income ratios of U.S. states to a positive productivity shock in California

Notes: This figure shows the responses of log house price-to-income ratios of U.S. states (except for California) to a one per cent positive shock to the labor productivity in California. States are ordered ascendingly by their distances to California. The unit on the horizontal axis is year. The unit on the vertical axis is per cent.

S1.3.2 Responses to regional shocks in Texas

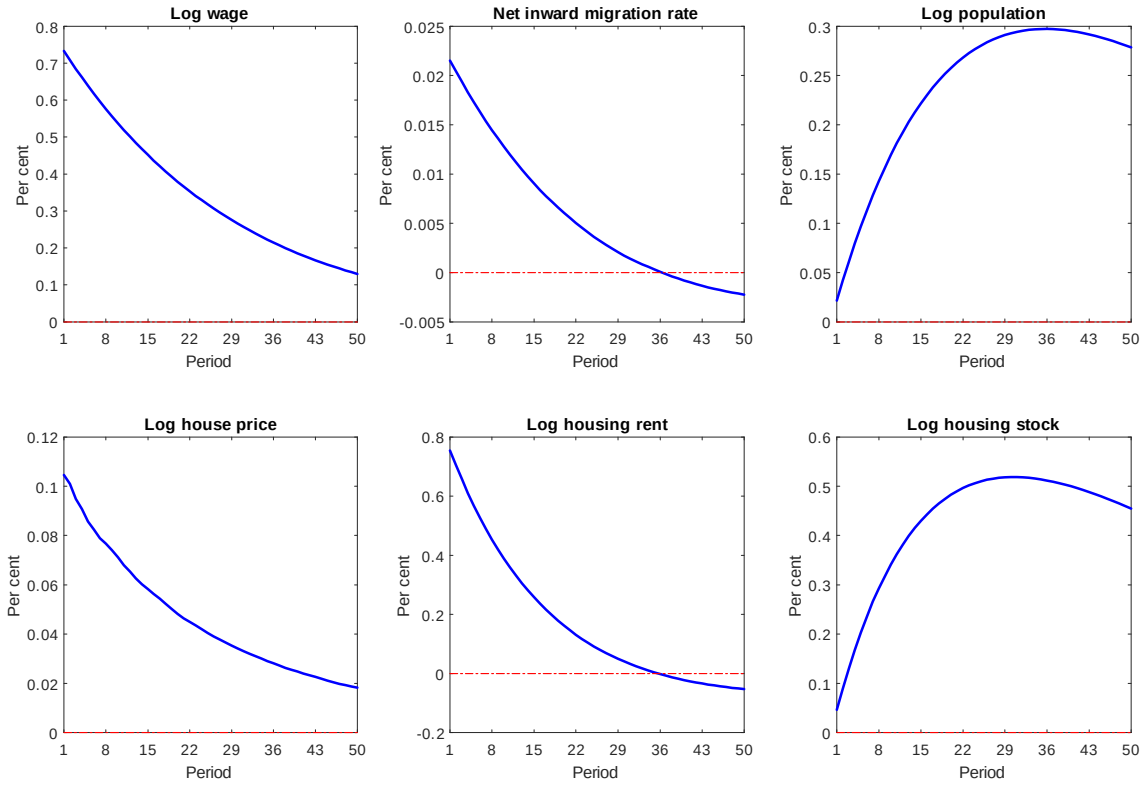

Figure S12: Reponses of Texas to a positive productivity shock in Texas

Notes: This figure shows the responses of log wage rate, net inward migration rate (i.e., the ratio of net inward migration to local population), log population, log house price, log housing rent and log housing stock in Texas to a one per cent positive shock to the labor productivity in Texas.

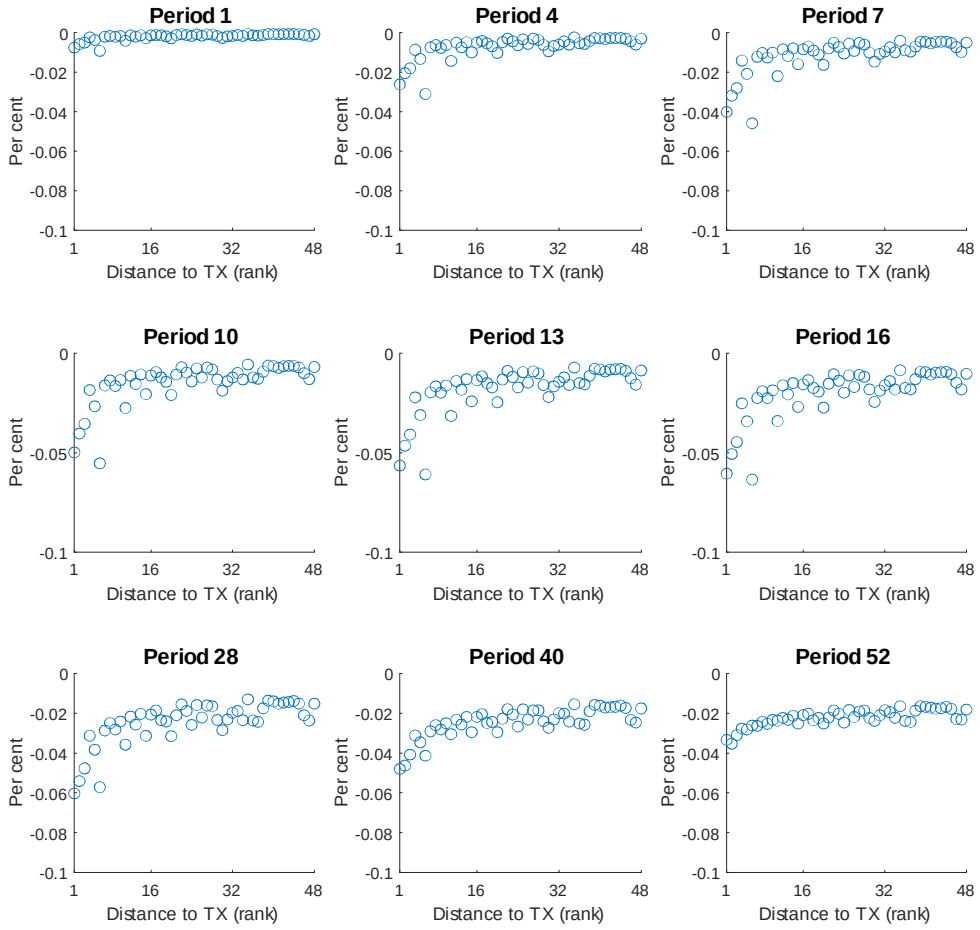

Figure S13: Spatiotemporal responses of log population of U.S. states to a positive productivity shock in Texas

Notes: Each panel shows the responses of log population of U.S. states (except for Texas) to a one per cent positive shock to the labor productivity in Texas, for the period noted at the top. Each dot represents a state. States are ordered ascendingly by their distances to Texas, and the horizontal axis corresponds to state's rank in terms of distance to Texas.

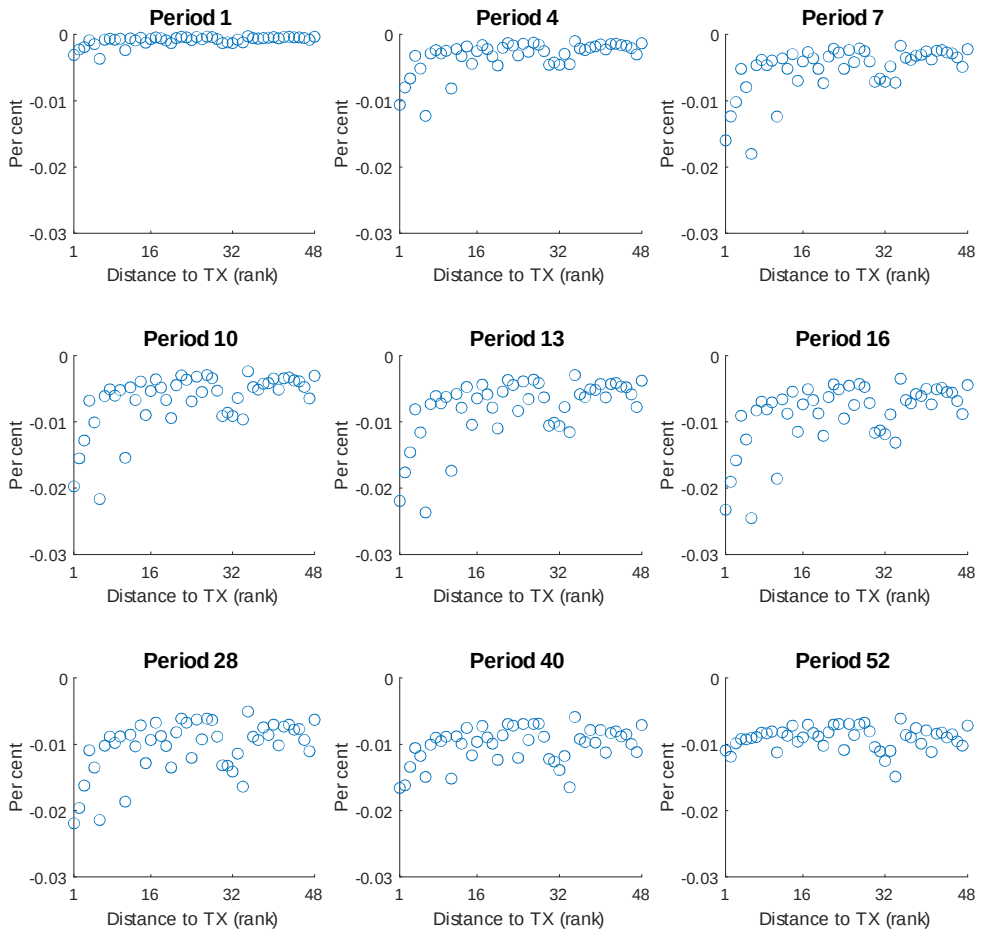

Figure S14: Spatiotemporal responses of log house price-to-income ratios of U.S. states to a positive productivity shock in Texas

Notes: Each panel shows the responses of log house price-to-income ratios of U.S. states (except for Texas) to a one per cent positive shock to the labor productivity in Texas, for the period noted at the top. Each dot represents a state. States are ordered ascendingly by their distances to Texas, and the horizontal axis corresponds to state's rank in terms of distance to Texas.

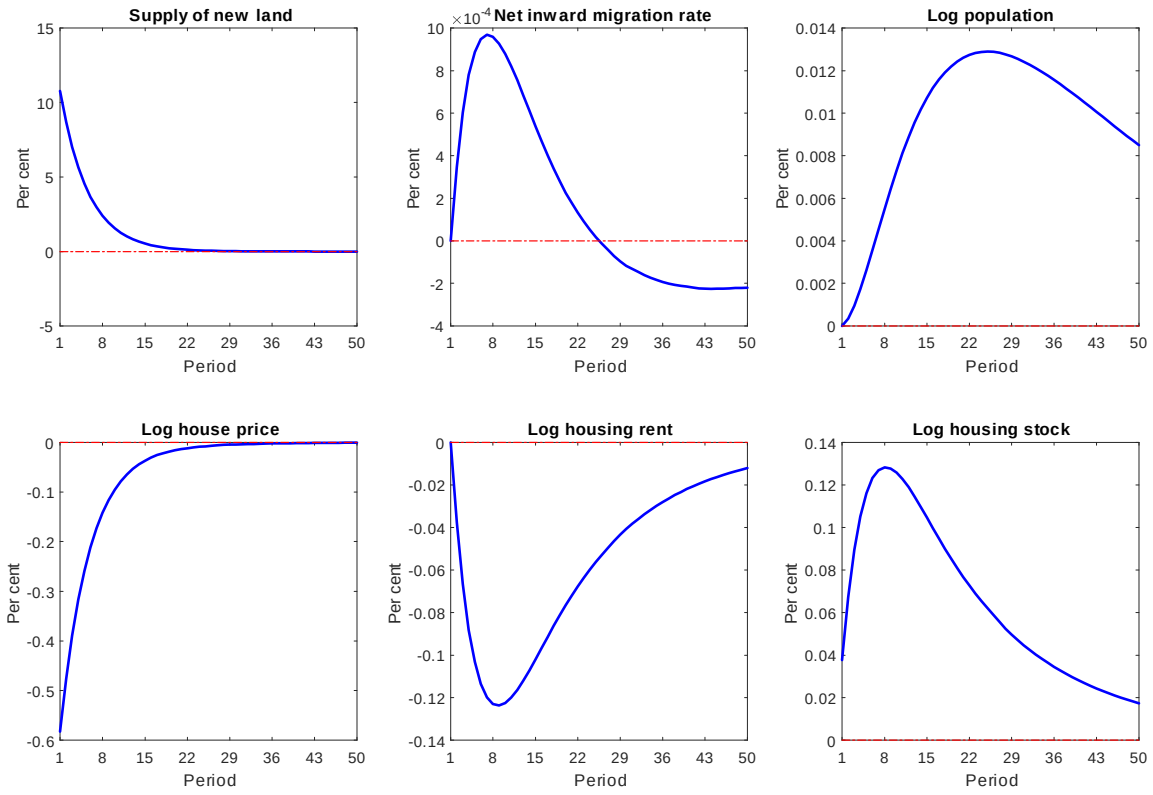

Figure S15: Reponses of Texas to a positive land-supply shock in Texas

Notes: This figure shows the responses of log wage rate, net inward migration rate (i.e., the ratio of net inward migration to local population), log population, log house price, log housing rent and log housing stock in Texas to a ten per cent positive shock to the annual supply of new land in Texas.

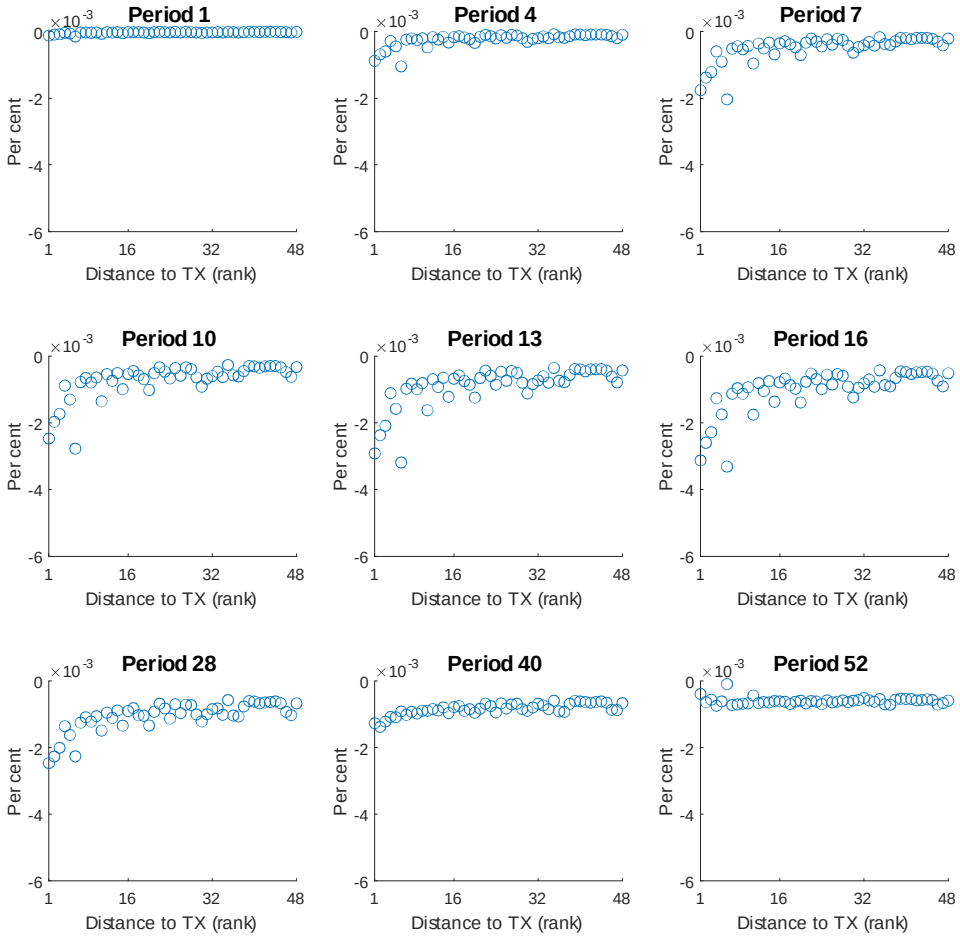

Figure S16: Spatiotemporal responses of log population of U.S. states to a positive land-supply shock in Texas

Notes: Each panel shows the responses of log population of U.S. states (except for Texas) to a ten per cent positive shock to the annul supply of new land in Texas, for the period noted at the top. Each dot represents a state. States are ordered ascendingly by their distances to Texas, and the horizontal axis corresponds to state's rank in terms of distance to Texas.

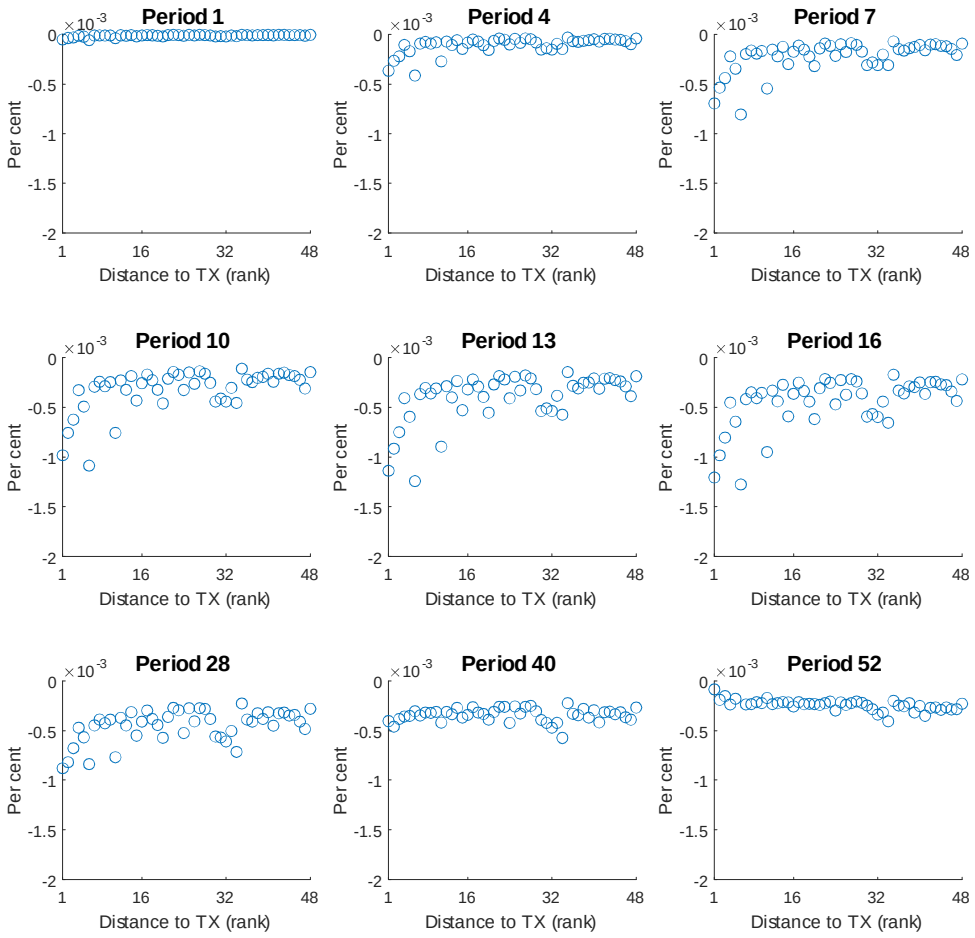

Figure S17: Spatiotemporal responses of log house price-to-income ratios of U.S. states to a positive land-supply shock in Texas

Notes: Each panel shows the responses of log house price-to-income ratios of U.S. states (except for Texas) to a ten per cent positive shock to the annul supply of new land in Texas, for the period noted at the top. Each dot represents a state. States are ordered ascendingly by their distances to Texas, and the horizontal axis corresponds to state's rank in terms of distance to Texas.

S1.3.3 Responses to regional shocks in Florida

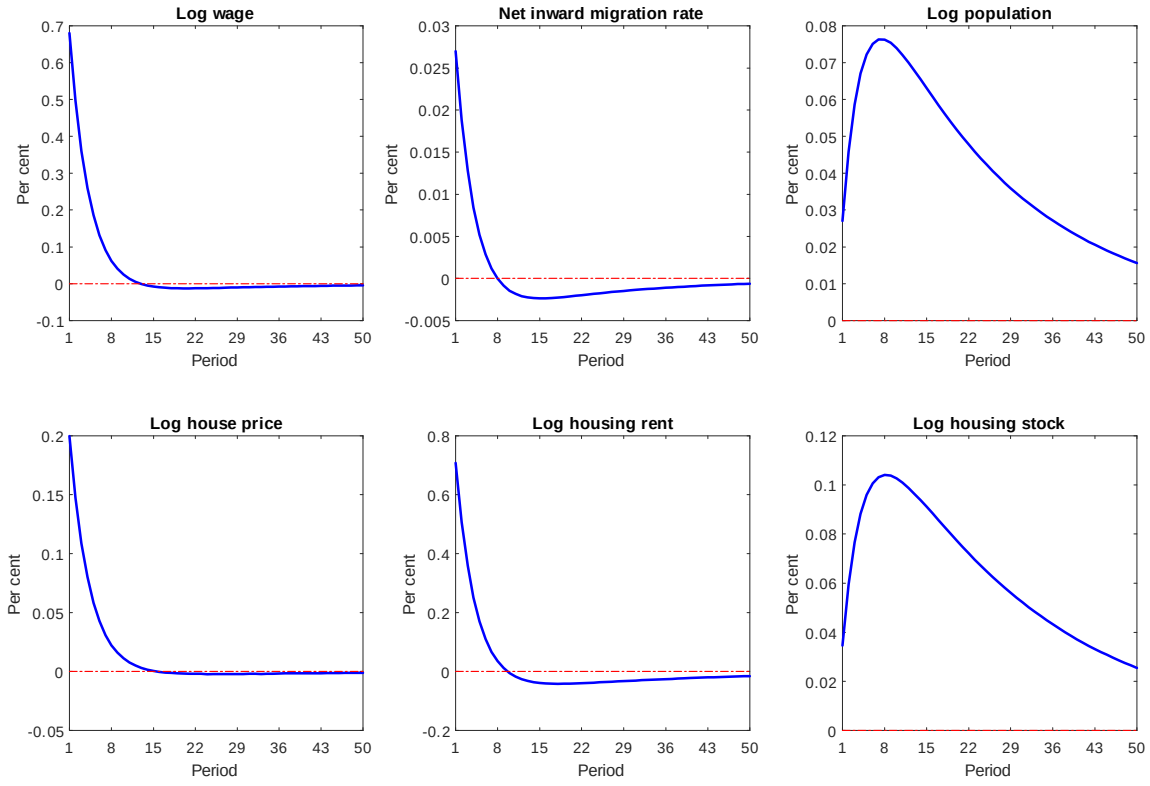

Figure S18: Reponses of Florida to a positive productivity shock in Florida

Notes: This figure shows the responses of log wage rate, net inward migration rate (i.e., the ratio of net inward migration to local population), log population, log house price, log housing rent and log housing stock in Florida to a one per cent positive shock to the labor productivity in Florida.

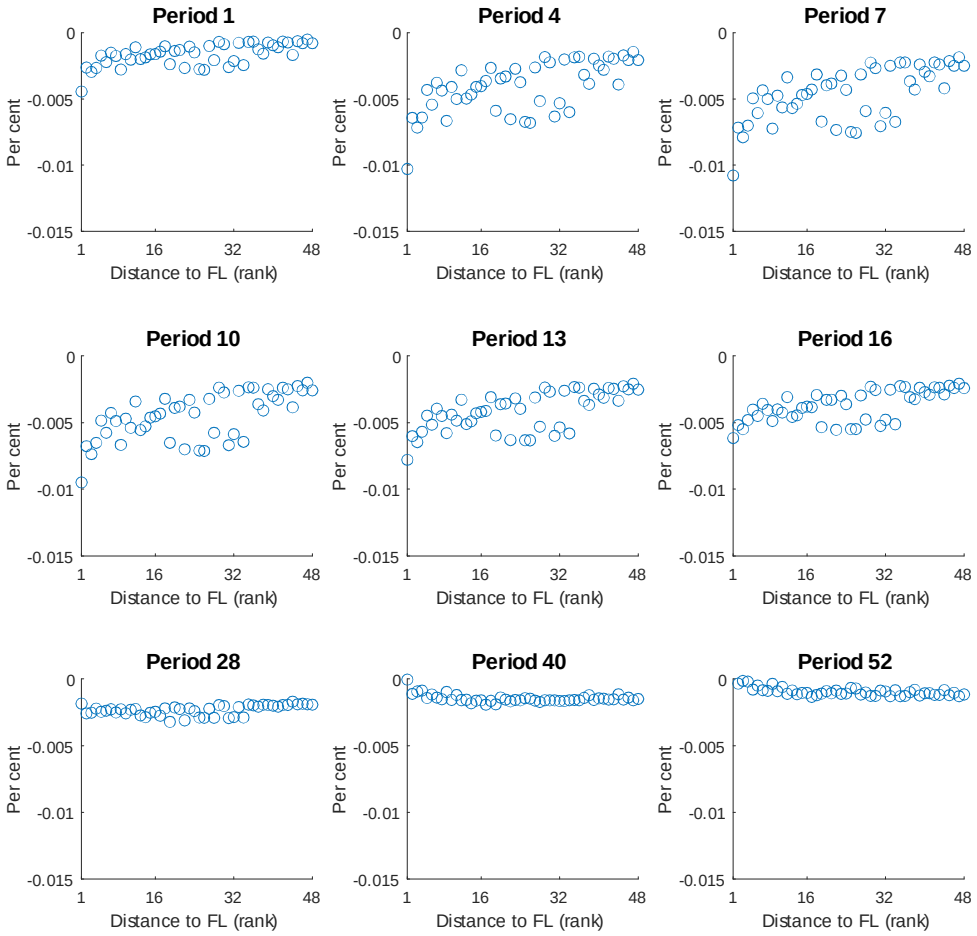

Figure S19: Spatiotemporal responses of log population of U.S. states to a positive productivity shock in Florida

Notes: Each panel shows the responses of log population of U.S. states (except for Florida) to a one per cent positive shock to the labor productivity in Florida, for the period noted at the top. Each dot represents a state. States are ordered ascendingly by their distances to Florida, and the horizontal axis corresponds to state's rank in terms of distance to Florida.

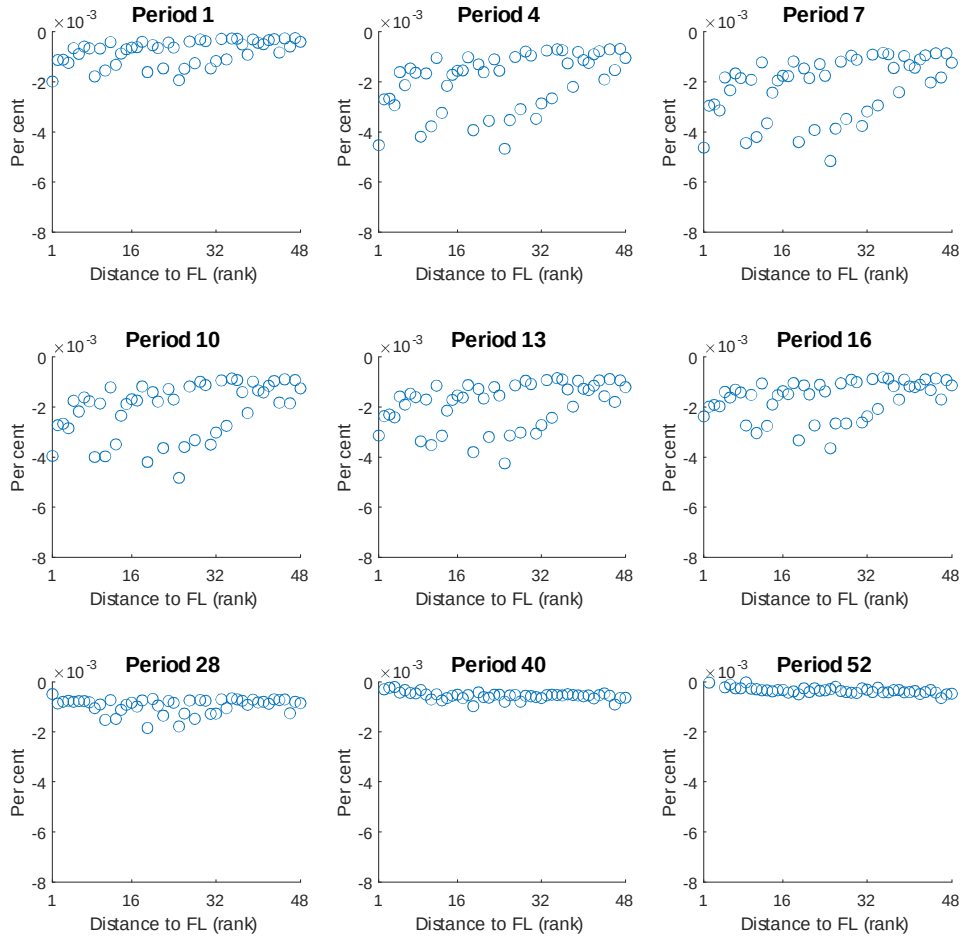

Figure S20: Spatiotemporal responses of log house price-to-income ratios of U.S. states to a positive productivity shock in Florida

Notes: Each panel shows the responses of log house price-to-income ratios of U.S. states (except for Florida) to a one per cent positive shock to the labor productivity in Florida, for the period noted at the top. Each dot represents a state. States are ordered ascendingly by their distances to Florida, and the horizontal axis corresponds to state's rank in terms of distance to Florida.

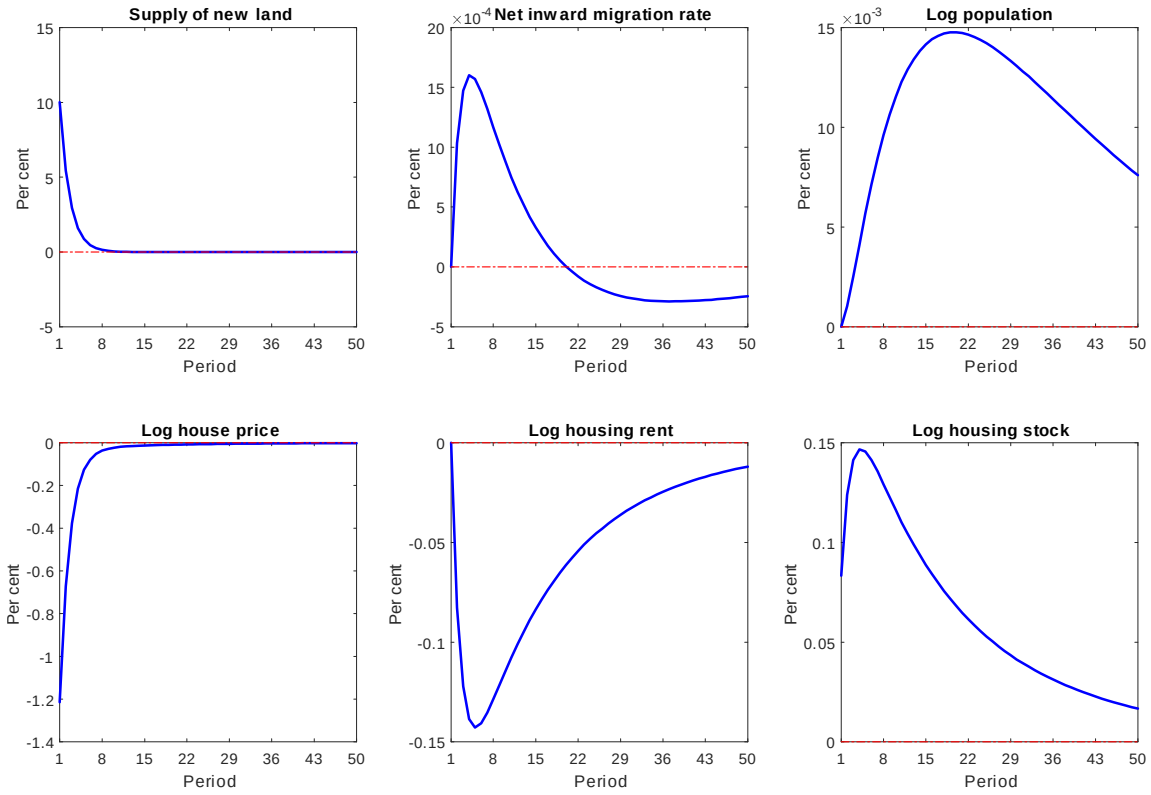

Figure S21: Reponses of Florida to a positive land-supply shock in Florida

Notes: This figure shows the responses of log wage rate, net inward migration rate (i.e., the ratio of net inward migration to local population), log population, log house price, log housing rent and log housing stock in Florida to a ten per cent positive shock to the annual supply of new land in Florida.

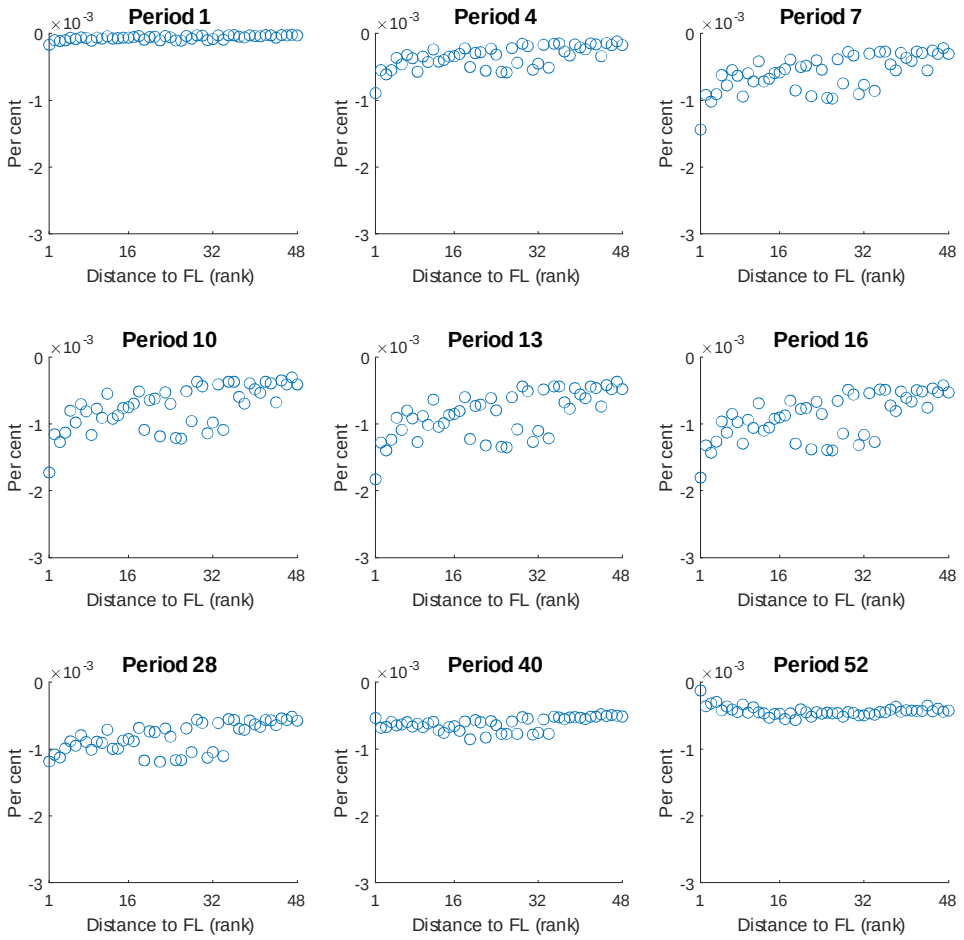

Figure S22: Spatiotemporal responses of log population of U.S. states to a positive land-supply shock in Florida

Notes: Each panel shows the responses of log population of U.S. states (except for Florida) to a ten per cent positive shock to the annul supply of new land in Florida, for the period noted at the top. Each dot represents a state. States are ordered ascendingly by their distances to Florida, and the horizontal axis corresponds to state's rank in terms of distance to Florida.

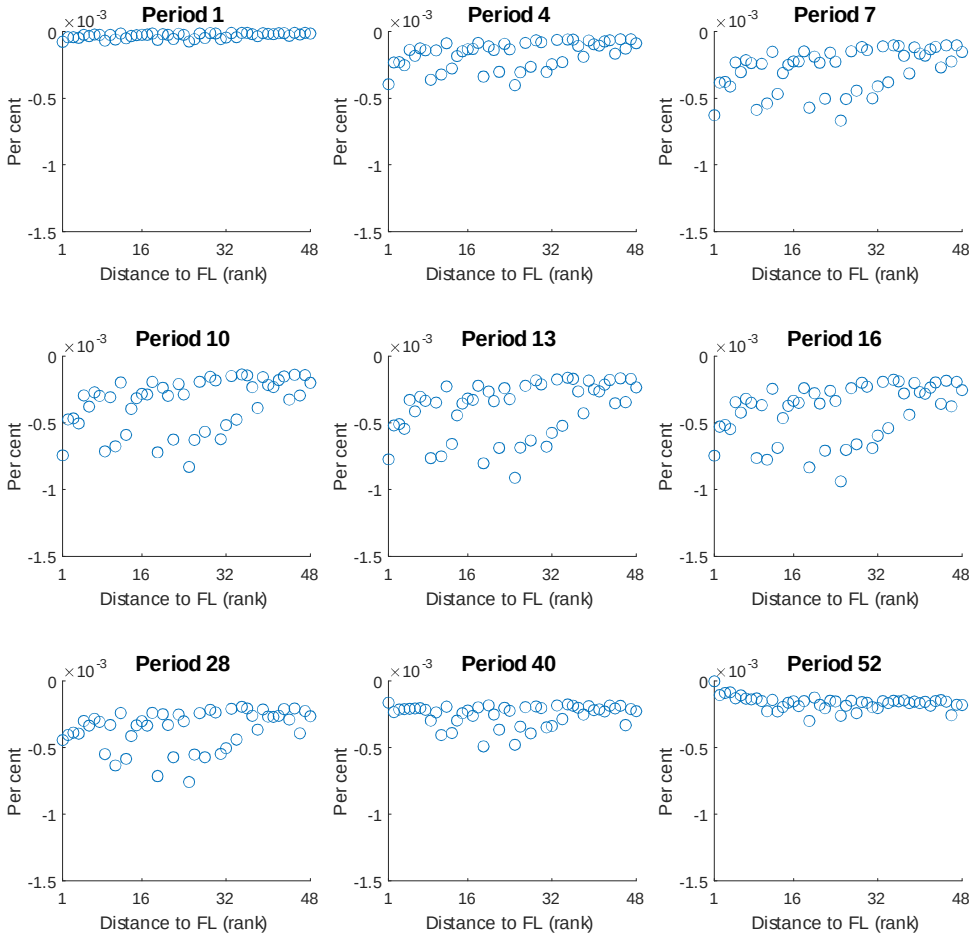

Figure S23: Spatiotemporal responses of log house price-to-income ratios of U.S. states to a positive land-supply shock in Florida

Notes: Each panel shows the responses of log house price-to-income ratios of U.S. states (except for Florida) to a ten per cent positive shock to the annul supply of new land in Florida, for the period noted at the top. Each dot represents a state. States are ordered ascendingly by their distances to Florida, and the horizontal axis corresponds to state's rank in terms of distance to Florida.

S1.3.4 Compare and contrast California with Texas and Florida

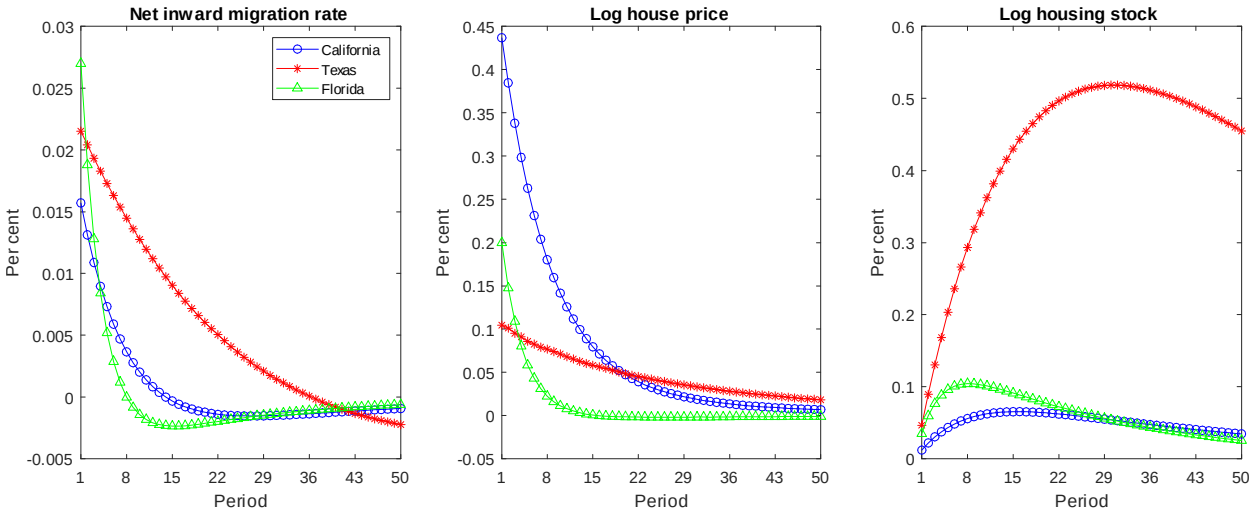

Panel 1: Responses of California, Texas and Florida to positive shocks to their local labor productivities

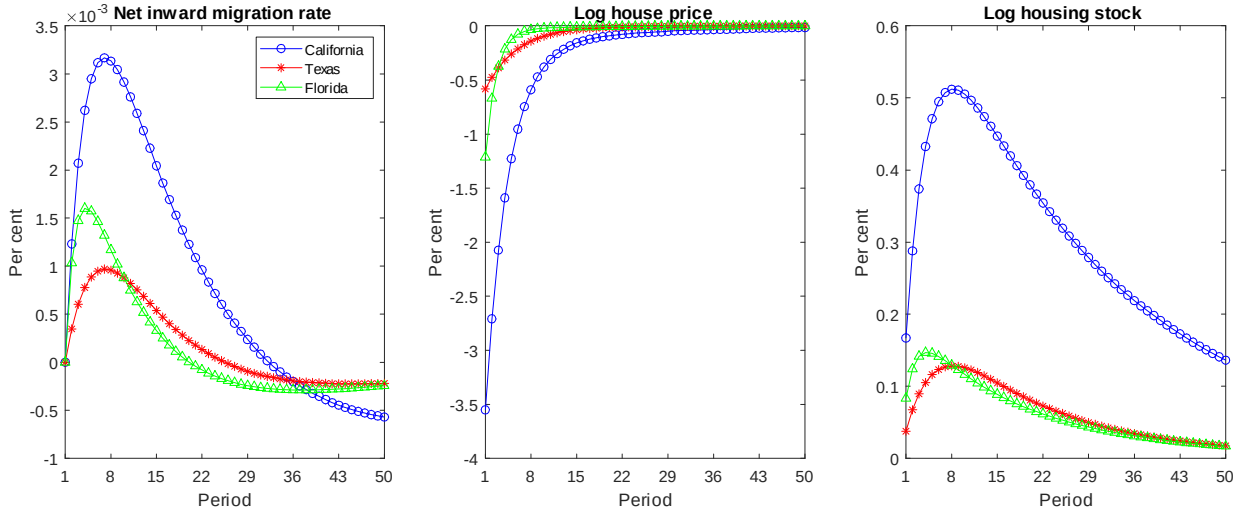

Panel 2: Responses of California, Texas and Florida to positive shocks to their local land supplies

Figure S24: Reponses of California, Texas and Florida to local shocks

In Panel 1, the blue lines designated with 'o' show the responses of net inward migration rate (i.e., the ratio of net inward migration to local population), log house price and log housing stock in California to a one per cent positive shock to the labor productivity in California. The red lines designated with '$\star$' show the responses of Texas to a one per cent positive productivity shock in Texas, and the green lines designated with 'Δ' show the responses of Florida to a one per cent positive productivity shock in Florida. Similarly, Panel 2 show the responses of California, Texas, and Florida after ten per cent positive shocks to their local supplies of new land.

S1.3.5 Calibration sensitivity

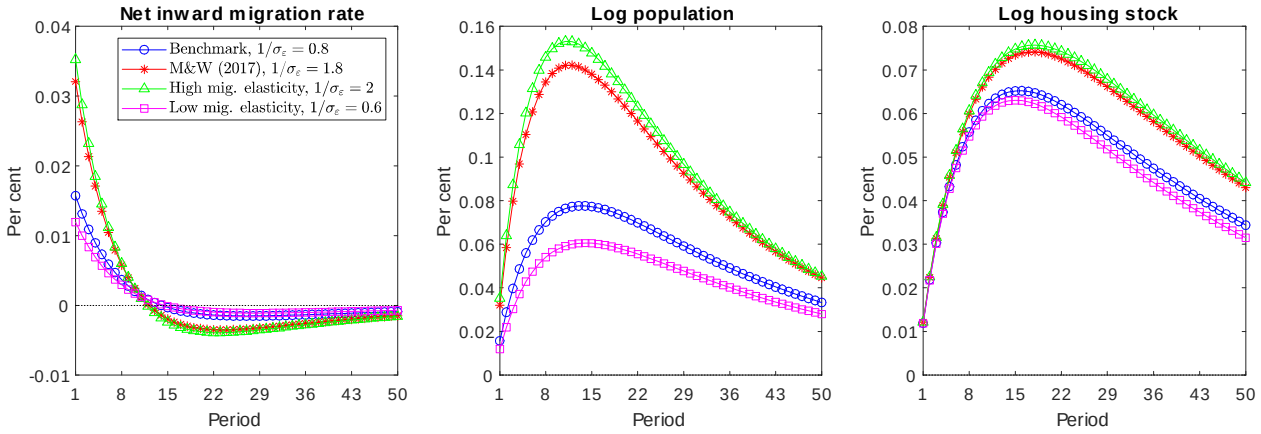

Panel 1: Reponses of California to a positive labor productivity shock in California

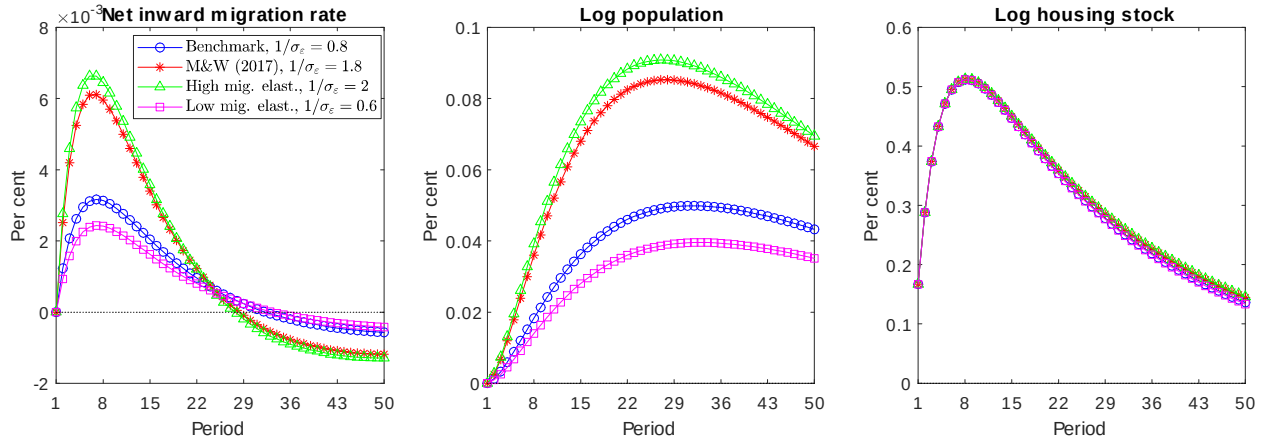

Panel 2: Reponses of California to a positive land-supply shock in California

Figure S25: Reponses of California to local shocks when the migration elasticity, $1/\sigma_\varepsilon$, is set to different values

Notes: Panel 1 shows the responses of net inward migration rate (i.e., the ratio of net inward migration to local population), log population and log housing stock in California to a one per cent positive shock to the labor productivity in California. The blue lines designated with 'o' correspond to the benchmark model calibrated in Section 6. The red lines designated with '$\star$' correspond to the re-calibrated model when the migration elasticity, $1/\sigma_\varepsilon$, is set to 1.8, which is the benchmark estimate for the migration elasticity of "star scientists" in Moretti and Wilson (2017). The green lines designated with 'Δ' correspond to the re-calibrated model when $1/\sigma_\varepsilon$ is set to 2, and the purple lines designated with '$\square$' correspond to the re-calibrated model when $1/\sigma_\varepsilon$ is set to 0.6. Similarly, Panel 2 shows the responses of California to a ten per cent positive shock to the annual supply of new land in California, when $1/\sigma_\varepsilon$ is set to different values.

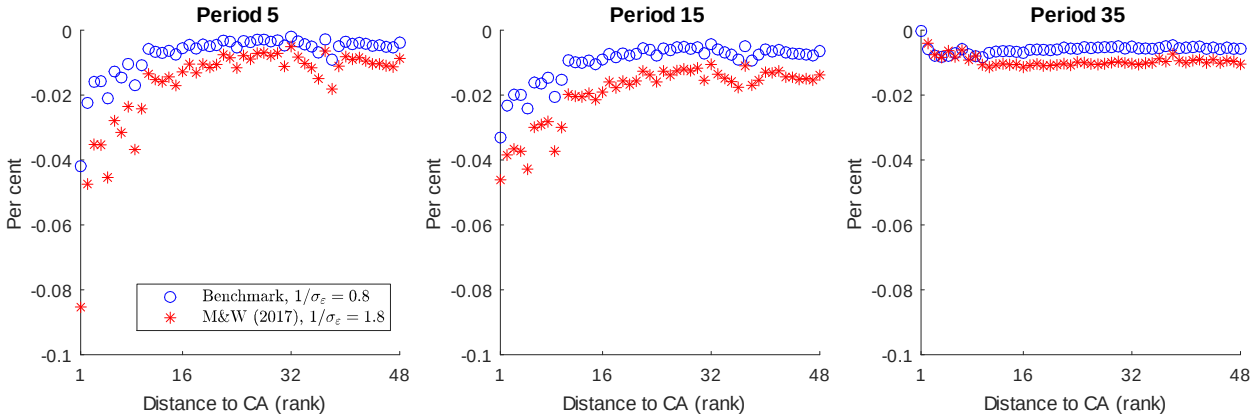

Panel 1: Spatiotemporal responses of log population of U.S. states to a positive labor productivity shock in California

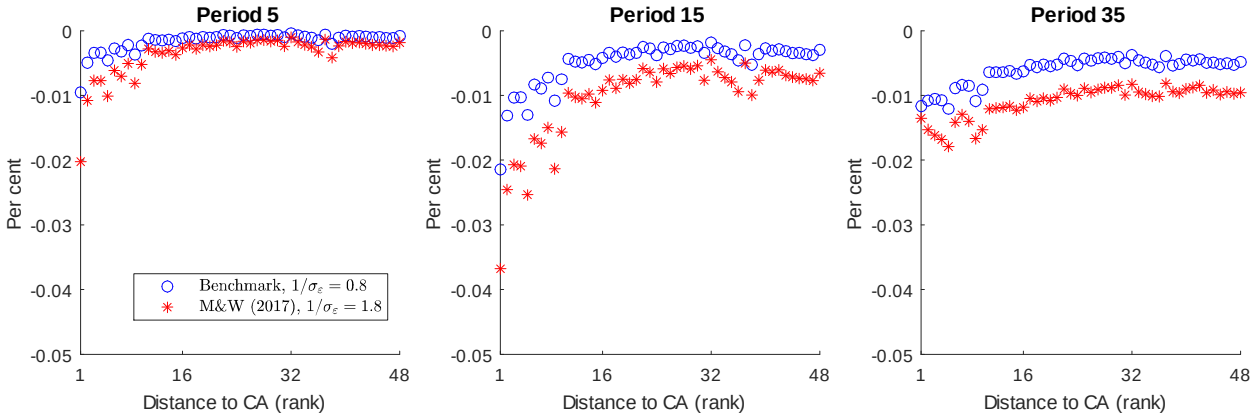

Panel 2: Spatiotemporal responses of log population of U.S. states to a positive land-supply shock in California

Figure S26: Spatiotemporal responses of log population of U.S. states to shocks in California when the migration elasticity, $1/\sigma_\varepsilon$, is set to different values

Notes: Panel 1 shows the responses of log population of U.S. states (except for California) to a one per cent positive shock to the labor productivity in California, for the periods noted at the top. Each dot represents a state. States are ordered ascendingly by their distances to California, and the horizontal axis corresponds to state's rank in terms of distance to California. The blue circles correspond to the benchmark model calibrated in Section 6. The red stars correspond to the re-calibrated model when the migration elasticity, $1/\sigma_\varepsilon$, is set to 1.8, which is the benchmark estimate for the migration elasticity of "star scientists" in Moretti and Wilson (2017). Similarly, Panel 2 shows the responses of log population of U.S. states (except for California) to a ten per cent positive shock to the annual supply of new land in California, when $1/\sigma_\varepsilon$ is set to different values.

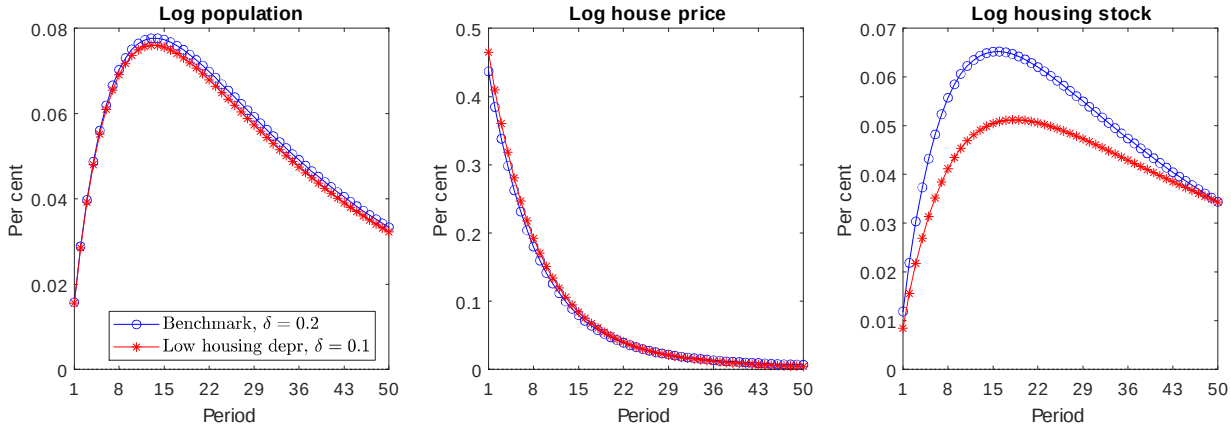

Panel 1: Reponses of California to a positive labor productivity shock in California

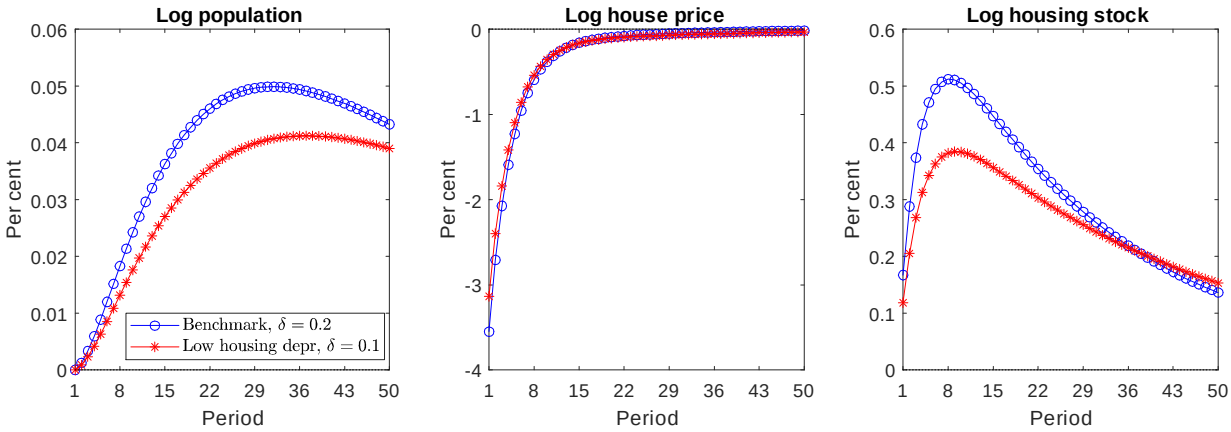

Panel 2: Reponses of California to a positive land-supply shock in California

Figure S27: Reponses of California to local shocks when the housing depreciation rate, δ, is set to different values

Notes: Panel 1 shows the responses of log population, log house price and log housing stock in California to a one per cent positive shock to the labor productivity in California. The blue lines designated with 'o' correspond to the benchmark model calibrated in Section 6. The red lines designated with '$\star$' correspond to the model in which the housing depreciation rate, δ, is set to 0.1. Similarly, Panel 2 shows the responses of California to a ten per cent positive shock to the annual supply of new land in California, when the housing depreciation rate, δ, is set to different values.

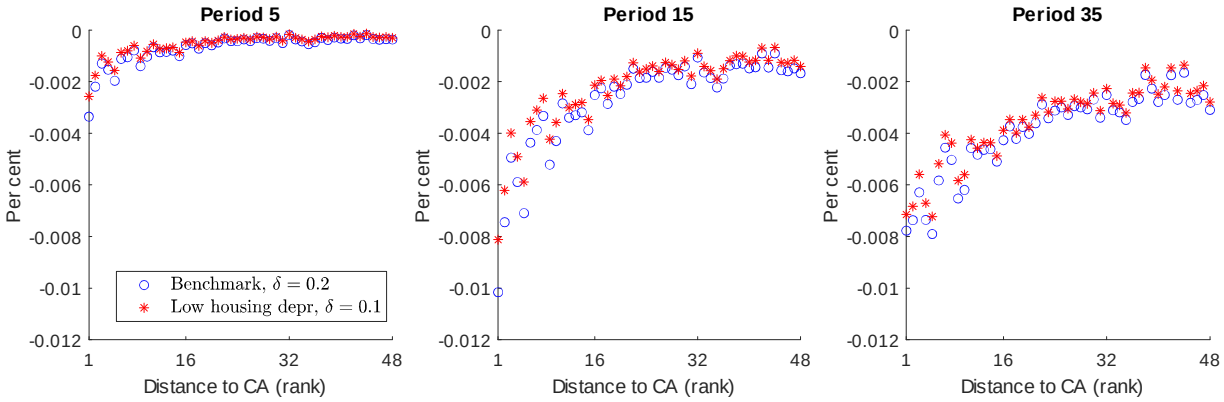

Panel 1: Spatiotemporal responses of log housing stocks of U.S. states to a positive labor productivity shock in California

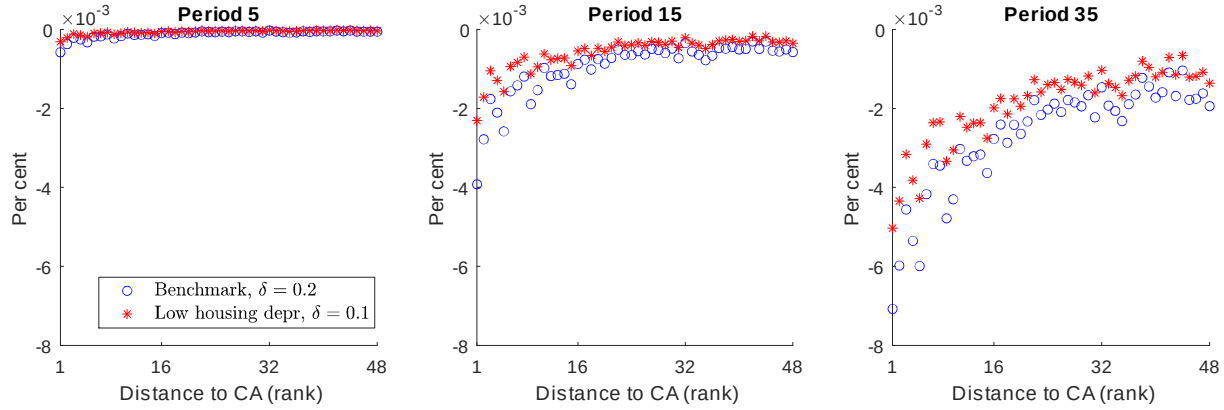

Panel 2: Spatiotemporal responses of log housing stocks of U.S. states to a positive land-supply shock in California

Figure S28: Spatiotemporal responses of log housing stocks of U.S. states to shocks in California when the housing depreciation rate, δ, is set to different values

Notes: Panel 1 shows the responses of log housing stocks of U.S. states (except for California) to a one per cent positive shock to the labor productivity in California, for the periods noted at the top. Each dot represents a state. States are ordered ascendingly by their distances to California, and the horizontal axis corresponds to state's rank in terms of distance to California. The blue circles correspond to the benchmark model calibrated in Section 6. The red stars correspond to the model in which the housing depreciation rate, δ, is set to 0.1. Similarly, Panel 2 shows the responses of log housing stocks of U.S. states (except for California) to a ten per cent positive shock to the annual supply of new land in California, when the housing depreciation rate, δ, is set to different values.

S2 Computation of the impulse responses

The impulse responses reported in the paper are computed using the Monte Carlo techniques developed by Koop et al. (1996). As discussed in Section 4, the model economy set out in Sections 2 and 3 can be written in a compact form as:

$$\boldsymbol{\zeta}_t = \boldsymbol{f}\left(\boldsymbol{\zeta}_{t-1}, \boldsymbol{a}_t, \boldsymbol{a}_{t-1}, \boldsymbol{\kappa}_{t-1}, \boldsymbol{g}_{l,t}; \Theta\right), \tag{S.1}$$

where Θ is a row vector that contains all the parameters, $\boldsymbol{\zeta}_t = [\boldsymbol{l}(t), \boldsymbol{q}_t]$ is a $1 \times 2n$ vector, and

$$\boldsymbol{\chi}_t = \boldsymbol{g}\left(\boldsymbol{\zeta}_t, \boldsymbol{a}_t, \boldsymbol{\kappa}_t; \Theta\right), \tag{S.2}$$

where $\boldsymbol{\chi}_t = [\boldsymbol{p}_t, \boldsymbol{h}_t]$ is a $1 \times 2n$ vector.

Define $\boldsymbol{\xi}_t = [\boldsymbol{\zeta}_t, \boldsymbol{\chi}_t]$, which is a $1 \times 4n$ vector. Then, the (S.1) and (S.2) can be combined and written as

$$\boldsymbol{\xi}_t = \boldsymbol{\psi}\left(\boldsymbol{\xi}_{t-1}, \boldsymbol{a}_t, \boldsymbol{a}_{t-1}, \boldsymbol{\kappa}_t, \boldsymbol{\kappa}_{t-1}, \boldsymbol{g}_{l,t}; \Theta\right). \tag{S.3}$$

The stochastic processes of $\boldsymbol{a}_t$ and $\boldsymbol{\kappa}_t$, are given by

$$\begin{aligned}
\ln \boldsymbol{a}_t &= \ln \boldsymbol{a} + \boldsymbol{g}_a t \ + \boldsymbol{\lambda}\, f_t + \boldsymbol{z}_{a,t}, && \text{(S.4)}\\
f_t &= \rho_f f_{t-1} + \sigma_f \varepsilon_{f,t}, && \text{(S.5)}\\
\boldsymbol{z}_{a,t} &= \boldsymbol{z}_{a,t-1}\mathbf{diag}(\rho_{a,1}, \rho_{a,2}, ...\rho_{a,n}) + \boldsymbol{\varepsilon}_{a,t}\mathbf{diag}(\sigma_{a,1}, \sigma_{a,2}, ...\sigma_{a,n}), && \text{(S.6)}
\end{aligned}$$

and

$$\begin{aligned}
\ln \boldsymbol{\kappa}_t &= \ln \boldsymbol{\kappa} + \boldsymbol{g}_\kappa t + \boldsymbol{z}_{\kappa,t}, && \text{(S.7)}\\
\boldsymbol{z}_{\kappa,t} &= \boldsymbol{z}_{\kappa,t-1}\mathbf{diag}(\rho_{\kappa,1}, \rho_{\kappa,2}, ...\rho_{\kappa,n}) + \boldsymbol{\varepsilon}_{\kappa,t}\mathbf{diag}(\sigma_{\kappa,1}, \sigma_{\kappa,2}, ...\sigma_{\kappa,n}), && \text{(S.8)}
\end{aligned}$$

and the values of state level intrinsic population growth rates, $\boldsymbol{g}_{l,t}$, for $t = 0, 1, 2, ...$, are exogenously given.

Impulse response function: To illustrate the computation algorithm, we take the computation of the impulse responses to a standard deviation negative productivity shock to state i^* as an example. Note that the model is Markovian. Thus, the relevant history is only the period before the start of simulation. Let the shock hits the economy in period 1. Then, the impulse response function is given by

$$\begin{aligned}
GI_\xi(t, \varepsilon_{a,i^*1}, \boldsymbol{\xi}_0, \boldsymbol{a}_0, \boldsymbol{\kappa}_0) &= E(\boldsymbol{\xi}_t|\varepsilon_{a,i^*1}, \boldsymbol{\xi}_0, \boldsymbol{a}_0, \boldsymbol{\kappa}_0) - E(\boldsymbol{\xi}_t|\boldsymbol{\xi}_0, \boldsymbol{a}_0, \boldsymbol{\kappa}_0)\\
\text{for } t &= 1, 2, ..., T,
\end{aligned}$$

where T is the horizon of the impulse response analyses, $E(\boldsymbol{\xi}_t|\boldsymbol{\xi}_0, \boldsymbol{a}_0, \boldsymbol{\kappa}_0)$ is the expectation of $\boldsymbol{\xi}_t$ conditional only on $\boldsymbol{\xi}_0, \boldsymbol{a}_0$ and $\boldsymbol{\kappa}_0$, and $E(\boldsymbol{\xi}_t|\varepsilon_{a,i^*1}, \boldsymbol{\xi}_0, \boldsymbol{a}_0, \boldsymbol{\kappa}_0)$ is the expectation of $\boldsymbol{\xi}_t$ conditional on both $\boldsymbol{\xi}_0, \boldsymbol{a}_0, \boldsymbol{\kappa}_0$ and ε_{a,i^*1}. Recall that ε_{a,i^*1} is the innovation to the local productivity shock in state i^* in period 1.

Initial values: In our impulse response simulations, we assume that the economy is on the balanced growth path when $t = 0$. Recall that in Section 5, we established the

uniqueness of the balanced growth path by showing that for given values of $L_0, \boldsymbol{\kappa}$ and $\boldsymbol{a}$, the steady states of the detrended variables are uniquely determined by the equation system (47)-(54). Note that detrended variables equal non-detrended variables when $t = 0$. Thus, we use the steady state values of the detrended variables as the initial values for the corresponding non-detrended variable in the impulse response simulations, which implies that the economy is on the balanced growth path when $t = 0$.

Deterministic variables: The intrinsic population growth rates of all states are set equal to the balanced growth path level given by (42):

$$\boldsymbol{g}_{l,t} = [\hat{g}_l, \hat{g}_l, ..., \hat{g}_l], \text{ for } t = 1, 2, ..., T,$$

where g_l is the balanced growth path intrinsic population growth rate, which is assumed to be common to all states, and estimated as the average growth rate of the national population over the period 1976-2014.

Stochastic processes: The state level productivities and land supplies, $\boldsymbol{a}_t$ and $\boldsymbol{\kappa}_t$, are simulated using the estimated (S.4) - (S.8), where f_0, $\boldsymbol{z}_{a0}$ and $\boldsymbol{z}_{\kappa 0}$ are set to 0.

We set the numbers of replications and horizons to R and T, and independently draw innovations from the standard normal distribution. Let $\varepsilon_{f,t}^{(r)}$, $\boldsymbol{\varepsilon}_{a,t}^{(r)}$ and $\boldsymbol{\varepsilon}_{\kappa,t}^{(r)}$ denote the simulated $\varepsilon_{f,t}$, $\boldsymbol{\varepsilon}_{a,t}$ and $\boldsymbol{\varepsilon}_{\kappa,t}$, for replication r, where $\boldsymbol{\varepsilon}_{a,t}^{(r)} = \left[\varepsilon_{a,1t}^{(r)}, \varepsilon_{a,2t}^{(r)}, ..., \varepsilon_{a,nt}^{(r)}\right]$ and $\boldsymbol{\varepsilon}_{\kappa,t}^{(r)} = \left[\varepsilon_{\kappa,1t}^{(r)}, \varepsilon_{\kappa,2t}^{(r)}, ..., \varepsilon_{\kappa,nt}^{(r)}\right]$. The innovations, $\varepsilon_{f,t}^{(r)}$, $\varepsilon_{a,it}^{(r)}$ and $\varepsilon_{\kappa,it}^{(r)}$, for $i = 1, 2, ..., n$, $t = 1, 2., ..., T$ and $r = 1, 2., ..., R$, are independently drawn from the standard normal distribution.

Productivity processes without shock: When there is no shock, for each replication r, we plug the simulated innovations, $\varepsilon_{f,t}^{(r)}$ and $\boldsymbol{\varepsilon}_{a,t}^{(r)}$, into (S.4) - (S.6), and obtain a series of simulated productivities, $\boldsymbol{a}_t^{(r)}$, for $t = 1, 2., ..., T$.

Productivity processes with shock: When there is shock, for each replication r, we plug the simulated innovations, $\varepsilon_{f,t}^{(r)}$ and $\boldsymbol{\varepsilon}_{a,t}^{(r)}$, with the i^*th element of $\boldsymbol{\varepsilon}_{a,1}^{(r)}$, i.e., $\varepsilon_{a,i^*1}^{(r)}$, being replaced by -1 (a negative shock), into (S.4) - (S.6), and obtain another series of simulated productivities, $\check{\boldsymbol{a}}_t^{(r)}$, for $t = 1, 2., ..., T$.

Land supply processes: For both the cases with and without shock, for each replication r, we plug the simulated innovations, $\boldsymbol{\varepsilon}_{\kappa,t}^{(r)}$, into (S.7) - (S.8), and obtain a series of simulated productivities, $\boldsymbol{\kappa}_t^{(r)}$, for $t = 1, 2., ..., T$.

Computation: To compute $E(\boldsymbol{\xi}_t|\boldsymbol{\xi}_0, \boldsymbol{a}_0, \boldsymbol{\kappa}_0)$ and $E(\boldsymbol{\xi}_t|\varepsilon_{a,i^*1}, \boldsymbol{\xi}_0, \boldsymbol{a}_0, \boldsymbol{\kappa}_0)$ numerically, we conduct the following two simulations.

- *Simulation 1 (no shock):* For each replication r, given the initial values, $\boldsymbol{\xi}_0$, $\boldsymbol{a}_0$ and $\boldsymbol{\kappa}_0$, and the deterministic processes of $\boldsymbol{g}_{l,t}$, we simulate the model (S.3) using the simulated productivity processes, $\boldsymbol{a}_t^{(r)}$ and $\boldsymbol{\kappa}_t^{(r)}$, for $t = 1, 2, ..., T$, and obtain a series of realized $\boldsymbol{\xi}_t$, i.e., $\boldsymbol{\xi}_t^{(r)}$, for $t = 1, 2, ..., T$:

$$\boldsymbol{\xi}_t^{(r)} = \boldsymbol{\psi}\left(\boldsymbol{\xi}_{t-1}^{(r)}, \boldsymbol{a}_t^{(r)}, \boldsymbol{a}_{t-1}^{(r)}, \boldsymbol{\kappa}_t^{(r)}, \boldsymbol{\kappa}_{t-1}^{(r)}, \boldsymbol{g}_{l,t}; \Theta\right).$$

- *Simulation 2 (with shock):* For each replication r, given the initial values, $\boldsymbol{\xi}_0$, $\boldsymbol{a}_0$ and $\boldsymbol{\kappa}_0$, and the deterministic processes of $\boldsymbol{g}_{l,t}$, we simulate the model (S.3) using the simulated

productivity processes, $\check{\boldsymbol{a}}_t^{(r)}$ and $\boldsymbol{\kappa}_t^{(r)}$, for $t = 1, 2, ..., T$, and obtain a series of realized $\boldsymbol{\xi}_t$, i.e., $\check{\boldsymbol{\xi}}_t^{(r)}$, for $t = 1, 2, ..., T$:

$$\check{\boldsymbol{\xi}}_t^{(r)} = \boldsymbol{\psi}\left(\check{\boldsymbol{\xi}}_{t-1}^{(r)}, \check{\boldsymbol{a}}_t^{(r)}, \check{\boldsymbol{a}}_{t-1}^{(r)}, \boldsymbol{\kappa}_t^{(r)}, \boldsymbol{\kappa}_{t-1}^{(r)}, \boldsymbol{g}_{l,t}; \Theta\right).$$

Here, $\boldsymbol{\xi}_t^{(r)}$ and $\check{\boldsymbol{\xi}}_t^{(r)}$ are the simulated $\boldsymbol{\zeta}_t$ in replication r in Simulation 1 and Simulation 2, respectively. Then, the two expectations, $E(\boldsymbol{\xi}_t|\boldsymbol{\xi}_0, \boldsymbol{a}_0, \boldsymbol{\kappa}_0)$ and $E(\boldsymbol{\xi}_t|\varepsilon_{a,i^*1}, \boldsymbol{\xi}_0, \boldsymbol{a}_0, \boldsymbol{\kappa}_0)$, are approximated as the averages across replications:

$$\hat{E}(\boldsymbol{\xi}_t|\boldsymbol{\xi}_0, \boldsymbol{a}_0, \boldsymbol{\kappa}_0) = \frac{1}{R}\sum_{r=1}^{R} \boldsymbol{\xi}_t^{(r)} \quad \text{and} \quad \hat{E}(\boldsymbol{\xi}_t|\varepsilon_{a,i^*1}, \boldsymbol{\xi}_0, \boldsymbol{a}_0, \boldsymbol{\kappa}_0) = \frac{1}{R}\sum_{r=1}^{R} \check{\boldsymbol{\xi}}_t^{(r)}.$$

Thus, the approximated impulse response in period t is given as

$$GI_{\boldsymbol{\xi}}(t, \varepsilon_{a,i^*1}, \boldsymbol{\xi}_0, \boldsymbol{a}_0, \boldsymbol{\kappa}_0) = \frac{1}{R}\sum_{r=1}^{R} \check{\boldsymbol{\xi}}_t^{(r)} - \frac{1}{R}\sum_{r=1}^{R} \boldsymbol{\xi}_t^{(r)}.$$

S3 Parameter values

Table S2: Location-specific parameters related to housing supplies and investment

State		$\hat{\vartheta}_{\kappa,i}$	$\hat{\theta}_i$			$\hat{\vartheta}_{\kappa,i}$	$\hat{\theta}_i$
AL	Alabama	0.0707	0.0175	NE	Nebraska	0.0598	0.0278
AZ	Arizona	0.1362	0.0155	NV	Nevada	0.2070	0.0071
AR	Arkansas	0.0571	0.0279	NH	New Hampshire	0.2394	0.0183
CA	California	0.5176	0.0092	NJ	New Jersey	0.4045	0.0130
CO	Colorado	0.2785	0.0138	NM	New Mexico	0.1067	0.0066
CT	Connecticut	0.4770	0.0056	NY	New York	0.2328	0.0160
DE	Delaware	0.1508	0.0178	NC	North Carolina	0.1390	0.0228
DC	District of Columbia	0.5312	0.0130	ND	North Dakota	0.0971	0.0184
FL	Florida	0.1442	0.0304	OH	Ohio	0.1109	0.0191
GA	Georgia	0.1210	0.0249	OK	Oklahoma	0.0857	0.0264
ID	Idaho	0.1058	0.0126	OR	Oregon	0.1665	0.0167
IL	Illinois	0.1854	0.0137	PA	Pennsylvania	0.1034	0.0233
IN	Indiana	0.0780	0.0200	RI	Rhode Island	0.2331	0.0097
IA	Iowa	0.1037	0.0283	SC	South Carolina	0.1062	0.0225
KS	Kansas	0.0687	0.0286	SD	South Dakota	0.0857	0.0248
KY	Kentucky	0.0654	0.0242	TN	Tennessee	0.0792	0.0247
LA	Louisiana	0.0826	0.0186	TX	Texas	0.0602	0.0343
ME	Maine	0.1330	0.0188	UT	Utah	0.2039	0.0102
MD	Maryland	0.3666	0.0179	VT	Vermont	0.2351	0.0158
MA	Massachusetts	0.3138	0.0137	VA	Virginia	0.3216	0.0218
MI	Michigan	0.0955	0.0286	WA	Washington	0.2029	0.0129
MN	Minnesota	0.0712	0.0217	WV	West Virginia	0.0975	0.0190
MS	Mississippi	0.0628	0.0258	WI	Wisconsin	0.1116	0.0206
MO	Missouri	0.0704	0.0258	WY	Wyoming	0.1678	0.0062
MT	Montana	0.0947	0.0121				
Average across the U.S. states		0.1682	0.0189				

Table S3: Location-specific parameters of the labor productivity processes

State		$\hat{\lambda}_i$	SE	p-value	$\hat{\rho}_{a,i}$	SE	p-value	$\hat{\sigma}_{a,i}$
AL	Alabama	1.3500	0.0830	0.0000	0.8589	0.1086	0.0000	0.0133
AZ	Arizona	0.9067	0.1355	0.0000	0.8089	0.1153	0.0000	0.0228
AR	Arkansas	0.9156	0.0932	0.0000	0.7286	0.1414	0.0000	0.0194
CA	California	0.3449	0.1533	0.0343	0.8694	0.1057	0.0000	0.0239
CO	Colorado	1.1385	0.1041	0.0000	0.8507	0.1390	0.0000	0.0191
CT	Connecticut	1.6242	0.1737	0.0000	0.8270	0.1132	0.0000	0.0280
DE	Delaware	1.3316	0.1136	0.0000	0.7059	0.1565	0.0002	0.0252
DC	District of Columbia	0.5195	0.1849	0.0099	0.7746	0.0992	0.0000	0.0269
FL	Florida	1.5818	0.1475	0.0000	0.7405	0.1315	0.0000	0.0276
GA	Georgia	2.1065	0.1119	0.0000	0.7394	0.1463	0.0000	0.0240
ID	Idaho	0.6251	0.1496	0.0004	0.7247	0.1147	0.0000	0.0252
IL	Illinois	0.9811	0.0533	0.0000	0.3842	0.1758	0.0398	0.0138
IN	Indiana	1.1175	0.0826	0.0000	0.8134	0.1025	0.0000	0.0123
IA	Iowa	0.2285	0.1354	0.1051	0.4526	0.1889	0.0255	0.0378
KS	Kansas	0.6216	0.0567	0.0000	0.3714	0.1929	0.0672	0.0159
KY	Kentucky	0.9512	0.0836	0.0000	0.7206	0.1464	0.0001	0.0178
LA	Louisiana	0.2497	0.1011	0.0214	0.6956	0.1178	0.0000	0.0173
ME	Maine	1.1732	0.1084	0.0000	0.8417	0.1267	0.0000	0.0196
MD	Maryland	1.3749	0.0959	0.0000	0.7012	0.1505	0.0001	0.0211
MA	Massachusetts	1.6583	0.1668	0.0000	0.8216	0.1227	0.0000	0.0294
MI	Michigan	1.0009	0.0898	0.0000	0.7040	0.1369	0.0000	0.0180
MN	Minnesota	1.2649	0.0570	0.0000	0.0955	0.2094	0.6527	0.0176
MS	Mississippi	1.0084	0.1246	0.0000	0.8873	0.1014	0.0000	0.0185
MO	Missouri	1.2509	0.0597	0.0000	0.5434	0.1879	0.0085	0.0159
MT	Montana	-0.3493	0.1437	0.0233	0.3939	0.1899	0.0500	0.0403
NE	Nebraska	0.8859	0.0708	0.0000	-0.1827	0.1980	0.3663	0.0206
NV	Nevada	1.4794	0.1905	0.0000	0.9022	0.0993	0.0000	0.0275
NH	New Hampshire	1.9806	0.2323	0.0000	0.7920	0.1068	0.0000	0.0358
NJ	New Jersey	1.4646	0.1077	0.0000	0.7568	0.1439	0.0000	0.0219
NM	New Mexico	0.5373	0.0585	0.0000	0.7661	0.1673	0.0001	0.0130
NY	New York	1.2613	0.1260	0.0000	0.8292	0.1375	0.0000	0.0243
NC	North Carolina	1.9992	0.1169	0.0000	0.6985	0.1519	0.0001	0.0263
ND	North Dakota	-0.1182	0.2531	0.6448	0.0022	0.2127	0.9917	0.0796
OH	Ohio	0.8190	0.0685	0.0000	0.6346	0.1530	0.0004	0.0155
OK	Oklahoma	-0.3802	0.1414	0.0131	0.6517	0.1587	0.0005	0.0325
OR	Oregon	0.7045	0.1365	0.0000	0.7930	0.1063	0.0000	0.0213
PA	Pennsylvania	1.0008	0.0845	0.0000	0.7710	0.1288	0.0000	0.0157
RI	Rhode Island	0.9745	0.1682	0.0000	0.8807	0.1042	0.0000	0.0252
SC	South Carolina	1.5644	0.0742	0.0000	0.6996	0.1511	0.0001	0.0164
SD	South Dakota	0.8927	0.1288	0.0000	0.2804	0.2052	0.1857	0.0388
TN	Tennessee	2.1752	0.1451	0.0000	0.7874	0.1265	0.0000	0.0271
TX	Texas	1.1899	0.1242	0.0000	0.9746	0.1236	0.0000	0.0195
UT	Utah	1.0823	0.1101	0.0000	0.9438	0.0994	0.0000	0.0149
VT	Vermont	1.4196	0.1048	0.0000	0.7451	0.1277	0.0000	0.0195
VA	Virginia	1.3727	0.1008	0.0000	0.7820	0.1264	0.0000	0.0186
WA	Washington	1.0695	0.0763	0.0000	0.7613	0.1380	0.0000	0.0154
WV	West Virginia	0.1421	0.0726	0.0624	0.4836	0.1887	0.0178	0.0201
WI	Wisconsin	1.2697	0.0689	0.0000	0.6330	0.1633	0.0008	0.0166
WY	Wyoming	-0.7628	0.1712	0.0002	0.5032	0.1872	0.0134	0.0446
Average across the U.S. states		1.0000			0.6723			0.0237

Table S4: Location-specific parameters of the land supply processes

State		WRI	$\widehat{g}_{\kappa,i}$	SE	p-value	$\widehat{\rho}_{\kappa,i}$	SE	p-value	$\widehat{\sigma}_{\kappa,i}$
AL	Alabama	-1.1401	0.0879	0.0273	0.0040	0.9017	0.1206	0.0000	0.4879
AZ	Arizona	0.9917	0.1009	0.0171	0.0000	0.8163	0.1307	0.0000	0.3275
AR	Arkansas	-1.0279	0.2017	0.0334	0.0000	0.8833	0.1299	0.0000	0.6364
CA	California	1.0057	-0.0081	0.0077	0.3003	0.7490	0.1143	0.0000	0.1377
CO	Colorado	0.8514	0.0225	0.0114	0.0614	0.9233	0.1082	0.0000	0.1785
CT	Connecticut	0.7112	-0.0067	0.0127	0.6033	0.8830	0.0994	0.0000	0.1981
DE	Delaware	0.8514	-0.0566	0.0198	0.0092	0.8576	0.1024	0.0000	0.3137
DC	District of Columbia		-0.0161	0.0070	0.0321	0.7467	0.1231	0.0000	0.1366
FL	Florida	0.6972	0.0782	0.0052	0.0000	0.5419	0.2119	0.0180	0.1508
GA	Georgia	-0.1163	0.0375	0.0109	0.0023	0.8757	0.1464	0.0000	0.2193
ID	Idaho	-0.7053	0.0724	0.0264	0.0120	0.9174	0.0965	0.0000	0.3950
IL	Illinois	-0.0882	-0.0141	0.0170	0.4156	0.8445	0.1159	0.0000	0.3115
IN	Indiana	-1.2383	0.0132	0.0266	0.6242	0.8812	0.1208	0.0000	0.4837
IA	Iowa	-1.2102	0.1207	0.0392	0.0055	0.9313	0.0960	0.0000	0.5719
KS	Kansas	-1.4066	0.1999	0.0341	0.0000	0.9754	0.1184	0.0000	0.5596
KY	Kentucky	-0.6212	-0.0064	0.0301	0.8329	0.9128	0.1144	0.0000	0.5116
LA	Louisiana	-1.3084	0.2236	0.0422	0.0000	0.8887	0.1041	0.0000	0.6419
ME	Maine	1.1319	-0.0676	0.0293	0.0312	0.8537	0.1052	0.0000	0.4875
MD	Maryland	1.2862	-0.0060	0.0066	0.3766	0.8722	0.1118	0.0000	0.1155
MA	Massachusetts	2.3661	-0.0731	0.0213	0.0024	0.9124	0.0852	0.0000	0.2864
MI	Michigan	0.2063	-0.0969	0.0340	0.0093	0.9010	0.1105	0.0000	0.5697
MN	Minnesota	0.2904	0.0285	0.0250	0.2671	0.8120	0.1543	0.0000	0.5412
MS	Mississippi	-0.9718	0.2309	0.0341	0.0000	0.9083	0.1348	0.0000	0.6544
MO	Missouri	-1.2663	0.0443	0.0269	0.1140	0.8103	0.1424	0.0000	0.5783
MT	Montana	-0.3267	0.0411	0.0346	0.2477	0.8736	0.1145	0.0000	0.6103
NE	Nebraska	-0.7755	0.0995	0.0418	0.0265	0.9879	0.0989	0.0000	0.5934
NV	Nevada	-0.4529	0.0711	0.0091	0.0000	0.6113	0.1325	0.0001	0.1877
NH	New Hampshire	2.0856	0.0053	0.0244	0.8313	0.8596	0.1003	0.0000	0.3874
NJ	New Jersey	1.4124	-0.0286	0.0137	0.0491	0.8934	0.0976	0.0000	0.2096
NM	New Mexico	0.0240	0.0382	0.0159	0.0249	0.7506	0.1249	0.0000	0.3071
NY	New York	0.1642	-0.0855	0.0225	0.0010	0.9254	0.0870	0.0000	0.3060
NC	North Carolina	-0.3126	0.0033	0.0100	0.7425	0.8698	0.1344	0.0000	0.1983
ND	North Dakota	-0.5791	0.1953	0.0321	0.0000	0.6902	0.1663	0.0004	0.8126
OH	Ohio	-0.3267	0.0090	0.0262	0.7357	0.9157	0.0980	0.0000	0.3951
OK	Oklahoma	-0.8035	0.2954	0.0414	0.0000	0.8535	0.1097	0.0000	0.6672
OR	Oregon	0.2904	-0.0435	0.0298	0.1583	0.9397	0.0863	0.0000	0.3977
PA	Pennsylvania	0.6972	-0.0828	0.0297	0.0107	0.8690	0.0988	0.0000	0.4594
RI	Rhode Island	2.3942	-0.0643	0.0230	0.0107	0.8991	0.1019	0.0000	0.3656
SC	South Carolina	-0.8877	0.0277	0.0113	0.0227	1.0186	0.1315	0.0000	0.1939
SD	South Dakota	-1.2804	0.0545	0.0292	0.0759	0.8546	0.1260	0.0000	0.5606
TN	Tennessee	-0.7755	0.0051	0.0220	0.8190	0.8618	0.1263	0.0000	0.4200
TX	Texas	-0.4529	0.2911	0.0401	0.0000	0.8064	0.1141	0.0000	0.6618
UT	Utah	0.0801	0.0169	0.0212	0.4323	0.9599	0.0847	0.0000	0.2717
VT	Vermont	0.6691	-0.0108	0.0134	0.4264	0.7502	0.1447	0.0000	0.3043
VA	Virginia	-0.0882	0.0135	0.0059	0.0327	0.8146	0.1240	0.0000	0.1171
WA	Washington	1.2161	-0.0574	0.0148	0.0008	0.8107	0.1222	0.0000	0.2866
WV	West Virginia	-1.0840	0.1989	0.0341	0.0000	0.9383	0.1046	0.0000	0.5298
WI	Wisconsin	0.2764	-0.0002	0.0313	0.9955	0.8987	0.1082	0.0000	0.5181
WY	Wyoming	-0.4529	0.1273	0.0266	0.0001	0.9425	0.0920	0.0000	0.3673
Average across the U.S. states		0.0000	0.0455			0.8611			0.4005

Notes: The average WRI is computed across the 48 states on the U.S. mainland, since Alaska and Hawaii are excluded from our analyses. The WRIs of the states we included are re-scaled such that the mean and the standard deviation of the sub-sample are zero and one, respectively.

Reference

Herkenhoff K.F., Ohanian, L.E., and Prescott, E.C. (2018). Tarnishing the golden and empire states: Land-use restrictions and the US economic slowdown. *Journal of Monetary Economics*, 93, 89–109.

Koop, G., Pesaran, M.H., and Potter, S.M. (1996). Impulse response analysis in nonlinear multivariate models. *Journal of Econometrics*, 74, 119–147.

Moretti, E. and Wilson, D.J. (2017). The effect of state taxes on the geographical location of top earners: evidence from star scientists. *American Economic Review*, 107, 1858–1903.